Intelligent supervision of flexible optical networks

Matthieu Kanj

ANNÉE 2016

UNIVERSITÉ DE RENNES 1

UNIVERSITE BRETAGNE LOIRE

THÈSE / UNIVERSITÉ DE RENNES 1
sous le sceau de l'Université Bretagne de Loire

pour le grade de

DOCTEUR DE L'UNIVERSITÉ DE RENNES 1

Mention : Informatique

Ecole doctorale MATISSE

présentée par

Matthieu KANJ

Préparée à l'IRISA (UMR 6074)
Institut de Recherche en Informatique et Système Aléatoires
Equipe Adopnet (Advanced Technologies for Operated Networks)

Intelligent supervision of flexible optical networks

Thèse soutenue à Rennes
le 20 Décembre 2016

devant le jury composé de :

Cédric WARE
Maître de conférences (HDR) à Telecom ParisTech / *Rapporteur*

David COUDERT
Directeur de recherche (HDR) à INRIA Sophia Antipolis / *Rapporteur*

Ramon CASELLAS
Ingénieur de recherche à CTTC Barcelone / *Examinateur*

Jean-Marie BONNIN
Professeur des universités à Telecom Bretagne / Examinateur

Esther LE ROUZIC
Ingénieur de recherche à Orange Labs/ *Co-encadrant*

Bernard COUSIN
Professeur à Université de Rennes 1 / *Directeur de thèse*

Dominique VERCHÈRE
Ingénieur de recherche à Nokia Bell Labs / *Invité*

To the memory of my father.

ACKNOWLEDGEMENTS

This dissertation would not have been possible without the guidance and the help of several individuals, who in one way or another contributed and extended their valuable assistance in the preparation and completion of this study.

Firstly and foremost, I would like to thank my supervisor Prof. Bernard Cousin for given me the opportunity to realize my PhD at B-com Technology Research Institute. I am deeply grateful for the advice and support that I have received from him over the past three years.

My most sincere thanks goes to Esther Le Rouzic, who supervised me throughout this thesis and contributed greatly to my training on optical networks. Working with you was an opportunity to learn a lot, and acquire precious knowledge on optical communication and R&D. It was a great pleasure to work with a person like you, who is active, full of energy and ideas.

I would especially like to thank Julien Meuric, Jean-Luc Augé and Nicolas Brochier, who provided their expertise to enable this thesis to work well and for their support. The many discussions we have had, has helped me a lot.

I would like to express my sincere thanks to the committee members, David Coudert, Cédric Ware, Ramon Casellas, Jean-Marie Bonnin, and Dominique Verchère, for accepting to evaluate this work and to be part of the jury. I am particularly honored that Cedric Ware and David Coudert have agreed to evaluate this dissertation. I am very grateful for their feedback on this work.

I would like to express my deep gratitude and sincere thanks to our team leader Rodolphe Legouable, and our lab chief Stéphane Paquelet, for their support and help during the preparation and the completion of this thesis. I would also like to thank our domain chief Michel Corriou and B-com director Bertrand Guilbaud for the support, the motivation and the excellent working conditions that they offered.

I wish to express my thanks to my colleagues in B-com and Orange Labs : Pape Abdoulaye FAM, Ali Zeineddine, Antoine Rozé, Hamidreza Khaleghi, Andrey Fedosov, Florian Lebeau, Jean Dion, Pauline Desnos, Vincent Savaux, Patrick Savelli, Imad Alawe, Olivier Weppe, Rémi Bonnefoi, Lilian Delaveau, Pierre Didier, Marc Lanoiselée, Francoise Liégeois, Djamel Amar and Ahmed Frikha.

I am very grateful to my family, especially my parents for their patience, motivation and support during these three years.

Finally, the deepest gratitude and heartiest thanks goes to my love Hiba for her continuous help and moral support.

RÉSUMÉ

Les réseaux optiques dynamiques et flexibles font partie des scénarios d'évolution des réseaux de transport optique. Ceux-ci formeront la base de la nouvelle génération des réseaux optiques de demain et permettront le déploiement efficace des services tel que le Cloud Computing. Cette évolution est destinée à apporter flexibilité et automatisation à la couche optique, mais s'accompagne d'une complexité supplémentaire, notamment au niveau de la gestion et de la commande de cette toute nouvelle génération de réseau.

Jusqu'à récemment, les protocoles de routage et de signalisation normalisés ont pris en compte plusieurs paramètres physiques tels que l'information spectrale de la bande passante, le format de modulation, et la régénération optique. Cependant, d'autres paramètres sont encore nécessaires (par exemple, les puissances optiques des liens, le gain des amplificateurs) afin de faire fonctionner efficacement de grands réseaux. Dans ce contexte, il y a un besoin d'étudier les réseaux optiques existants ainsi que les différentes méthodes de prise en compte de la couche photonique dans le plan de contrôle. Le but est d'avoir un réseau optique automatique, flexible et programmable, mais surtout efficace de point de vue économique et opérationnel.

L'utilisation de la technologie à grille flexible a un impact sur les réseaux optiques existants, où presque tous les équipements devront être remplacés, ce qui entrainera un cout additionnel pour les opérateurs. Dans ce travail, nous étudions les réseaux optiques actuels et évaluons l'impact de la flexibilité sur les infrastructures existantes. Ensuite, nous identifions plusieurs paramètres optiques à contrôler et proposons des extensions protocolaires afin d'intégrer ces paramètres dans un plan de contrôle GMPLS. De plus, nous développons les algorithmes de routage et de signalisation qui permettent la mise en oeuvre d'un plan de contrôle efficace qui répond au besoin de la flexibilité. Enfin, l'ensemble de nos propositions et de nos solutions sont évaluées sur plusieurs topologies réseaux avec des modèles de trafic différents dans le but de valider leur pertinence.

ABSTRACT

Dynamic and flexible optical networks are among the evolution scenarios of the optical transport networks. These form the basis of the new generation of optical networks of tomorrow and enable the effective deployment of services such as cloud computing. This evolution is intended to provide flexibility and automation to the optical layer. However, it results in additional complexity, particularly in terms of the management and control of this new network generation.

Until recently, the standardized routing and signaling protocols have been taking into account several optical parameters like the spectral bandwidth information, modulation format, and optical regeneration. However, other parameters (e.g., link optical powers, gain of optical amplifiers) are still required in order to efficiently operate large optical networks. In this context, there is a need to study the existing optical networks and the different integration methods of the photonic layer in a control plane. The goal is to get an automatic optical network that is flexible, programmable, and at the same time efficient from an economical and operational perspective.

The use of flexible grid technology has an impact on existing optical networks, where almost all the equipment must be replaced, resulting in an additional cost to network operators. In this work, we study the current optical networks and evaluate the impact of flexibility on the existing infrastructures. Then, we identify several physical parameters to be controlled and propose protocol extensions in order to integrate these parameters in the GMPLS control plane. In addition, we develop the routing and signaling algorithms that allow the implementation of an efficient control plane that addresses the need for flexibility. Finally, the set of our proposals and solutions are evaluated on multiple network topologies with different traffic patterns in order to validate their relevance.

RÉSUMÉ ÉTENDU EN FRANÇAIS

Introduction

Les réseaux de transport optiques constituent la base des systèmes de télécommunications d'aujourd'hui. Grace à la grande capacité et la longue portée des fibres optiques qui les constituent, ils sont utilisés pour interconnecter les grandes villes et les pays à internet et aux fournisseurs de services dans le monde entier. La convergence technologique vers un plan de données unifié fait que tout le trafic issu de n'importe quelles couches de services (IP / MPLS, Ethernet, DSL, ATM, etc.) est transporté sur les réseaux optiques grâce aux systèmes de transmission WDM. Ce rôle crucial des réseaux optiques, ainsi que leurs coûts considérables en termes de CAPEX (dépenses en capital) et OPEX (dépenses opérationnelles) explique la forte attention accordée par les opérateurs à ces réseaux, en particulier en termes de performance et de gestion de ressources.

Au cours des dernières années, nous avons assisté à l'explosion du trafic Internet en raison de la croissance phénoménale des applications d'Internet telles que les vidéos, la HDTV, le trafic de données mobiles, les jeux en ligne, le partage de fichiers, les sites de réseautage social, etc. Cette demande croissante de bande passante est estimée de produire encore une augmentation significative dans les années à venir. Tout cela a stimulé le besoin de réseaux IP à haute vitesse, mais aussi la nécessité d'accroître la capacité des réseaux de transport optiques. Pour faire face à cette tendance, les progrès technologiques en communication optique ont été déclenchés, afin d'obtenir des systèmes de transmission optique efficaces, offrant des débits élevés avec une utilisation efficace de la bande passante. L'objectif est d'évoluer vers des infrastructures de réseau coeur optique flexible et dynamique.

Les réseaux de transport optiques d'aujourd'hui sont construits en utilisant le système de transmission WDM. Plusieurs canaux optiques sont présents au sein de chaque fibre optique. Chaque noeud optique du réseau contient un ensemble de modules WSS (*Wavelength Selective Switch*) qui permettent de commuter optiquement n'importe quel canal optique. Cependant, ces systèmes WDM sont conçus avec la technologie *fixed-grid*, avec l'inconvénient de ne pas pouvoir exploiter efficacement les ressources en bande passante optique du réseau : chaque canal optique occupant une bande passante identique et offrant un débit fixe. La nécessité d'une plus grande capacité dans les réseaux optiques stimulée par l'augmentation du trafic a déclenché

de nombreuses avancées technologiques [1], conduisant à l'introduction des technologies *flex-grid* pour la commutation optique. Cette technologie permet une gestion dynamique et efficace des ressources de bande passante disponibles au sein du réseau. En effet, les réseaux *flex-grid* sont attrayants en raison de leur potentiel d'amélioration de l'efficacité spectrale d'environ 30%. Ils offrent la possibilité de fournir des canaux de bande passante variable (i.e., plus petit ou plus grand de 50GHz), et permettent ainsi le développement futur de transpondeurs à débit binaire supérieur. Cependant, le déploiement des réseaux *flex-grid* nécessitera beaucoup plus qu'un WSS *flex-grid* [1]. Ces réseaux nécessiteront des ROADMs (*Reconfigurable optical add/drop multiplexer*) flexibles, des transpondeurs conçus pour fonctionner sur une grille ayant des longueurs d'onde plus étroites, de nouveaux logiciels de gestion du réseau et des outils de planification du réseau plus sophistiqués. De plus, ils devraient être en mesure de gérer la problématique de la fragmentation de la bande passante qui apparaîtra à cause de l'établissement et de la suppression de canaux optiques ayant des largeurs de bande variables dans un environnement présentant un trafic dynamique.

En général, l'objectif principal d'un opérateur de réseau est d'assurer un équilibre entre la gestion optimale des ressources et la minimisation des coûts associés à l'exploitation du réseau. Les opérateurs sont de plus en plus à la recherche de solutions automatisées pour optimiser le routage et l'allocation des ressources dans la phase opérationnelle. A cet égard, un plan de contrôle intelligent joue un rôle important dans l'évolution des réseaux optiques. Le plan de contrôle permettra d'activer les équipements constituant le réseau optique et de gérer de nouveaux services dynamiques et donc la demande variable de trafic. Il améliore également l'efficacité du réseau et la résilience du réseau. Enfin, il aide à réduire les frais d'exploitation en simplifiant la mise en service et la maintenance du réseau, ce qui permet la fourniture rapide de bande passante et d'éviter les processus manuels de configurations complexes et longues.

Le protocole GMPLS (*Generalized Multiprotocol Label Switching*) est une des implémentations possibles du plan de contrôle. Il est bien connu, couramment et majoritairement utilisé pour la gestion des réseaux optiques. Il est proposé et développé par l'IETF (*Internet Engineering Task Force*) en tant qu'un plan de contrôle générique pour les réseaux utilisés pour le provisionnement des chemins de bout-en-bout pour les réseaux des fournisseurs de services Internet et télécoms. Cependant, la norme GMPLS actuelle ne prend pas en charge toutes les fonctionnalités annoncées par la technologie *flex-grid*. Pour cela, de nombreuses améliorations doivent être apportées aux protocoles du plan de contrôle GMPLS afin de prendre en compte les phénomènes tels que les dégradations optiques et la fragmentation. De plus, ils devront prendre en compte aussi les mécanismes tels que le routage et affectation du spectre (RSA), l'interopérabilité entre les fournisseurs d'accès internet, et la virtualisation des services de transport.

Dans ce contexte difficile, cette thèse vise à améliorer les fonctionnalités de gestion du plan de contrôle GMPLS afin de faciliter l'intégration de la technologie *flex-grid* dans les réseaux optiques actuels. Le travail réalisé est divisé en deux parties principales. La première partie se concentre sur les conséquences de la migration vers un

réseau *flex-grid* sur la couche optique. Plus précisément, nous nous concentrons sur le niveau de puissance des amplificateurs optiques et nous proposons une solution au problème d'intégration de la flexibilité sur les infrastructures existantes des réseaux optiques *fixed-grid*. La deuxième partie se concentre davantage sur les aspects du plan de contrôle où des améliorations et de nouvelles extensions protocolaires sont proposées pour inclure les paramètres optiques identifiés dans le plan de contrôle GMPLS. Des nouveaux algorithmes de routage et de mécanismes de signalisation sont développés dans le cas des réseaux optiques transparents et translucides.

Contributions

La croissance exponentielle du trafic dans les réseaux optiques a déclenché l'évolution vers des réseaux optiques flexibles, promettant un gain significatif pour les opérateurs de réseau en termes d'efficacité spectrale sur leurs infrastructures de réseau optique. Cependant, le déploiement de nouveaux liens optiques et le remplacement des équipements optiques existants rendent la technologie flexible très coûteuse pour les opérateurs des réseaux malgré ses promesses de capacité accrue. Dans ce contexte, les opérateurs de réseaux tentent de réduire les coûts (c'est-à-dire les coûts d'achat et d'exploitation) de la migration vers les réseaux flexibles en maintenant l'utilisation de leurs infrastructures existantes.

Dans ce travail de thèse, nous avons abordé la technologie flexible et ses impacts sur le plan de données et le plan de contrôle des réseaux de transport optiques actuels. Nous nous sommes concentrés sur le problème de la saturation de la puissance qui pourrait éventuellement être rencontré lors de la migration des réseaux optiques *fixed-grid* vers les réseaux optiques *flex-grid* lorsqu'on tente de conserver les infrastructures optiques actuelles. En particulier, nous avons abordé le problème qui n'a jamais été étudié précédemment, concernant la saturation de puissance dans les amplificateurs optiques due à l'augmentation du nombre de canaux optiques établis.

L'objectif principal de notre travail était, d'une part, d'évaluer ce problème de saturation de puissance et de proposer une solution qui puisse être facilement implémentée dans un plan de contrôle optique. D'autre part, démontrer que l'amélioration de l'intelligence du plan de contrôle permet d'optimiser les ressources du réseau et de bénéficier ainsi de l'augmentation de capacité offerte par la technologie flexible tout en conservant les infrastructures optiques existantes.

C'est dans ce contexte que le travail a été réalisé, les contributions et les résultats sont résumés comme suit :

- Nous avons d'abord introduit au chapitre 1, l'évolution des réseaux optiques en distinguant le plan de données et le plan de contrôle car ils constituent les deux parties principales d'un réseau optique automatisé. Nous avons présenté la phase de conception du réseau et les éléments physiques qui peuvent avoir un impact sur la conception et le contrôle des réseaux optiques. Enfin, nous nous sommes concentrés sur la suite de protocoles de contrôle, GMPLS, largement

utilisée et nous avons fourni une description fonctionnelle de ses protocoles de routage et de signalisation.

- L'évolution vers des réseaux flexibles et l'impact de la flexibilité sur le plan de données et le plan de contrôle des réseaux optiques actuels sont présentés au chapitre 2. Nous avons montré comment les changements dans le plan de données rendus nécessaires par l'ajout d'équipements optiques flexibles peuvent augmenter la complexité de l'algorithme de routage, et donc ils nécessiteront une amélioration des protocoles du plan de contrôle de tout réseau optique automatisé. Ensuite, nous avons présenté les travaux existants dans la littérature qui traitent de la flexibilité, démontrant que l'évolution vers des réseaux flexibles automatisés permet d'optimiser les ressources et d'augmenter la capacité des réseaux optiques actuels. Enfin, nous avons souligné que l'augmentation du nombre de canaux offerts par la technologie flexible peut augmenter le niveau de puissance optique dans les liens optiques, soulevant l'importance de prendre en compte la puissance optique comme une limitation lors de la migration vers un réseau flexible.

- Dans le chapitre 3, nous avons abordé le problème de saturation de puissance qui pourrait apparaitre après la migration du réseau *fixed-grid* vers le réseau *flex-grid* lorsque l'on maintient en service les infrastructures optiques existantes. Nous nous sommes concentrés tout d'abord dans ce chapitre, sur les réseaux optiques transparents avec un modèle de trafic incrémental, pour simuler le cas du réseau statique. Le problème de saturation de puissance a été abordé comme suit : Tout d'abord, nous avons développé une méthode de conception de liens optiques qui nous a permis de déterminer le niveau de puissance sur les liens du réseau. Ensuite, nous avons identifié les paramètres essentiels requis par un plan de contrôle optique pour contrôler et évaluer ces niveaux de puissance. Deuxièmement, nous avons proposé un processus d'adaptation de puissance par canal qui bénéficie des marges de transmission pour réduire la puissance transmise des canaux optiques. Finalement, nous avons proposé un algorithme de calcul de chemin, avec des extensions protocolaires pour les protocoles de routage et de signalisation de la suite protocolaires GMPLS, afin de fournir la mise en oeuvre pratique d'un tel processus d'adaptation de puissance. Les résultats de la simulation ont démontrés que les niveaux de puissance de l'infrastructure *fixed-grid* ne sont pas suffisants pour permettre l'augmentation du nombre de canaux optiques lors de la migration vers un réseau *flex-grid*. Ils ont également montré que l'utilisation du processus d'adaptation de puissance permet de réduire le problème de saturation de puissance et donc d'augmenter la capacité du réseau. Enfin, ils ont démontré aussi que l'augmentation du nombre des plus courts chemins calculés ne permet pas d'éviter complètement le problème de saturation, même si le processus d'adaptation de puissance est utilisé.

- Dans le chapitre 4, nous avons étendu notre étude au cas des réseaux translu-

cides (donc avec régénération) sous un modèle de trafic dynamique, pour simuler le cas des futurs réseaux optiques automatiques et flexibles. Le processus d'adaptation de puissance et l'algorithme de calcul de chemins ont été adaptés au cas des canaux optiques régénérés. Ensuite, nous avons proposé de nouvelles extensions aux protocoles de routage et de signalisation pour permettre la gestion de la régénération optique et l'adaptation de puissance. Les résultats de la simulation ont montré que le problème de saturation de puissance se pose même à une faible charge du réseau et sous des modèles de trafic dynamique. En plus, comme dans le chapitre 3, l'augmentation de la capacité du réseau ne peut pas être exploitée si le processus d'adaptation de puissance n'est pas utilisé dans les scénarios flexibles. Il a été montré également que la méthode de régénération utilisée dans l'algorithme de calcul de chemins peut impacter les performances et le coût du réseau. Pour aller plus loin, nous avons répété les simulations sur des topologies de réseau supplémentaires. Les résultats ont montré une forte dépendance entre la topologie du réseau et l'apparition du problème de saturation de puissance. Les topologies possédant des liens optiques introduisant une faible dégradation du signal auront probablement des marges de puissance suffisantes pour éviter le problème de saturation de puissance et pourront supporter les canaux flexibles supplémentaires lorsque le processus d'adaptation de puissance sera utilisé.

- Dans le chapitre 5, nous nous sommes intéressés au problème persistant de saturation de puissance dans les réseaux optiques translucides flexibles. Par conséquent, nous avons proposé un nouvel algorithme de régénération qui utilise les informations de puissance des liens du réseau pour sélectionner les sites de régénération. L'algorithme a été appliqué dans les scénarios flexibles en utilisant le processus d'adaptation de puissance, où le problème de saturation se pose encore. Les résultats de simulation ont montré que l'algorithme réussit à éviter le problème de saturation de puissance en modifiant la répartition de puissance sur les liens du réseau. Cependant, la performance de l'algorithme a montré une dépendance vis-à-vis de la topologie du réseau.

Conclusion

Ce travail a mis en évidence l'importance de prendre en compte l'information de puissance des liens optiques lors de la migration vers les réseaux *flex-grid*. Il a permis de comprendre l'impact des niveaux de puissance des liens optiques sur le gain de capacité attendu de la technologie flexible. De plus, ce travail a permis de développer les extensions protocolaires et les algorithmes de calcul de chemins nécessaires pour réaliser l'implémentation de l'adaptation de la puissance par canal dans les futurs réseaux optiques flexibles.

CONTENTS

LIST OF ACRONYMS

ASE	Amplifier Spontaneous Emission
BER	Bit Error Rate
BP	Blocking Probability
CAPEX	Capital Expenditure
CBR	cumulative blocking ratio
CT	Crosstalk
CD	Chromatic Dispersion
DCF	dispersion compensation fiber
DCM	dispersion compensating module
DSP	digital signal processing
EDFA	Erbium doped fiber amplifier
EDWA	Erbium doped waveguide amplifier
ERO	Explicit Route Object
FEC	Forward Error Correction
FWM	four-wave mixing
GMPLS	Generalized Multiprotocol Label Switching
IETF	Internet Engineering Task Force
ILP	Integer Linear Programing
IM	Inverse Multiplexing
ITU-T	International Telecommunication Union Telecommunication
LCoS	liquid Crystal on Silicon
LMP	Link Management Protocol
LSA	Link State Advertisement
LSDB	Link States Database
LSP	Label Switch Path
MEMS	Micro-Electro Mechanical System
MIB	Management Information Base
MTOSI	Multi-Technology Operations System Interface
MXCE	Maximum channel number exceeded
NETCONF	Network Configuration Protocol
NF	Noise Figure
NFV	Network Functions Virtualization
NLI	Non-linear Impairment

OEO	Optical-to-Electrical-to-Optical
ONF	Open Networking Foundation
OPEX	Operational Expenditure
OSPF-TE	Open Shortest Path First with Traffic Engineering extensions
OXCs	Optical Cross Connects
OSNR	Optical Signal to Noise Ratio
PA	Power Adaptation
PAR	Power Aware Regeneration
PCE	Path Computation Element
PDH	Plesiochronous Digital Hierarchy
PDL	Polarization Dependent Loss
PMD	Polarization Mode Dispersion
PSD	Power Spectral Density
PV	Power Verification
QPSK	Quadrature Phase-Shift Keying
RF	Regenerator Flag
RAO	Regenerator Availability Object
RO	Regenerator Object
ROADM	Reconfigurable Optical Add/Drop Multiplexer
RSA	Routing and Spectrum Assignment
RSVP	Resource Reservation Protocol
RWA	Routing and Wavelength Assignment
SBS	Stimulated Brillouin Scattering
SDH	Synchronous Digital Hierarchy
SDN	Software Defined Networking
SNMP	Simple Network Management Protocol
SNR	Signal to Noise Ratio
SOA	Semiconductor Optical Amplifier
SPM	self-phase modulation
SRS	Stimulated Raman Scattering
TE	Traffic Engineering
TED	Traffic Engineering Database
TLV	Type-Length-Value
UNI	User Network Interface
WDM	Wavelength Division Multiplexing
WSS	Wavelength Selective Switch
XPM	cross-phase modulation

NOTATIONS

α	Fiber attenuation coefficient
$\aleph_l$	Set of amplifiers of the link l
a_n	Attenuation of the n^{th} span
$C_{adaptation}$	Channel power attenuation value
G_n	Gain of the n^{th} amplifier
G_{OA_max}	Maximum amplifier gain
k	Index of the optical path
K	Number of shortest paths
L	Optical fiber length
l	Index of the optical link
N	Number of network nodes
$N_{channel\_max}$	Maximum number of channels per link
$N_{channel\_max,l}$	Maximum number of channels of the link l
NF	Noise figure
$OSNR_{est,p}$	Estimated OSNR for the path p
$OSNR_{margin,p}$	Difference between the estimated and required OSNR for the path p
$OSNR_{req,p}$	Required OSNR for the path p
p	Optical path
$P_{design,l}$	The optical power designed for the link l
P_{in}	Input optical power
$P_l(t)$	Current optical power over the link l at time t
$P_{margin,l}$	Optical power margin over the link l
$P_{max,l}$	Maximum optical power allowed at the input of the link l
P_n	Input optical power of the n^{th} span
$P_{OA\_margin,n}$	Optical power margin over the n^{th} amplifier
P_{OA_max}	Amplifier maximum output power
$P_{OA\_max,n}$	Maximum output power of the n^{th} amplifier
$P^{opt}_{channel,l}$	Channel optimum power over link l
$P^{opt}_{channel,p}$	Channel optimum power over the path p
$P^{adapted}_{channel,p}$	Channel optical power after power adaptation over the path p
P_{out}	Output power
S	Number of spectrum slots
t	Time

LIST OF FIGURES

LIST OF TABLES

INTRODUCTION

OPTICAL transport networks constitute the backbone of today telecommunications systems. Thanks to their high capacity and long reach, they are used to interconnect the major cities and countries to internet and service providers around the world. The technological convergence towards a unified data plane makes that all traffic from a variety of service layers (IP/MPLS, Ethernet, DSL, ATM, etc.) is carried over optical networks thanks to Wavelength division multiplexing (WDM) transmission systems. This critical role of optical networks as well as their considerable costs in terms of CAPEX (Capital Expenditure) and OPEX (Operational Expenditure) explains the high attention given by operators to such networks, especially in terms of performance and resource management.

In the recent past years, we have witnessed the explosion of internet traffic due to the phenomenal growth of Internet applications such as videos, HDTV, mobile data traffic, online gaming, file sharing, social networking sites, cloud services, etc. This growth in demand for bandwidth is estimated to still provide a significant increase in the coming years. All this has stimulated the need for high speed IP networks but also the need to increase the capacity of optical transport networks. To cope with this trend, technological advances in optical communication have been triggered in order to get efficient optical transmission systems offering high data rates with efficient bandwidth utilization. The goal is to evolve to a more flexible and dynamic optical core network infrastructures.

Today's optical transport networks are built using WDM transmission systems. Every link fiber supports several optical channels (one on each available wavelength). Every optical node in the network contains a set of Wavelength Selective Switch (WSS) modules that allow to optically switching any optical channel. However, these WDM systems are designed with fixed-grid technology; with the disadvantage of not being able to effectively exploit the optical bandwidth resources of the network. The need for more capacity in optical networks driven by the traffic increase has triggered many technological advances [1] leading to introduction of the flexible grid technologies for optical switching. This technology allows the dynamic and efficient management of the available bandwidth resources of the network. Indeed, flexible-grid networks are attractive because of their potential to improve spectral efficiency by approximately 30% [3]. They give the possibility to provision channels with greater than 50 GHz of bandwidth enabling the future deployment of higher bit-rate transponders. How-

ever, the deployment of flexible-grid networks will require far more than flexible grid WSS [1]. Such networks will require flexible grid reconfigurable optical add/drop multiplexer (ROADMs), transponders designed to operate over a finer wavelength grid, new management software, and more sophisticated planning tools. Moreover, they should be able to manage bandwidth fragmentation problematic that will appear due to the setup and teardown of mixed sizes of bandwidths in a dynamic network environment.

In general, the major objective of an operator is to ensure a balance between optimal management of resources and minimization of costs associated with the operation of the network. Operators are increasingly looking for more automated solutions to optimize routing and allocation of resources in operational phase. In this respect, an intelligent control plane plays an important role with the evolution of optical networks. A control plane enables the optical network to support and manage new, dynamic services and traffic demands. It also improves network efficiency and resiliency when applied for dynamic service restoration. Finally, it helps reducing operating expenses by simplifying service turn-up and network maintenance, allowing quickly bandwidth provision and automating complex configuration processes.

The Generalized Multiprotocol Label Switching (GMPLS) protocol is one of the well-known and commonly adopted control plane used for managing optical networks. It is proposed and developed by the Internet Engineering Task Force (IETF) as a generic network control plane framework. It is used for end-to-end lightpath provisioning and core tunneling technologies of the Internet and telecom service providers. However, the current GMPLS standards do not support yet all features announced by flexible grid technology. Therefore, many improvements should be made to the GMPLS control plane protocols in order to support mechanisms such as impairment awareness, routing and spectrum assignments (RSA), spectrum defragmentation, multi-vendors and multi-layer interoperability, and network services virtualization.

In this challenging context, this thesis aims to improve GMPLS control plane management functionalities in order to facilitate the integration of flex-grid technology in current optical networks. The realized work is divided into two main parts: the first part focus on the physical layer consequences when migrating to flexible grid network. More specifically, we focus on the power level of optical amplifiers and propose a solution to the flexibility integration problem over the existing fixed-grid network infrastructures. The second part focuses more on control plane aspects where enhancements and new protocol extensions are proposed to include the identified optical parameters in a GMPLS control plane. New routing algorithms and signaling mechanisms are developed for the case of transparent and translucent optical networks.

The thesis work is organized as follows:

Chapter 1 presents the background knowledge that is used in this thesis. Firstly, it gives a description of optical networks evolution and describes the physical impairments affecting the optical signal during its propagation in the network. Then, it high-

lights the relation between optical link design, impairments estimation and the optical control plane. Secondly, it presents briefly the basic functionalities of an optical control plane and detailed the routing and wavelength assignment problem in optical networking. Finally, some of the existing control plane protocols are presented with a focalization on the GMPLS-based protocol suite functionalities.

Chapter 2 is dedicated to the state of the art of the flexible grid technology and to its impact on the optical and control plane of optical networks. The first part, presents some hardware aspect on optical switching and the improvements realized to the optical plane to improve its flexibility. The second part is dedicated to the impact of flexibility on the control plane and how it affects path computation, impairment estimation and GMPLS control plane protocols. The last part presents some of the recent studies on flexibility and resources optimization in flexible optical networks. Then, it introduces the problematic and the motivations of this thesis.

Chapter 3 presents the problem that could be faced when migrating from fixed grid to flexible grid networks. More specifically, the power saturation problem at optical amplifiers level when keeping in uses the already deployed optical links (i.e., optical fibers and amplifiers). A power adaptation method is proposed to avoid this power saturation. Moreover, protocol extensions, routing algorithm and signaling mechanism are also proposed for transparent optical networks.

In **Chapter 4**, the case of the translucent optical network is considered, where a state of the art on the existing protocol extensions and signaling mechanisms that deals with optical regeneration is first presented. Secondly, protocols extensions, routing algorithm and signaling mechanisms are proposed to implement the power adaptation process in the case of optical regeneration. Finally, the power saturation problem and the power adaptation process are evaluated over different network topologies.

Chapter 5 focuses on the power saturation problem over highly loaded links, where the power adaptation process was not sufficient to resolve saturation problem. Therefore, a power aware regeneration algorithm is proposed in order to reduce the power level over highly loaded link and thus avoiding power saturation.

Finally, this work is summarized by providing **conclusions and perspectives** that arise from this study.

CHAPTER 1

OPTICAL NETWORK

THIS chapter aims to present the background of this thesis. It offers a general description of the data and control planes of the automated optical networks. In the first part, the data plane aspects such as the evolution of the optical networks, the optical impairments, the link design and the estimation of impairments are presented. They allow understanding the importance of optical impairments and network design phase, on the determination of the optical resources and on the performance of any optical network. In the second part, the role and the objectives of the optical control plane are presented, with a focus on the GMPLS protocol suite that will be used in this work.

These two parts will help understanding how an automated optical network works. The flexibility aspects in optical networks and its impact on the data and control planes are left to the Chapter 2.

1.1 The optical transport networks: evolutions and problematic

One of the main trends of our time is the growing bandwidth demands of business and carrier networks, due primarily to new uses related to Internet (multimedia services, electronic commerce, etc.) [4]. This change was accompanied by a profound technological transformation of transport networks in order to carry the ever-growing traffic volumes.

The optical fiber is a part of these trends and brings significant improvements in terms of rates, reaches, but not only. It is more reliable, more efficient and has a lower cost and more returns on investment compared to copper cables. However, new problems arise, especially in terms of routing. Indeed, the control of photons circulating in

the optical fiber is not an easy task as the electrical signal processing in copper networks. Therefore, optical-electrical conversion solutions have been implemented. The optical signals are converted into electrical signals with a transceiver to be processed by upper layers, while optical nodes based on Reconfigurable Optical Add/Drop Multiplexer (ROADM) steer the optical signals on the optical fibers. This approach takes the advantage of the high capacity of the optical layer.

The transport networks have evolved through three main steps: asynchronous networks PDH (Plesiochronous Digital Hierachy), SDH synchronous networks (Synchronous Digital Hierarchy) and Optical transport networks (OTN) for the rates beyond 10 Gbits/s. These networks were originally used to transport the traffic of operators (e.g., IP/MPLS flows, ATM, Ethernet, xDSL). The OTN layer uses the optical fibers to ensure a converging transport layer, integrating all functions usually performed by higher layers and encapsulating all their traffic. The OTN transport layer allows the multiplexing, routing, management and supervision of optical channels carrying client data in the network. The traffic transported by the OTN layer is usually sent over WDM (Wavelength Division Multiplexing) optical networks when the distances exceed few tens of kilometers. In Figure 1.1, we show a network architecture where the packet backhaul traffic in the metro segment and the IP traffic in the core segment of the network are transported by the WDM layer. In this architecture the OTN is a network standard that only serves as encapsulation of the traffic (there is no OTN switching equipment). In this work, we are interested only in WDM optical networks (Figure 1.1) and we do not take into account the possible grooming in OTN sub-layer.

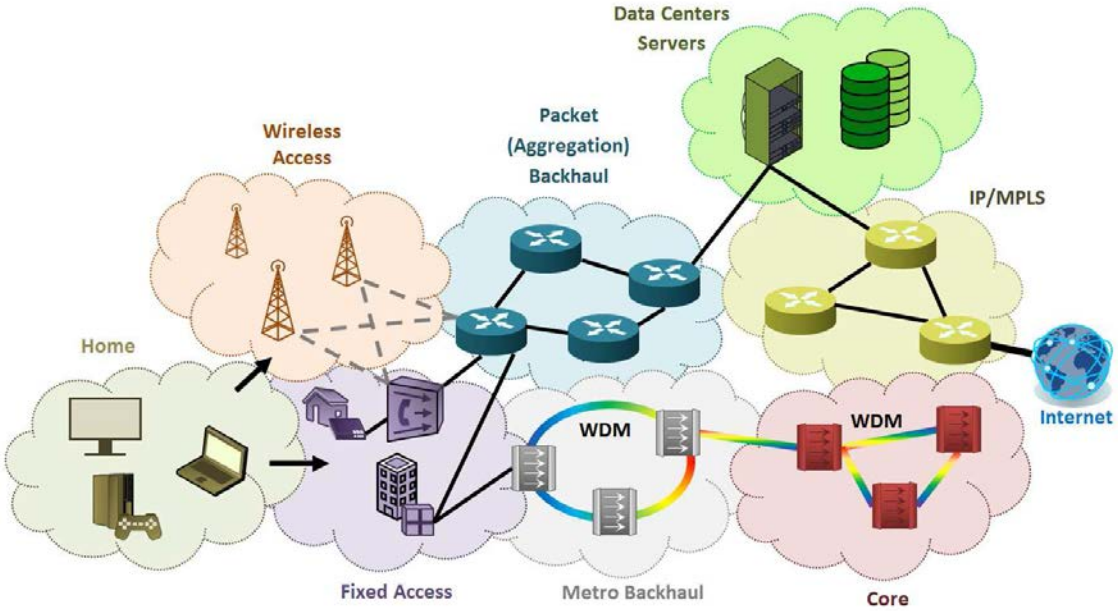

Figure 1.1: Operator networks hierarchy

The WDM optical networks use the wavelength division multiplexing technique to

allow transporting simultaneously a high number of wavelengths (i.e., optical channels) per fiber. This transmission technique allows better utilization of fiber bandwidth, thereby reducing costs and making best usage of the existing network infrastructures. Optical transport network based on WDM can operate in three different transport modes, depending on the resort to optical-to-electrical-to-optical (OEO) conversions. These modes are known as opaque, transparent and translucent [5]. In the following, we briefly describe the main characteristics of them.

1.1.1 Opaque mode

In this mode optical-electrical conversions are systematically performed when crossing any node. Opaque mode uses point-to-point connectivity, which means that all optical channels between any source and destination node are OEO converted at each intermediate node. This conversion enables the different services to be aggregated according to their needs at each node. The reception and retransmission of the optical signal in each crossed node is called "signal regeneration", which means that all impairments accumulated before the OEO conversion are cancelled.

In fact, optical signals are degraded when propagating in the optical fibers due to physical impairments. The advantage of this mode is that it eliminates the cascading of physical impairments (i.e., optical impairments) and allows services to be flexibly steered on any route without any limit of distance. Moreover, the OEO conversion allows benefiting from the aggregation and disaggregation of traffic in the electrical layer to better fill the optical channels. However, this mode increases the cost of the network when a large amount of traffic transits in nodes without the need to be groomed (i.e., grooming is not required): the systematic OEO conversion in this case is not required and could be saved by bypassing the nodes. This drives us to the second mode: transparent mode.

1.1.2 Transparent mode

In order to reduce the cost of optical transport network by eliminating the OEO conversions, new concepts of nodes have emerged [6, 7]. ROADMs are the best example of this kind of photonic nodes. This type of node is capable of switching in optical domain an optical signal arriving from an input fiber to another output fiber without necessarily undergoing an OEO conversion, giving the possibility to have transparent optical networks.

In transparent optical networks, all optical connections between a source and a destination node are optically switched when passing through intermediate nodes. The OE and EO conversions are only present at the source and destination nodes in order to allow the insertion and extraction of the signal (i.e., data packets) from the optical network. The advantages of such networks are in terms of cost and power consumption since no longer OEO conversions are performed in intermediate nodes. It is

thus a viable choice for small-scale networks with short diameter and limited number of nodes.

However, it is not likely to be a practical solution for large scale networks for the following reasons:

- Physical impairments: the optical signal propagation in optical fiber undergoes physical degradation that depends on several aspects, like the characteristics of fiber and optical amplifiers. This limits the reach of optical signals, especially when crossing a high number of optical links and nodes.

- The continuity of wavelength: In transparent networks, the chosen wavelength at the transmitter side cannot be changed in transit nodes, because the resort to intermediate OEO devices is forbidden[1]. Therefore, the same wavelength is used over all crossed optical links.

It is not easy to choose between opaque and transparent networks. An opaque network appears easier to manage and to optimize; but this simplicity comes at the expense of the number of resources consumed. A transparent network gives the possibility to reduce OEO conversion. However, this creates complexity due to the physical impairments and wavelength continuity. Therefore, in order to resolve transparency problems while keeping its advantages, another network concept is privileged: translucent network.

1.1.3 Translucent mode

The translucent mode is a compromise between economy and performance. In this mode, the optical signal is optically switched until its quality degrades below a threshold or wavelength contention occurs. In this case an OEO conversion is performed in order to eliminate the physical impairments or to avoid wavelength contention or for traffic aggregation needs. In other words, the optical signal is regenerated/groomed only if necessary. Moreover, in case only regeneration is required, and no grooming, a regenerator (i.e., OEO device) is used, which is a repeater that helps to clean up the signal and improve transmission quality.

A translucent optical network resolves the scalability and impairment problem. Moreover, it allows cost reduction for the network operator since much less regeneration resources are needed and offers more flexibility. This type of network represents our nowadays and future transport optical networks. As mentioned before, the optical regeneration is performed when the signal quality degrades below a certain threshold. However, the difficulty is to evaluate this degradation. Therefore, two evaluation techniques exist: reactive and proactive.

[1] There are optical equipment capable of optically regenerating/changing the wavelength of an optical signal, and thus without requiring OEO conversion. However, this solution is very expensive and not sufficiently mature to support all types of signals (e.g., all modulation formats). This is why optical continuity is an important constraint in optical networks and must be taken into account.

The reactive technique consists in establishing the optical channel, then evaluating if the channel quality is acceptable through a real time signal quality measurement. It is a non-stable and risky technique, especially, if the optical channel is not feasible (i.e., the signal quality not acceptable) and there is a need for a regenerator that could potentially not be available over the optical path. Moreover, this technique is not effective for future automatic optical networks since it reduces the performance of networks in terms of connection blocking and channel establishment delay (i.e., high establishment delay for unfeasible channels).

The proactive technique consists in estimating the physical feasibility of the optical channel before establishing it. In this case, the feasibility of the channel is known in advance and thus regenerators can be placed in intermediate nodes in case of unfeasible channel. However, a re-evaluation can be done after the establishment of the channel, because if the channel quality is not acceptable (due to inaccurate impairment estimation) a restoration mechanism can be triggered. In fact, the estimation of channel quality is done through an impairment estimator that is based on the modeling of optical impairments. This requires an accurate modeling of impairments in order to reduce the error margin between estimation and measurement, and thus reducing connection blocking.

1.2 Optical impairments

As optical signal propagates through the optical fibers and nodes, it encounters several physical degradation that affect its intensity, quality, temporal and spectral properties. These physical impairments can be classified into two major groups: linear and non-linear [8]. The linear impairments are independent from signal power. The non-linear impairments depend on the optical power and on the number of established channels. They induce interference due to the interaction between them. However, in this work, we are not interested specifically to each impairment types, but more to their impact on signal quality and on the design of optical links.

In the following we briefly present these two groups of impairments in order to understand them. We highlight the most important between them and cite some mitigation techniques. Then, we discuss the importance of having accurate estimation and models for these impairments, and explain their relation with the design of optical links. Finally, a state of the art on existing physical impairment estimator is then presented, identifying relevant parameters and deducing specific engineering rules.

1.2.1 Linear impairments

1.2.1.1 Power attenuation

The power attenuation is the loss in optical power that a signal encounters when propagating through an optical fiber. The output power P_{out} after propagating through an optical fiber of length L is given by $P_{out} = P_{in}e^{-\alpha \times L}$, with P_{in} is the input power and α

is the fiber attenuation coefficient. This power attenuation is due to absorption, reflections, refractions, bending losses, Rayleigh scattering [8]. Usually, power attenuation is regularly compensated by optical amplifiers.

1.2.1.2 Amplifier Spontaneous Emission (ASE)

The most important source of linear impairment in optical transmission systems is the ASE noise. It is generated by spontaneous decay of electrons in the upper energy levels to lower energy levels in the atoms of Erbium doped material. It is produced by the optical amplifiers used to amplify the power of optical signals due to the encountered power attenuation during their propagation. ASE noise is evaluated by the noise figure (NF) of the optical amplifiers, and it is amplified as the optical signal goes through other optical amplifiers[2].

The ASE noise acts on the Optical Signal to Noise Ratio (OSNR) which is the parameter used to evaluate the quality of the optical signal. The OSNR is an important parameter that characterizes the performance of the optical channel. It represents the power ratio of the useful signal and the produced noise.

1.2.1.3 Polarization Dependent Loss (PDL)

The PDL occurs in passive optical components like optical couplers, filters, isolators, multiplexers/demultiplexers, and photodetectors. The PDL value increases with the number of the crossed components. However, the accumulation of penalties generated by this phenomenon is taken into account in terms of system margins (i.e., as a limitation on the number of the crossed components or OSNR penalty), which are explained in Chapter 2.

1.2.1.4 Chromatic Dispersion (CD)

The chromatic dispersion originates from the dependence between the index of the optical fiber and the wavelength. This distortion causes inter-symbols interference. The CD depends on the modulation format, bit-rate and on the physical characteristics of the optical fiber. Moreover, it is cumulative where the total dispersion at the end of a light-path is the sum of dispersion on each optical link constituting the taken path. It is easily compensated and one of the most deployed compensation techniques is based on dispersion compensation fiber (DCF) on conventional dispersion managed systems. Recent coherent transmission systems do not need such modules, therefore, they are replaced by digital signal processing (DSP) techniques at the receiver side [9].

[2]This noise does not decrease with the power attenuation encountered during signal propagation. That is why we need to amplify regularly and not all at once.

1.2.1.5 Polarization Mode Dispersion (PMD)

The PMD originates from the impurities in optical fiber making that the two orthogonal polarization of the optical signals propagate with different velocities resulting in variable in time pulse spread and overlap. The PMD is one of the major linear impairments. It is cumulative and is proportional to the square root of propagation distance and its effects are random and time-dependent. In coherent transmission system the PMD is compensated through DSP algorithms.

1.2.1.6 Linear Crosstalk (CT)

The crosstalk arises due to the imperfect isolation in optical components (add/drop ports, multiplexers/demultiplexers, and optical switches) causing power leakage between WDM channels during the filtering operation and insertion/extraction of optical signals. The impact of this type of impairment on the optical channels is taken into account during the design of WDM systems, because the computation complexity of the CT increases with the number of crossed elements. This phenomenon can be reduced by installing network devices having good isolation.

1.2.1.7 Filter concatenation

The filter concatenation causes the narrowing of spectral width of the optical channel as it goes through a set of filters along the crossed path. In this work, this impairment is taken into account as an optical OSNR penalty.

1.2.2 Non-linear Impairments (NLIs)

The non-linear effects arise from the materials properties (refractive index, loss, etc.) of the optical fibers and from the optical power intensity. The dependence between the refractive index and the optical power causes the Kerr effect, creating three kinds of impairments: self-phase modulation (SPM), cross-phase modulation (XPM), and four-wave mixing (FWM). Various factors contribute to the increase in non-linear impairments: the aggregated optical power of all optical channels, the type of fiber, inter-channels spacing. Moreover, when the optical power level is high, a scattering phenomenon appears due to the interaction between fiber materials and optical channels. The intensity of this phenomenon increases rapidly when the optical power exceeds a certain threshold. This inelastic scattering phenomenon causes the SRS (Stimulated Raman Scattering) and SBS (Stimulated Brillouin Scattering).

In summary, several optical impairments impact the signal quality, where the non-linear impairments are the most difficult to compensate. However, some of them have more impact than the others. Therefore, taking them into account is the only way to ensure good reception of any optical signal. This lead us to the optical link design step during the creation of optical networks.

1.3 Link design and impairment awareness

As explained before, with the introduction of transparency in optical networks, the paths that were previously feasible in opaque network may no longer be feasible due to impairments accumulation. Therefore, it is important to take into account the physical feasibility of optical paths during network planning and dimensioning but not only. Determining the physical feasibility of optical paths through impairments estimation is the key for having an automatic transparent optical network [10]. Therefore, these impairments should be modeled and integrated in the control plane of future optical network in order to allow automatic and dynamic establishment of optical channels.

In fact, taking into account optical impairments is usually realized in the design phase of optical networks. The characteristics of the optical components deployed in optical links (e.g., optical amplifiers, optical spans) determine the degradation that an optical signal may undergo when crossing these links. However, most of the works in literature have neglected this design phase and simple methods were used instead to evaluate the reaches of optical channels (e.g., considering a maximum distance for every channel [11, 12]). Therefore, these methods are not accurate, since the feasibility estimation of the optical channels is realized without modeling or computing the real degradation. In this work, the link design phase is considered to better evaluate impairments impact and at the same time understanding the power levels over network links.

In the following, we briefly describe the link design process in optical networking. The existing impairment estimators and impairment awareness techniques are then presented. Finally, the accuracy of estimator models and impairment measurements is discussed.

1.3.1 Link design and impairment modeling

The most important, critical and complex phase in optical networking is the link design. It determines the capacity and the performance of an optical network. Therefore, a special attention is usually given to this phase during network planning and dimensioning.

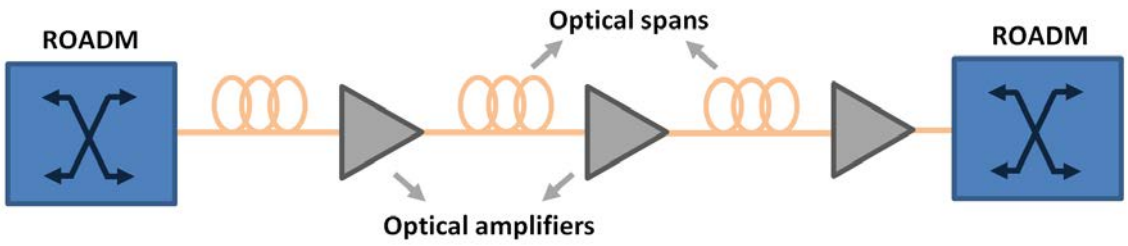

Figure 1.2: Set of optical spans and amplifiers constituting an optical link between two ROADMs.

The link design consists in selecting, installing and configuring the optical components that are required to build an optical transmission link between every two optical nodes. Therefore, it requires taking into account a large set of parameters [13, 14], like the optical power attenuation between amplifiers, technical specification of optical components, the number of planned channels for the link, the specification of available amplifiers and optical impairments. Figure 1.2, shows the set of optical spans (i.e., optical fibers) and amplifiers constituting an optical link between two ROADMs (i.e., optical nodes).

Three main elements are essential to the design of an optical link: the number of channels to establish over the link, optical spans characteristics (i.e., attenuation, physical parameters) and the set of available optical amplifiers. Figure 1.3 shows a set of three optical amplifiers with different characteristics in terms of gain, power and generated noise. Usually, the optical spans constituting the optical link have not necessarily the same lengths and thus they have different attenuations requiring probably different types of amplifiers. Therefore, depending on the required gain and the required output power the designer will select the amplifier that generates less noise.

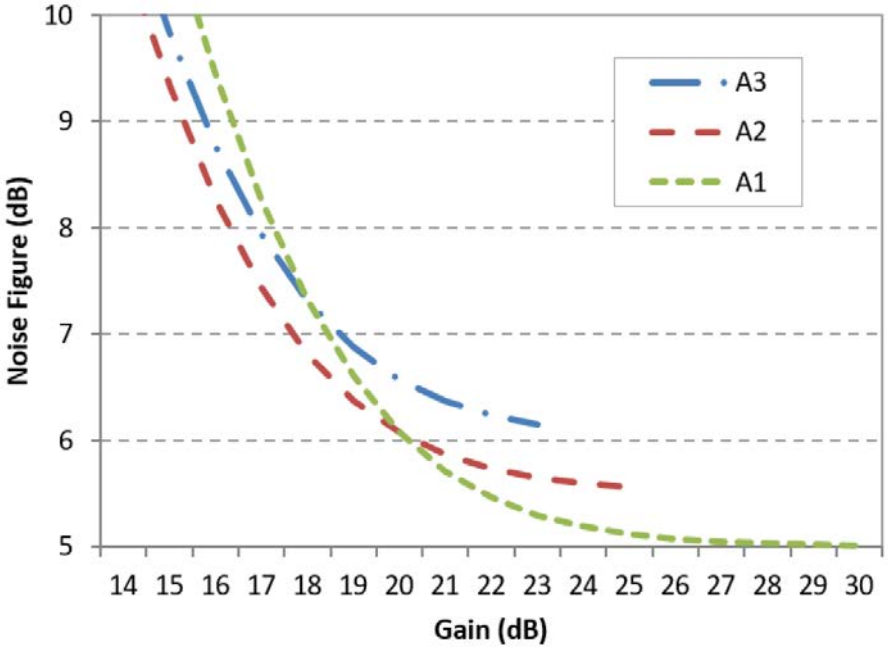

Figure 1.3: Gain variation versus the NF for a set of three optical amplifiers.

The complexity of the link design process arises from the set of opposite objectives. The selected and configured amplifiers should at the same time compensate optical spans attenuations, satisfy the required aggregated optical power while minimizing the generated noise and non-linear effects. The goal is to maximize the capacity and the performance of the optical link by minimizing the generation of linear and non-linear impairments.

In general, the link design phase requires modeling these impairments and studying their impacts, in order to facilitate choosing and configuring the optical amplifiers to be deployed over any link between two nodes. That's why the design phase is the first step to develop an impairment estimator (i.e., performance estimator). Such an estimator is usually built using the set of modeled impairments and it is considered after the design phase to evaluate the generated noise over network links (after deploying and configuring the amplifiers). It is through it that the evaluation of the physical feasibility of any optical channel is done when crossing several optical links (i.e., by computing the accumulated impairments over these links). This demonstrates the tight relation between impairments modeling, link design and the development of an accurate impairment estimator.

1.3.2 Existing impairment estimators

Estimating the transmission quality of an optical signal during its propagation is a theme increasingly relevant. It is the key to have automatic and translucent optical networks. To this end, many research efforts were conducted and various impairment estimators were developed in the literature. The goal is to evaluate the physical feasibility of any optical channel between any source and destination node.

In general, a transmission system is characterized by a typical Bit Error Rate (BER) threshold through which it can be determined the quality of the signal. However, in optical networking, installing BER measurement equipment is costly and not a suitable method when monitoring a high number of optical channels. Therefore, several impairment estimators have been developed in the literature, some are based on the number of crossed optical links [15, 16], others on Quality factor (Q) [17–19] or OSNR [20, 21], or on distance in kilometers (i.e., fixing a maximum distance for every signal). However, relation exists between BER and Q, and between OSNR and Q [22], which facilitates the determination of an OSNR or Q reference threshold that ensures a proper signal reception [23]. These models aim to estimate the signal to noise ratio (SNR) of optical channels in order to evaluate their feasibility. Basically, the term OSNR is used to evaluate only the linear impairments and the SNR term is used to evaluate the linear and non-linear impairments at the same time. However, in this work, we use the OSNR term (rather than SNR) to represent the signal degradation (i.e., linear and non-linear impairments), since most of the studies in the literature are using it.

These impairments estimators usually take into account several linear and non-linear impairments by modeling their effects. Therefore, depending on the number and types of modeled impairments, a model may be more or less complete. In fact, the interest of having a complete model is the reliability of the results, but often the computational complexity does not allow an easy integration of such an estimator model into a design tool or in routing algorithms. Therefore, a tradeoff is to be taken between the model completeness and complexity. The default method consists in developing a model (e.g., OSNR model) than incorporates the maximum number and types of impairments and a set of thresholds for the impairments that cannot be included in the

model (e.g., CD, PMD and PDL). However, sometimes the threshold for impairment is not respected, but the signal is still decodable due to its acceptable OSNR value. Therefore, it is important to develop impairment estimators that model in a balanced way the different types of impairment effects.

In this study, the OSNR model developed in [21] is used, since it allows the estimation of the linear and nonlinear impairments, and because it offers an easy implementation in the control plane. In contrast, the impairments such as CD, PMD were not considered since they are compensated though DSP in coherent transmission. However, impairment such as filtering concatenation is considered as an OSNR penalty.

1.3.3 Impairments models accuracy

In already deployed networks and well before the introduction of transparency concept, there was no need to have impairment awareness during the network operation. However, this cannot work for the future transparent/translucent optical networks where impairments play an important role in the determination of the capacity of the network, the reach and the performance of optical channels (detailed in Chapter 2). In such a context, impairment estimator accuracy is very critical in the determination of the feasibility of optical channels. It helps reducing the number of rejected optical channels and also reducing the number of OEO regenerators used in translucent optical networks. As explained previously in Section 1.3.2, the absence of accurate models for some impairments, forces network operators to set system margins that correspond to each unconsidered effect (or difficult to model) in order to avoid system disturbance and guaranteeing good performance. However, this leads to an accumulation of margins (i.e., in form of penalties) and thus to the blocking of some connections that could be feasible in reality [24]. In this respect, improving impairment estimator accuracy helps reducing the erroneous feasibility estimation and system margins, allowing the increase in network capacity and in optical channels reaches.

1.4 Optical control plane

Traditional transport networks can be modeled as the interaction of two operating planes: a data plane and a control plane. Figure 1.4 shows a simplified representation of the two planes, where usually the control plane is directly on top of the data plane. In this model, the data plane carries user traffic and comprises network equipment, such as interface cards, optical switch, optical fibers. In contrast, the control plane is responsible for establishing and maintaining user services (represented here by GMPLS protocol suite and UNI).

In fact, the increase in the traffic and the improvement of optical physical layer that we will discuss in Chapter 2 has pushed towards automatic optical networks. Indeed, this evolution has increased the management complexity of such networks, making the implementation of an intelligent optical control plane an urgent need for operators

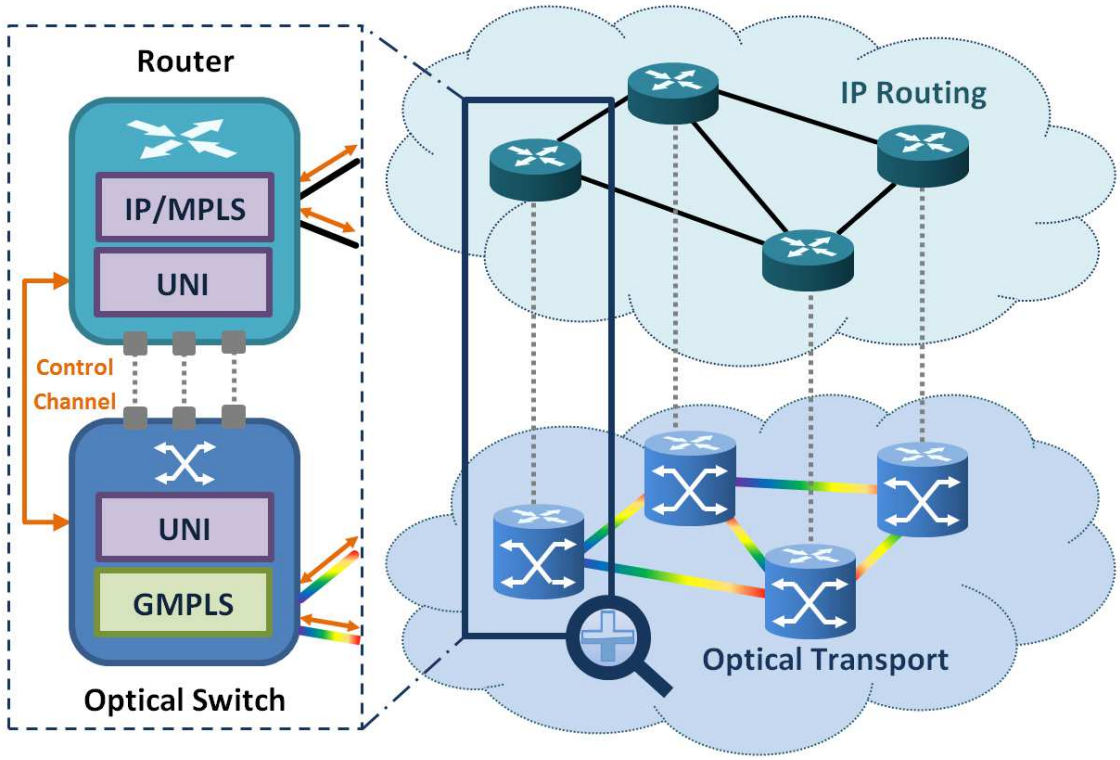

Figure 1.4: Simplified representation of the data and control plane in optical networks.

but not only. Reducing operational cost and time to set up services is also important for operators since current provisioning and scaling-up of new services requires complex engineering, planning and several weeks of waiting time.

In this section, we explain the role of the control plane in optical networks and focus on the routing and wavelength assignment problem in optical networks. Then, we briefly present some of the existing control plane protocols and focus on the GMPLS protocol suite that is considered for this study. Some future tendencies in optical networking are finally presented.

1.4.1 Role of the control plane

In general, the control plane can be seen as a set of control applications that support the capability of establishing a service (e.g., Optical connection) through the network. These control plane applications are:

- Call and Connection Control.
- Discovery.
- Routing.
- Path Computation.

- Signaling.

1.4.1.1 Call and connection control

This application is responsible for supporting the concept of calls and connections between the end users to support a service [25] (i.e., the reception of connection request from a user or a network operator to establish an optical channel). It is used for information signaling between the user (or network operator) and the optical network, to control the initiation, setup, modification, and teardown of the any connection request.

The initiation of the call is realized through a User-Network Interface (UNI) as shown in Figure 1.4. The UNI is the boundary between a user and the network. The user sends its service request over the UNI interface and the network responds by establishing calls and connections to meet the request. The decision on how to instantiate a service is determined by the local provisioning policy defined by the network operator.

1.4.1.2 Discovery

The discovery application is responsible for the discovery of neighbors and the links between neighbors [26]. This application is automated and realized through communication channels between neighboring nodes. Usually, every node sends a discovery message to neighboring nodes. In turn the nodes receiving this message respond to the originating node, completing the neighbor discovery process. This process allows exchanging IP addresses and identifiers of network nodes.

Moreover, the discovery protocol also supports the discovery of link connectivity between neighbors. This is accomplished through performing a link verification process in each node. Link verification works by sending a unique test message over the link being discovered. In this manner the local and remote link identifiers are discovered. The local node repeats this process for each of its links. This verification process allows detecting any connectivity failure over the links.

The discovery application maintains neighbor and link connectivity information and updates it in real time. This information is used by the routing application to distribute topology information throughout the network.

1.4.1.3 Routing

The routing application is responsible for propagating the link connectivity information (i.e., routing information) to all nodes within the network (or to a specific controller) [27]. This results in the creation of the traffic engineering (TE) database. The TE database contains the information on the network topology, as well as on the link resource information (e.g., link bandwidth availability, link impairments).

1.4.1.4 Path computation

The path computation application performs for the control plane the route computation for optical channels. This application uses the TE database information to compute one or several routes through the network in response to a connection request. At the end of computation, it provides the necessary information required for the establishment of the optical channel, such as the source (i.e., ingress), intermediate and destination (i.e., egress) nodes, and service constraints (e.g., reserved channel bandwidth).

The path computation application usually includes a Constrained Shortest Path First algorithm that is usually used to find the lowest cost route from source to destination. However, this algorithm can be improved to take into account additional service constraints [28]. Examples of service constraints that can be considered by path computation for an optical channel are bandwidth availability, wavelength continuity, and physical feasibility.

1.4.1.5 Signaling

The signaling application is responsible for setting up, modifying, and tearing down end-to-end services [29] (i.e., optical channels in optical networking). When the ingress node receives a connection request, the signaling controller requests a path computation with a set of constraints. The signaling controller then proceeds to establishment of the service using the signaling protocol and the computed path. The performed signaling mechanism depends on the signaling protocol used.

It is noteworthy that, two signaling options exist: in-band signaling and out-of-band signaling. In the in-band signaling option, the signaling traffic shares the same channel as the data traffic. However, in the out-of-band, the signaling channel is separated and independent of the data channel [30, 31].

1.4.2 Routing and wavelength assignment problem in optical networks

In optical networks, the path computation function is responsible in finding a path (i.e., route) and a free wavelength between a source and destination nodes in response to a connection request. In the literature, this problem of establishing an optical channel and reserving optical resources is referred to as the Routing and Wavelength Assignment (RWA) problem [32]. The general aim of the RWA problem is to increase the number of established connections. However, the difficulty resides in finding a path and assigning a wavelength for an optical channel while minimizing the amount of resources used. In fact, this problem becomes more difficult in transparent optical networks, where wavelength continuity and physical feasibility constraints should be respected. Moreover, this complexity can increase much more when dealing with re-

generator placement in translucent networks, flexible grid technology and with multi-layer dimensioning [33].

Indeed, RWA is a complex problem, especially when the number of optical links, nodes and parameters to take into account is high. However, depending on the traffic assumptions [34,35]: static or dynamic, the RWA problem is treated in two ways: offline and online.

1.4.2.1 Offline RWA and network dimensioning

In the static case, the entire set of connections is known in advance, and the problem is then to setup lightpaths for these connections in a global fashion while minimizing network resources. In the literature, this is referred to the network dimensioning phase [36]. The dimensioning of optical networks consists in determining the required resources (i.e., transponders, optical regenerators, etc.), their location and their quantities so that the maximum number of optical connections is routed with minimum cost and no blocking. Therefore, network dimensioning is usually performed taking into account several network information (i.e., traffic load, network architecture, protection aspects) in order to identify the most cost effective connection planning that meets operators needs and traffic evolution.

In such a context, where the set of optical connections to be established is known in advance, network modeling and optimization is used to find the set of routes and wavelengths to allocate for the planned connections. This is done through mathematical formulation of the problem using integer linear programing (ILP) for example. However, RWA is NP-complete problem where getting an optimal solution can take much time [37]. In this work, we will only consider the online RWA problem because it is more representative of future automated optical networks.

1.4.2.2 Online RWA

In the dynamic case, the optical connections requests are not known in advance. Therefore, the routes and wavelengths are computed in real-time upon reception of a connection request. This usually concerns the operational phase of automated optical networks where connection requests arrive randomly, and they are established and released dynamically. In this phase, heuristics and routing algorithms are implemented in a control plane instead of offline optimization (i.e., ILP formulation). This allows for a fast and efficient network operation, providing solution to problems such as nodes and links failures that requires dynamic and fast re-routing.

The objective in dynamic RWA is to compute a route and a wavelength that maximize the probability of establishing a given connection, while minimizing the blocking of future connections. However, the problem is less difficult compared to the static case, since the path computation algorithm deals with only one connection request. Traditionally, the RWA problem is decomposed into two sub-problems to decrease its complexity: the routing problem and the wavelength assignment problem. The routing

problem consists in finding an optical path (i.e., route) between a source and destination nodes. This computation is usually based on a criterion like path length or cost. The wavelength assignment problem consists in finding an available wavelength over the path computed by the routing algorithm.

In transparent and translucent optical networks, several constraints can be added to the RWA problem. These constraints include wavelength continuity, physical impairments, regenerator placement. The wavelength-continuity constraint requires finding a wavelength that is available over all optical links constituting the computed path. In general, several wavelength assignment strategies can be developed to satisfy this constraint (e.g., First-fit and Random-fit [38]). The physical impairment constraints are used to guarantee good signal quality. However, in case the path is not physically feasible, the RWA algorithm should be able to place regenerators in intermediate nodes.

It is noteworthy that, the optical path and wavelength are computed and assigned by taking into account the instantaneous state of the network at the time of connection request reception. However, this requires an up-to-date network database that contains detailed information on the available wavelengths and potential impairments over each link of the network. This database could be created in centralized or distributed manner depending on the operator management policy and on the control plane protocol used.

1.5 Existing protocol implementations of the control plane

In optical networking, different implementations of the control plane are used to manage the optical networks. The first one was the Simple Network Management Protocol (SNMP) [39]. It is used as an Internet standard protocol to communicate with network devices to perform management, alarm notification and performance monitoring. SNMP uses standard Management Information Bases (MIBs) to store information on the network devices and topology.

In fact, due to the limitations of SNMP in terms of configuration complexity and security weakness, the Network Configuration Protocol (NETCONF) [22] and the Multi-Technology Operations System Interface (MTOSI) have been developed. They are two promising technologies for IP-over-WDM transport networks. The MTOSI was developed to overcome the limitation of SNMP in terms of interoperability. In contrast, the NETCONF was proposed as alternative to SNMP, since it offers better configuration performance and allows reducing operational expenditures [40]. It is usually associated to YANG standard data model language due to its readability and simplicity.

However, the future deployment of these existing protocols will require an important effort from the IETF to improve these protocols in terms of extensibility (i.e., take into account flex-grid technology), multi-vendors and multi-domain interoperability and data models. Therefore, the acceptance and wide deployment of SNMP or NET-

CONF protocols will take a lot of time. In this work, we focus only on GMPLS protocol since it is a well-defined and standardized protocol, offering high flexibility in terms of functionalities, extensibility, performance, interoperability and security.

1.6 GMPLS control plane

1.6.1 GMPLS

The Generalized Multiprotocol Label Switching (GMPLS) [41] is one of the most deployed control plane technologies for optical networks. It was defined and proposed by the Internet Engineering Task Force (IETF) in order to support the increasing volume of IP traffic and to enable the automation of the management, configuration and resource provisioning in optical networks. It is a well-defined and stable protocol suite involving signaling, routing and link management protocols to automatically provision end-to-end traffic-engineered connections. It is a network protocol suite that extends the MPLS control plane by supporting other data transport technologies like optical cross connects (OXCs), photonic switches, IP routers, ATM switches, SONET and DWDM systems. It allows the setup of several connectivity services upon different switching type equipment (e.g., TDM, wavelengths and packet switching). Moreover, it offers a logical convergence and non-expensive heterogeneous architectures of transmission systems, control mechanisms and traffic engineering (TE).

GMPLS is a distributed control plane based on the TE extensions, where extensions could be added to the traditional MPLS routing and signaling protocols to encode new TE information concerning optical links or nodes, or to add new signaling configurations. This facilitates the operation of optical networks by providing an effective solution to control and optimize network resources and performance. In fact, GMPLS offers a complete separation of control and data planes. It is composed of three main protocols: Resource Reservation Protocol with Traffic Engineering extensions (RSVP-TE) signaling protocol, Open Shortest Path First with Traffic Engineering extensions (OSPF-TE) routing protocol, and Link Management Protocol (LMP). They help to ensure several control functionalities such as routing, network topology and link state dissemination, neighbor discovery and link management, path computation and signaling. Figure 1.5 shows a representation of the different interactions that exist between GMPLS protocols.

1.6.2 OSPF-TE

OSPF-TE is a link-state routing protocol used to exchange and distribute information about network links and topology [42]. It is an enhanced version of the OSPF protocol proposed by the IETF that allows carrying only one metric (e.g., cost metric). In fact, OSPF-TE gives the possibility to distribute several link properties, such as bandwidth, available resources and link quality. These attributes are taken into account in order to create what we call an extended link state database (LSDB).

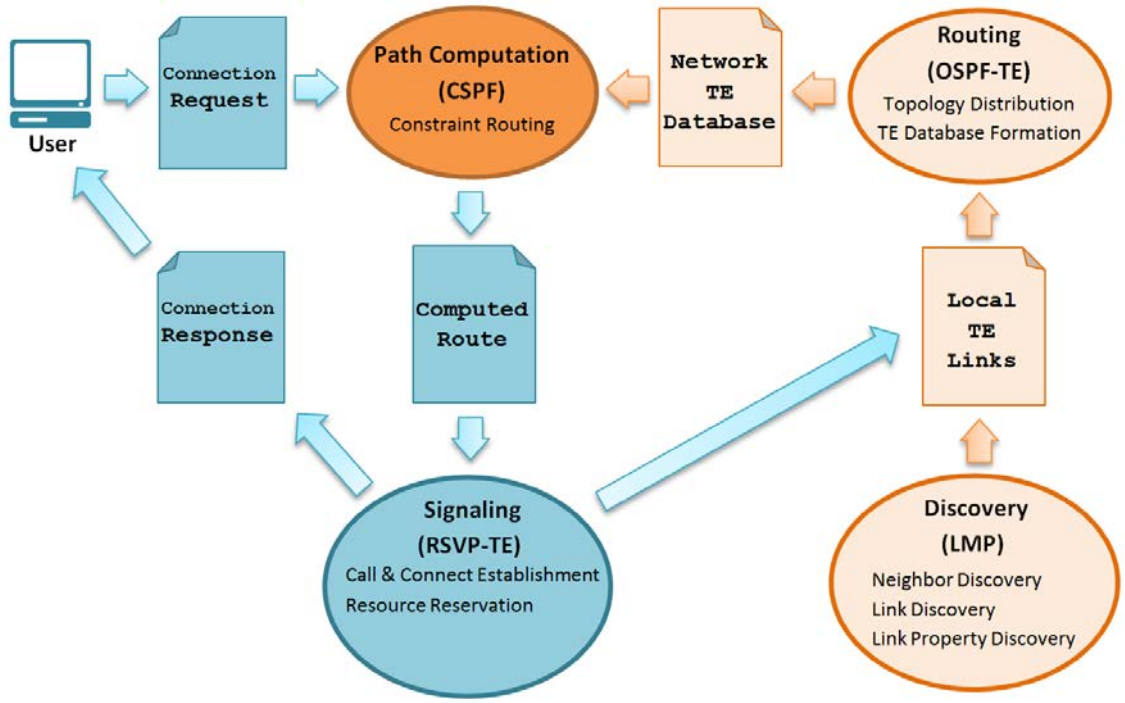

Figure 1.5: Simplified representation of the interactions between GMPLS control plane protocols.

OSFP-TE is in charge of advertising the traffic engineering information between network nodes. This advertising technique is ensured by a flooding mechanism in form of Link State Advertisements (LSAs) messages. The flooding mechanism ensures that all nodes in a network will have the same information in their local LSDB. In fact, the LSDB is created from TE information transported by LSA messages. These LSAs are organized in structures called Type-Length-Value (TLV) triplets, where they could be nested to offer an extensible technique to carry any additional information.

Furthermore, OSPF-TE allows also the advertisement of any change in link attributes (e.g., resources availability, link failure) by instantly sharing it with all network nodes, and thus guaranteeing the synchronization of their databases in order to always get a real time updated LSDB. This facilitates the management of the network by always providing a fine and accurate information on network resources. Therefore, any optical node can use its LSDB to perform a path computation upon reception of a connection request.

The OSPF-TE is a widely used routing protocol that provides good convergence time, security, and guarantee loop-free paths. However, some disadvantages appear at scalability level when the number of the added TE parameters is high. It may result in long TE database synchronization delay (i.e., longer convergence time after each update of the LSDB) and a huge number of advertised messages. At the same time, the lack of information on network resources may increase the blocking probability of

connection requests, since it limits the development of an intelligent path computation algorithm that takes into account the current state of the network. Therefore, a tradeoff is to be made between the number of link information to distribute and network performance requirements.

1.6.3 RSVP-TE

In order to set up a lightpath, GMPLS uses the signaling protocol RSVP-TE [43] to exchange control information among nodes. The RSVP-TE protocol is an extension of Resource Reservation Protocol (RSVP). It is the main signaling protocol used by GMPLS to set up, maintain and tear down optical connections and to perform resource allocation. It allows taking into account the concept of Quality of Service and traffic engineering.

RSVP-TE allows the establishment of Label Switched Paths (LSPs) by taking into account additional constraints like physical impairments, available resources, compatibility aspect between ingress and egress node. RSVP-TE uses $Path$ message to convey LSP information and specific configuration for the downstream nodes to request reservation of optical resources (i.e., bandwidth/wavelength). This message is propagated hop by hop until it reaches destination. The egress node usually responds by $Resv$ message and sends it in the upstream direction. The $Resv$ message is also propagated hop by hop until it reaches back the ingress node. It carries during its way to ingress node the specification of the traffic that has been requested, allowing the performance of resources reservation at every intermediate node.

1.6.4 LMP

The last brick of GMPLS protocol suite is the LMP [44]. This protocol runs between adjacent nodes to localize and isolate failures and thus triggers protection and restoration procedures. The LMP is responsible of the maintenance of the control channel between adjacent nodes. It helps verifying of traffic-engineering requirements between links of adjacent nodes (i.e., association maintenance between links and labels), allows the connectivity verification between data links if the control and data channels are separated (i.e., connection loss detection) and finally facilitating fault management and isolation.

1.6.5 Path computation and protocol extension in GMPLS control plane

In GMPLS distributed control plane, every optical node has its own local database. It is updated and synchronized with all other nodes databases through OSPF-TE protocol. This gives the possibility for every node to perform a path computation upon the reception of any connection request. The signaling process after path computation is ensured through RSVP-TE.

The path computation is a fundamental block in a distributed GMPLS controlled optical network. It is tightly related to OSPF-TE and RSVP-TE protocols, where any improvement in the RWA algorithm (e.g., to take into account physical impairments) will require adding protocol extensions to collect the needed information. In fact, as the number of optical parameters to take into account increases, the complexity of path computation algorithms (i.e., RWA algorithms) increases as well. This will affect the number and the size of the routing and signaling messages, and probably will increase the size of the databases and affect the performance of the network. However, the GMPLS control plane offers the possibility to perform path computation and information exchange in different ways [45], resolving the performance and scalability problem.

Indeed, GMPLS control plane offers different implementation possibility for path computation and information collection. The path computation module can for example be implemented in two different ways: centralized or distributed [46]. At the same time, information collection can also be realized through OSPF-TE protocol (i.e., in form of extensions stored in the LSDB) or through RSVP-TE protocol (i.e., by collection information during $Path/Resv$ message propagation) depending on the network operator policy.

1.7 Tendencies in optical networking

In the recent years, a new networking paradigm has emerged driven by IT community called Software Defined Networking (SDN) [47, 48]. It was proposed in order to change the way of managing networks, by enabling dynamic and automated networks and removing the limitations of current network infrastructures. The SDN paradigm offers like GMPLS the separation between control and data plane, and thus provides flexibility in managing networks, facilitating their evolution. Therefore, an important effort was realized to make SDN operate over optical networks, especially after the success achieved in the packet switching domain.

Indeed, today's optical networks are very static, therefore, once built; it is difficult and expensive to change them. SDN aims to increase the scalability, interoperability and agility of optical networks, allowing resources optimization and intelligent monitoring. It offers a centralized network control allowing better utilization of resources and simplified operation. It is usually associated to Network Functions Virtualization (NFV) [49] to get more flexible network applications and new services. SDN combined to NFV aims to create an abstraction of network resources and facilitate optical layer virtualization and programmability, transforming the network into more effective business enabler.

Despite the benefits from using SDN/NFV in optical networking, many improvements are still required for their control protocols (e.g., OpenFlow) to include all the required optical parameters. To this end, several studies have proposed hybrid network architectures that use the already deployed control planes like GMPLS to control the optical layer, and delegates SDN controllers to manage the high level networking

layers [50,51]. In this study we have considered GMPLS since it is adopted by almost all the industrials, and because it contains all the required protocols bricks to efficiently control optical equipment, whilst SDN is not yet mature to fully control optical networks.

1.8 Conclusion

The aim of this chapter was to present an overview of optical networks through presenting the different characteristics of their data and control planes. This overview allows better understanding how an optical network operates and at the same time identifying the dependencies between the optical and the control layer of an optical network.

In this chapter, we first recalled the evolution of optical networks and presented the optical impairments and their impact on the optical signal. Then, we discussed the importance of taking them during network design phase and in the operational phase and how this can improve the capacity and the performance of the network. Secondly, we presented the optical control plane functionalities and addressed the RWA problem in optical networking. Finally, we presented some of existing and future control plane protocols, and detailed the fundamental bricks of the GMPLS control plane protocol that is considered for this study.

CHAPTER 2

FLEXIBILITY IN OPTICAL NETWORK

THE evolution in optical transmission systems and optical switching techniques, driven by the traffic growth has given birth to the flexible technology. Indeed, the introduction of the flexibility in optical networking can improve significantly the spectrum efficiency of the network and thus increase its capacity. However, this flexibility increases also the management complexity of optical networks, impacting at the same time the optical layer and the control layer.

In this chapter, we focus on the impact of flexibility on the data and control planes of current networks. We begin first by presenting the major optical components used in optical networks, to facilitate identifying the ones that are impacted by the flexibility. Secondly, we present the changing in the optical and control plane when using the flexible optical components. Then, we explain how flexibility impacts the GMPLS control plane protocol and present some of the recent works in the literature that tries to accommodate flexibility in this protocol. Finally, we present the recent studies on flexibility benefits in terms of optical resources optimization. We conclude by presenting the migration problematic towards flexible networking and situating our work in relation to the ones realized in the literature.

2.1 Optical network components

In order to facilitate understanding how the flexible technology impacts the physical layer of optical network, we present in this section the essential components of optical networks.

2.1.1 Optical transceiver

It is the optical component that is used to send and receive optical signals. It uses a semiconductor laser diode and a modulator to generate the optical signal, and uses a photo-detector to receive optical signals and convert it to electrical domain, as well as digital signal processing element and analog to digital / digital to analog converters for the most recent transceivers based on coherent detection [1] [52]. The optical transceiver is usually built to support predefined functionalities (e.g., symbol rate and modulation format). However, with the technological improvements, it is possible to design flexible transceivers that support a high number of functionalities.

2.1.2 ROADM

The Reconfigurable Optical Add/Drop Multiplexer (or optical switch) is the most important component in optical network. Its basic function is to switch optical wavelength from one input fiber to another output fiber. It allows to configure/switch the wavelengths remotely. If no wavelength converters are deployed in the switch, then every input wavelength is the same as the output wavelength. The main components of today's optical switches are the Wavelength Selective Switch (WSS) modules. They are responsible of the switching and multiplexing/demultiplexing functions of wavelengths.

Figure 2.1 shows a simplified two degree ROADM architecture base on WSS modules. In this architecture, any incoming wavelength on a given direction (degree) can be switched to the other direction or simply dropped. Moreover, WDM multiplexer and demultiplexer are used for Add and Drop ports to facilitate insertion and extraction of wavelengths. However, in the literature many ROADM architectures exist [53]. In fact, depending on the switching requirements, the network operator can install more sophisticated architecture (e.g., higher switching degree, contentionless ROADM).

2.1.3 Optical amplifier

There are several different types of optical amplifiers, including semiconductor optical amplifiers (SOAs), erbium-doped fiber amplifiers (EDFAs), erbium-doped waveguide amplifiers (EDWAs), semiconductor optical amplifiers (SOAs) and Raman amplifiers. However, EDFAs are the most commonly used amplifiers in current optical networks, especially for long distance networks. EDFAs provide good performance, including high gain, wide bandwidth, and low noise. The EDFA is characterized by its maximum gain, bandwidth, maximum output power and noise (i.e., Amplified Spontaneous Emission/noise figure). It is used to compensate the signal power attenuation undergone over the optical spans (i.e., optical fibers) as shown in Figure 1.2. In this study, EDFA can be impacted by the flexibility in terms of optical power level (which will be treated in chapter 3).

[1] In reality, the coherent tranceiver has a very complex tranmission/reception chain design.

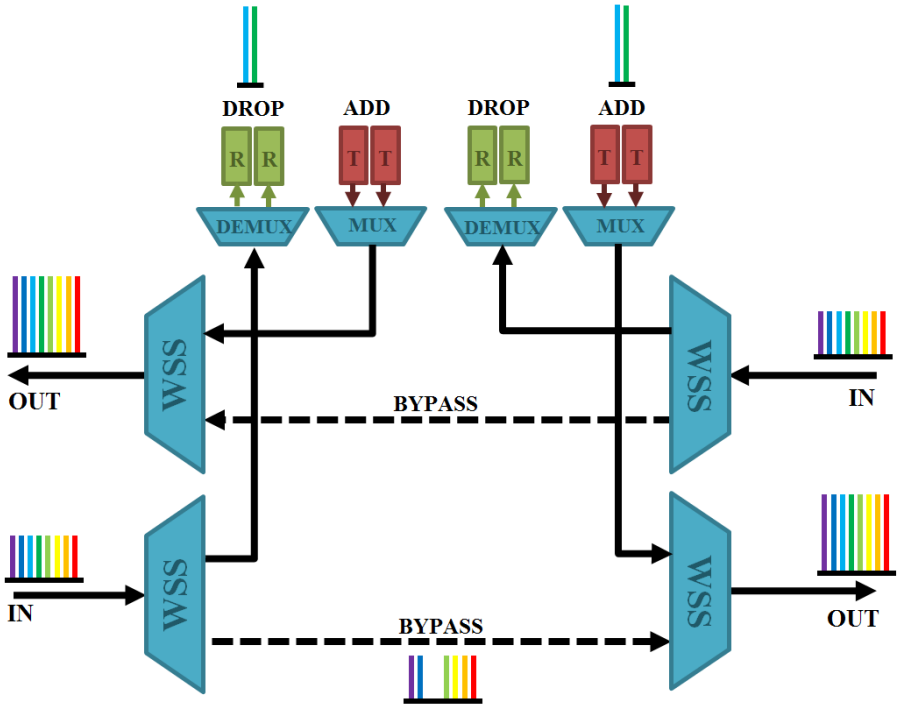

Figure 2.1: Example of ROADM architecture

Usually, a Dispersion Compensation Module (DCM) is placed between amplifier stages (for dual-stage amplifiers) in order to manage and compensate for chromatic dispersion accumulation of the optical fiber. In this work, we consider only coherent transmission systems where CD is compensated through DSP in the receiver. In fact, the recent 100Gbits/s coherent transmission systems and beyond showed a degradation in performance when DCM modules are used. Therefore, for our study, we only consider variable gain dual-stage amplifiers with no in-line chromatic dispersion compensation.

2.1.4 Optical fiber

It is the medium used in optical networking to transmit optical signal (i.e., carried on wavelength). It is usually made from silica glass. Single-mode fibers types are the most used in today's optical communication networks. The optical fiber impact the propagation of optical signals in terms of power attenuation and impairments. Therefore, depending on its fabrication properties the impact on optical signal can be low or high. Optical fiber is not impacted by flexibility; however, if it carries a high optical power, it can generate non-linear impairments.

2.2 Flexibility impact on the optical layer

Traditional WDM-based networks are based on the 50GHz frequency grid (called also fixed-grid) defined by the international telecommunication union telecommunication (ITU-T) in recommendation G.694.1 [54]. In this grid, each optical channel occupies one spectrum slot (i.e., 50 GHz) whatever its real bandwidth. On the one hand, this produces losses of spectrum resources when the occupied bandwidth by the established channel is smaller than the size of the allocated spectrum slots. On the other hand, up to recently, this 50 GHz channel spacing value was also corresponding to the bandwidth switching capabilities of optical nodes, preventing the establishment of optical channels with baud-rates larger than 40 Gbauds due to inacceptable filtering impairments. Of course, Inverse Multiplexing[2] (IM) techniques [55,56], was developed to overcome this limitation. However, these techniques are costly and also waste spectrum [57]. The need to overcome these limitations and to better use the spectrum of current optical networks and its capacity has pushed toward the improvement of three technological aspects of the physical layer of optical networks. These improvements are the development of: flexible optical switches, flexible transceivers and the flexible frequency grid.

2.2.1 Flexible optical switches

As explained in section 2.1, the optical switch enables the optical channel to bypass electrical switching when crossing any intermediate node. It allows the creation of transparent optical channels and the elimination of OEO conversion and thus reducing network cost. However, the WSS modules used in the ROADMs was limited in terms of switching (i.e., the switching grid specification is determined during the design and fabrication of the WSS) where only channels with bandwidth less or equal to 50 GHz can be switched[3]. This limitation came from WSS fabrication technology that was not capable of developing a WSS with smaller switching granularity (i.e., smaller than 50 GHz).

Therefore, in order to get flexible ROADMs, new technologies were developed such as grid-less WSS and programmable channel bandwidth filters [58], using liquid crystal on silicon (LCoS) technologies [59,60]. Indeed, the use of grid-less WSS allows dynamic switching of any optical channel with variable bandwidth (i.e., smaller or bigger than 50GHz). These improvements allow the establishment of any optical channel by fitting exactly the required bandwidth, reducing respectively the wasted bandwidth.

It is noteworthy that, other technological advances were realized to get multi-degree ROADMs and to have more flexibility in add/drop ports, offering the possibility to be colorless, directionless and contentionless [61]. In this respect, the assigned direction (i.e., switching configuration) for any optical channel can be reconfigured at

[2] It consists in dividing a high-speed data stream into multiple lower data rate streams at the transmission side, then combining these streams at the reception side.

[3] The portion of spectrum switched by the ROADM will be 50 GHz in all cases.

any time, improving the switching functionalities of optical switches and the manageability of optical networks [62].

2.2.2 Flexible transceivers

The improvement in optical switching was accompanied with an improvement in the optical transmission systems. In fact, the desire for greater system capacity was the driver to increase the spectral efficiency and the data rates of optical channels. These improvements were achieved in high-speed electronics (e.g., analogue-to-digital and digital-to-analogue converters), and in optical components such as lasers and modulators.

On the other hand, other developed techniques such as coherent detection [63] and digital signal processing have helped to get a remarkable improvement[4] in optical transmission reach and data rates (i.e., higher than 100 Gb/s). Moreover, these techniques allow for closer channels spacing, making possible to establish optical superchannels [64, 65] that consist in grouping into a single entity multiple channels, which must not be filtered except at the add drop stages (it is also called Nyquist-WDM techniques).

All these improvements have pushed toward the development of flexible transceivers [66,67] offering several degrees of flexibility in terms of symbol rates, modulation formats, bit rates and forward error correction (FEC). This flexibility allows adapting the optical channel bandwidth to fit exactly the real spectrum requirement of any traffic demand. As a result, the usage of spectrum resources is optimized, increasing the capacity of optical networks.

The flexible transceivers allow several applications such as dynamic bandwidth configuration, provisioning, and performance optimization that will be discussed in the next section. In this respect, they increase the network planning efficiency and reduce the operational costs for operators [68]. This is because a fewer number of transceivers could be used to establish all types of channels without the need to sparing equipment. Indeed, getting a fixed data rate for each possible requested data rates is very expensive and thus limits the possibility to have adaptable optical channels in a dynamic traffic context. However, increasing the degree of flexibility improve the programmability of the transceiver but at the expense of more complex and costly transceiver design.

2.2.3 Flexible frequency grid

As presented previously, the current fixed-grid (i.e., 50 GHz) defined by the ITU-T does not allow benefiting efficiently from the network capacity due to the generate bandwidth losses, pushing towards the development of flexible networking. Therefore, the ITU-T has defined a new standard grid called flex-grid [54] with finer spectrum granularity of 12.5 GHz, in order to migrate toward flexible networks. This new grid allows

[4] Especially, in terms of spectral efficiency and PMD compensation

benefiting from flexible transceivers to establish optical channels with spectrum occupation larger than 50GHz, and at the same time benefiting from spectrum saving due the finer spectrum granularity. Figure 2.2, shows an example of channel allocation in fixed-grid and flex-grid networks. The figure shows a set of optical channels with different data rates and spectrum occupation can be squeezed in order to save spectrum in flex-grid network. This flex-grid concept consists in a new definition of

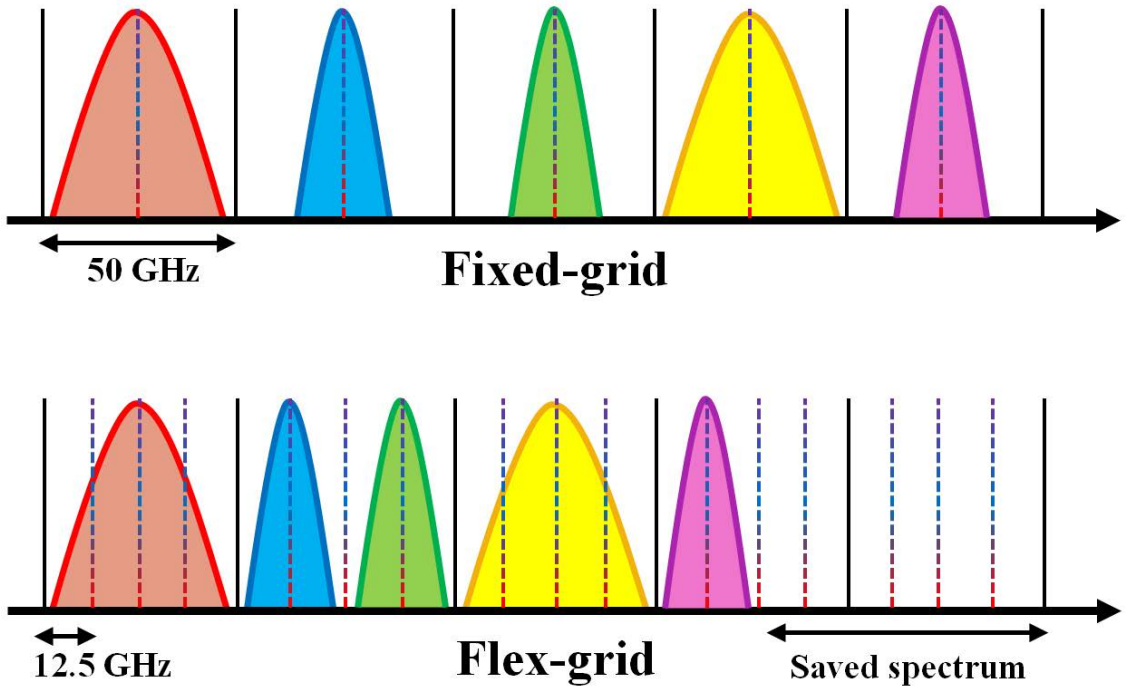

Figure 2.2: Fixed-grid versus flex-grid

DWDM grid with a set of nominal central frequencies and channel spacing. An optical channel is thus characterized by its nominal central frequency (with a 6.25 GHz step) and by the number of occupied spectrum slots (proportional to 12.5 GHz). The nominal central frequency of any channel is determined by the following formula: $f = 193.1 + n \times 0.00625$ THz, where n is a positive or negative integer including 0; and the bandwidth by $m \times 12.5$ GHz, where m is an integer greater or equal to 1.

In the literature, several studies [69–71] were realized in order to determine the spectrum slot granularity that allows benefiting at most from the flexibility. It has been shown that the choice of 12.5 GHz slicing is the best compromise between operational complexity, cost, flexibility and physical limitations (such as the cost of producing narrow optical filters and WSSs).

2.3 Flexibility impact on the control plane

The introduction of the flexible technology in optical networks has an important impact on the control plane and on the management of optical resources. This impact is translated into a complexity in terms of the routing algorithms used and connection provisioning. Indeed, the connection establishment in flexible optical network requires extensions to the signaling and routing control plane protocols, in order to collect additional physical parameters and to perform improved path computation.

In the following we present the impact of flexibility on the RWA problem, impairment estimation and we present the realized work to improve GMPLS control planes protocols in the standardization bodies.

2.3.1 Impact on path computation and impairment estimation

2.3.1.1 RWA vs RSA

In fixed-grid WDM networks, the conventional RWA algorithm is used to compute an optical path and assign a wavelength between two optical nodes. As the flex-grid concept is introduced in optical networks, new challenges are posed on the networking level. Indeed, the RWA algorithm of traditional WDM networks is no longer applicable and thus it is transformed to a routing and spectrum assignment algorithm (RSA). The main difference comes from the change in the way of switching in optical nodes, where it is based now on the frequency slot rather than on wavelength. In this respect, the RSA algorithm consists in finding an optical path between two nodes and a set of available spectrum slots (i.e., multiple of 12.5 GHz) that are continuous and contiguous over the computed path (in the case of transparency).

2.3.1.2 Spectrum fragmentation problem and spectrum assignment policy

Usually an established optical channel occupies several optical links between the source and destination nodes. In fact, due to the transparency constraint, this channel should occupy the same wavelength over these links. In flexible networks, this constraint is conserved and the optical channel should occupy the same spectrum slots over these links. However, the continuity constraint, in addition to the use of a mixture of optical channels with different spectral occupation, creates what we call spectrum fragmentation.

Indeed, during the establishment of an optical channel two types of fragmentation could appear: horizontal and vertical fragmentation. Figure 2.3 shows an example of these two types of fragmentation that could appear in flex-grid networks. In the example, we consider four optical nodes (A, B, C and D) connected by three optical links, and we suppose that two types of optical channels having different spectral occupation (37.5 GHz and 50 GHz) are established between the optical nodes. The horizontal fragmentation appears when there are non-continuous available spectrum slots over the optical links constituting the optical path. For example, this occurs when trying to

establish a 50 GHz channel between the node A and node D of Figure 2.3, since there is no continuous 50 GHz spectrum slots available over all the optical links between node A and node D. The vertical fragmentation appears when the combination of channels with different spectrum occupation creates unusable spectrum blocks (i.e., spectrum blocks that are not sufficient to satisfy the smallest connection request). This occurs for example over the link BC of Figure 2.3 where a spectrum slot of 12.5 GHz is available but not usable since the smallest connection request occupy 37.5 GHz.

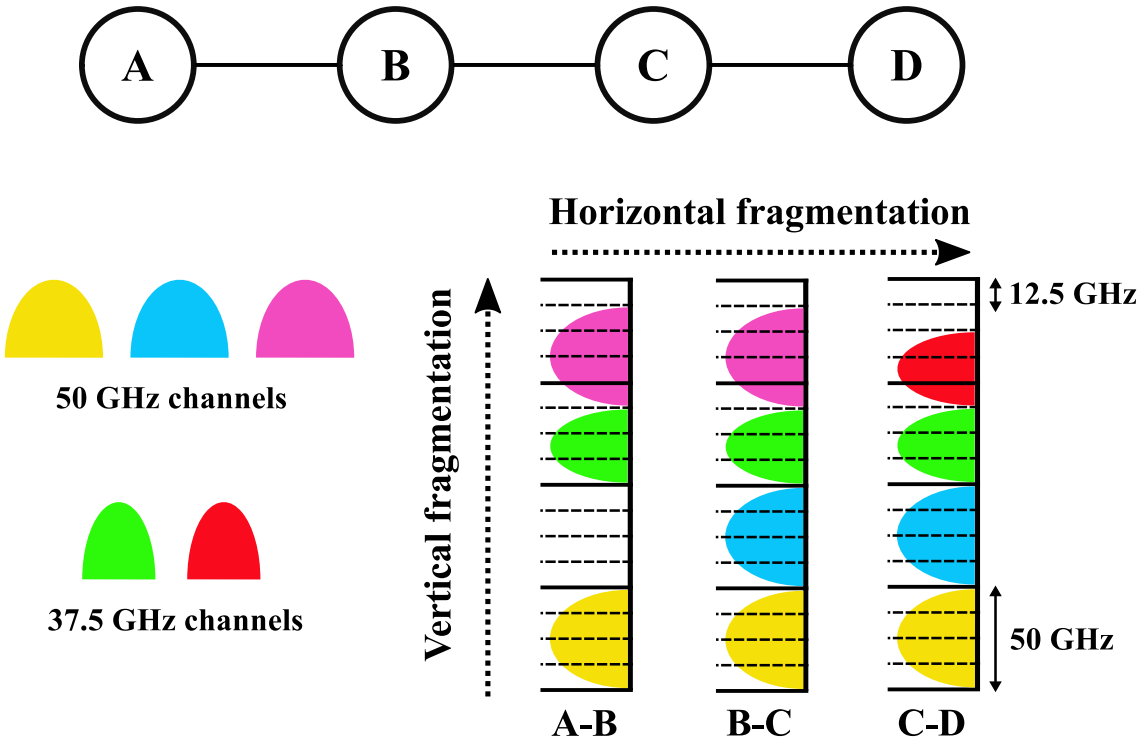

Figure 2.3: Example of horizontal and vertical spectrum fragmentation

In flexible networking, the spectrum fragmentation is an important problem since it reduces the benefits of the flexibility and thus limits the capacity of the optical networks. Indeed, the problem will become more important in dynamic scenarios where connection demands arrives without a prior knowledge, making difficult to predict the best way to establish them without creating fragmentation. In this respect, several dedicated spectrum defragmentation mechanisms have been developed in the literature [72–77]. However, these techniques do not guarantee a complete resolution of this problem.

In such a context, there are two ways to solve this problem. The first method consists in rerouting and reallocating the spectrum of the established channels in such a way the isolated spectrum slots are reduced. To this end several techniques like push-and-pull [77], make-before-break [78] and others [79] are used. However, the efficiency of these techniques depends on the deployed transceivers and on their capability to

guarantee no traffic disruption during network operation [5]. The second method is to develop a spectrum assignment policy that reduces the fragmentation as the one developed in [80].

In [32, 81], several spectrum assignment policy (e.g., First-fit, Random-fit, Least-loaded) were compared in terms of complexity and blocking probability. It has been demonstrated that the complexity of routing algorithm and the effect of fragmentation could be significantly reduced/increased depending on the spectrum assignment policy used. This makes from the spectrum assignment policy an important block in the RSA algorithm, since it impacts the performance and the capacity of the network.

In this work, for simplicity reasons, we use the first-fit spectrum assignment algorithm in order to find a set of available slots over an optical path. This algorithm consists in selecting the first available spectrum slots that satisfy the connection request.

2.3.1.3 Physical feasibility of optical channels

Usually, after the computation of an optical path between two nodes, the physical feasibility of the optical channel to establish is evaluated. This evaluation is based on an impairment estimator such as the ones mentioned in chapter 1. This estimation is usually performed considering a fixed set of optical transceivers with predetermined signal characteristics (e.g., modulation formats and bit rates) and performances (e.g., OSNR threshold). In fact, the selected characteristics for an optical channel allow determining the required OSNR threshold at the receiver side. Indeed, the OSNR and CD thresholds for example depend on the used baud rate, modulation format, signal power and other parameters [82]. Therefore, another degree of complexity is added to the physical feasibility estimation with the improvement in transceivers flexibility. This complexity is translated in form of impairment estimator (more complicated) that is capable of determining impairment thresholds depending on transceiver configuration parameters.

In summary, in flexible networks, the possibility of automatically establishing an optical channel with variable degree of flexibility in terms of optical power, symbol rates, modulation formats, FEC and channel width, requires an improved impairments estimator. This estimator should take into account the impact of each one of these parameters on the signal quality to determinate the feasibility of the optical channels. However, some parameters such as baud-rate and channel spacing impact the spectral occupation of the optical channel. Therefore, the complexity of the RSA algorithm is also increased. This is because RSA algorithm has to make a trade-off between channel performance and bandwidth occupation in order to satisfy the connection request, while minimizing the consumption of network resources.

[5] These technics are tranceivers dependent and introduce additional management complexity.

2.3.2 Impact on GMPLS control plane protocols

As mentioned before, the emerging flexibility in optical networks has introduced new challenges around efficient bandwidth provisioning and network automation. It had an impact on the optical control plane, requiring the development of new RSA algorithms as well as appropriate extensions to the control and management protocols. In this respect, there was a dedicated effort realized in standardization bodies to the development of control plane solutions to support the capabilities offered by the flexible networking.

The GMPLS control plane is one of the concerned control plane solutions where new standards and protocols drafts have been developed in [83–86] to take into account the different degree of flexibility presented in Sections 2.1 and 2.2. These standards and drafts concern specifically the two main bricks of the GMPLS control plane: the OSPF-TE and RSVP-TE protocols. They propose extensions to collect information such as link available spectrum slots, physical impairments, modulation formats and OSNR parameter.

Additionally the flexibility can introduce a scalability problem for GMPLS networks (i.e., in case of large networks) due to the high number of parameters to take into account. Indeed, this will results in a bigger OSPF-TE databases with higher number of information to synchronize and thus raising potentially a stability and latency problem. In this context, a framework was proposed in [87] to suggesting different approaches to collect network information and to perform impairment-aware RWA algorithms. These approaches are based on the combination between OSPF-TE and RSVP-TE where some optical parameters could be collected via signaling and thus eliminates the need to distribute them through OSPF-TE [88]. The goal was to improve the performance and the flexibility of GMPLS protocol.

Recently, several standards and studies [89–91] have addressed the issue of the increasing number of optical parameters and the multi-domain interoperability. They proposed the design of a GMPLS-based control plane with Path computation element (PCE) [92]. This PCE is a centralized entity that executes RSA algorithm though maintaining a centralized TED [93] that aggregates all the required optical parameters. Moreover, it allows performing path computation and, possibly, wavelength, modulation, FEC assignment [94, 95] and thus providing efficient routing and resources allocation. The reason behind this proposition was to increase the performance of GMPLS and overcome some limitation in optical networking (e.g., intensive computation, limited visibility of optical nodes, absence of TED in each node). Indeed, sometimes optical nodes do not dispose sufficient resources to make intensive computation, or they do not have a full visibility of the network (e.g., multi-domain), or even they do not dispose of traffic engineer databases (TEDs). Therefore, PCE can be a suitable solution to this kind of limitations.

All these standards and works show the capability of GMPLS protocol to handle the flexibility in optical networking (which is the reason behind deploying it in the most networks) and explain the reason behind considering it for our study.

2.4 Network margins and resources optimization

As mentioned previously, the first concern for optical operators is to increase their network capacity to follow the traffic growth while at the same time reducing the costs. Therefore, a set of technological advances (i.e., the flexibility in optical components) were realized to achieve this goal as presented in Section 2.2. Indeed, these advances in optical layer technologies coupled with enhanced control plane solutions, provide the basis to optimize the overall performance of the network and thus increase its capacity.

In fact, current optical networks are designed in such a way it maximizes the capacity of optical links and the reaches of optical channels, resulting in an overdimensioning in optical resources and in network margins. However, during network operation not all of these margins and resources are necessary. Sometimes, it is possible to optimize them (thanks to flexibles technology) in order to increase network capacity [2, 96].

In the following, we begin by explaining these margins in order to facilitate understanding the possible optimization methods. Then, we present some of the recent works in the literature on this topic.

2.4.1 Network margins

During the planning and the design phase of optical networks, several types of margins are considered to ensure the good operation of the network from the beginning to the end of its life. These margins can be classified into three categories: system margins, unallocated margins and design margins. Figure 2.4, illustrate the set of network margins and their evolution in time.

2.4.1.1 System margins

System margins represent the set of precaution (i.e., OSNR penalties) to protect network from time varying condition. They take into account for two types of impairments: fast varying impairments such as PDL and slow varying impairments such as the aging of optical components (e.g., fibers, amplifiers, transceivers) aging and nonlinear impairments (e.g., due to the increasing in link optical power level after the establishment of optical channels).

2.4.1.2 Unallocated margins

These margins represent the difference in the maximum transmission reach of the transceivers and the real distance traveled by the optical channel. In other words, these margins account for the excess in performance when the optical channel can work with less transmission performance. These margins are not known in advance, since they depend on the traffic demands, on the deployed transceivers and on the selected transmission parameter for the optical channel (e.g., modulation format, bit-rates, etc.).

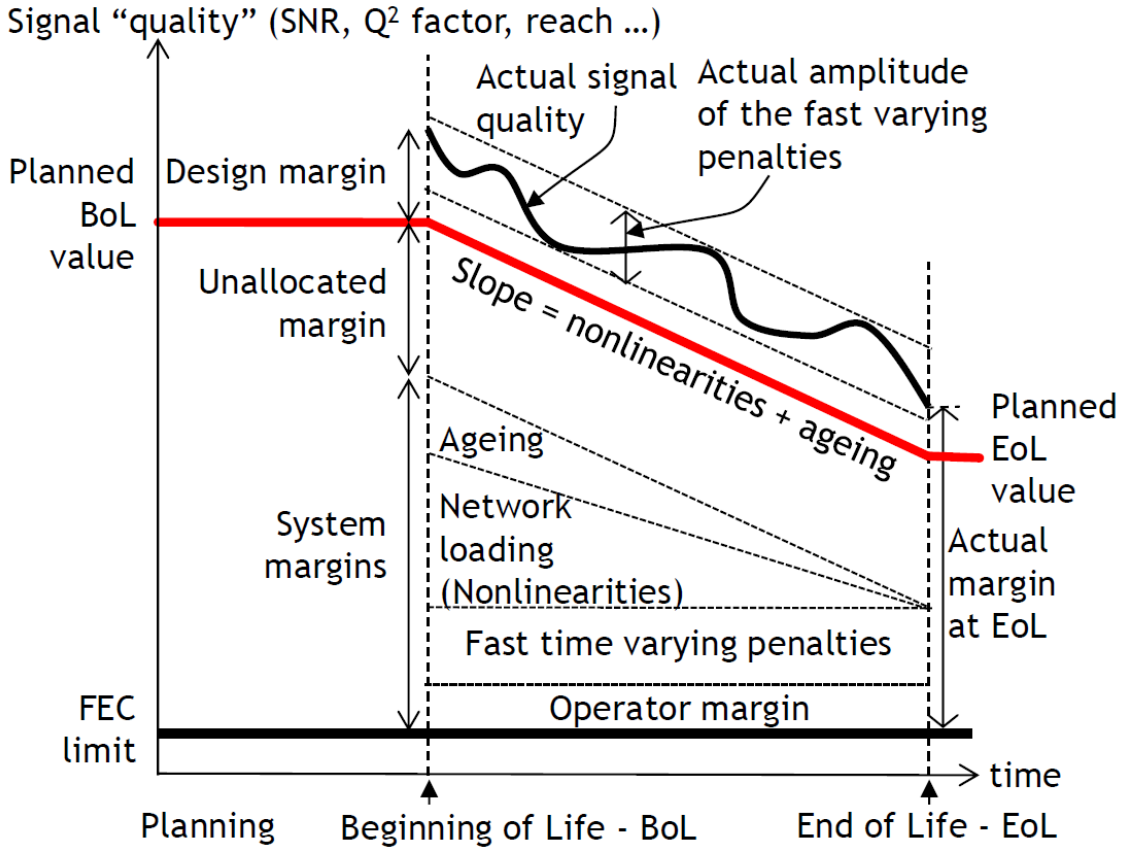

Figure 2.4: Margins and their evolution in a transport optical network [2]

2.4.1.3 Design margins

These margins concern the link design phase where an optical estimator (i.e., quality of transmission tool) is used to account for the optical impairments. Two reasons are behind these margins: inaccuracy of the impairment estimation model and inaccuracy of model input parameters. These margins cannot be known in advance without performing a measurement in the field, because they represent the difference between the estimated channel quality and the real one. In fact, these margins are set by operators to guarantee in all circumstance the operation of the established optical channel. Benefiting from these margins require improving the accuracy of impairment estimators as discussed in chapter 1.

2.4.2 Resources optimization

In the literature, several studies [97–100] tried to use network margins to increase network capacity. They have proposed optimization techniques based on different transmission parameters. Their goal was to maximize the quantity of transmitted data by optimizing the use of optical spectrum, taking advantage from transceivers flexibil-

ity [67, 101] and network margins [2, 96]. However, in this work, we consider only the unallocated margins since they are related to the introduced flexibility in optical networks. System and design margins are out of the scope of this thesis.

In fact, to optimize unallocated margins, several adaptation techniques could be applied. These techniques are: channel spacing, modulation format, baud/bit rates, coding scheme, and optical power adaptation. The first technique presented in [102], consists in reducing channel spacing by sacrificing the reach of the channel for increasing its spectral efficiency. The second one is the adaptation of the modulation formats [103, 104], where applying a higher-order modulation formats (when baud-rates are fixed) allows increasing the spectral efficiency of optical channels and thus increase the capacity of the fiber. The third technique is the baud rates adaptation [105–107] which is related the previously described technique in terms of acting on the spectral efficiency of channels. The fourth one is coding scheme adaptation also called FEC adaptation. Indeed, today the ratio between the amount of FEC and payload is fixed, but this could be made adaptive to enable greater distances or higher data rates [108–110]. The last technique is the optical power adaptation of optical channels [99, 111], where adapting their powers can improve the overall performance of optical links [112].

In summary, each of these techniques has an impact on the reach, OSNR and spectral occupation of the optical channel. Therefore, depending on the optimization objective (i.e., spectrum occupation reduction, performance improvement or capacity increase), one or a mixture of these techniques can be used to achieve the required objective [100, 113–116].

2.5 Conclusion and motivations

In this chapter, we addressed the impact of flexible technology on the optical and control plane of optical networks. Firstly, we showed how flexibility allows reducing the spectrum occupation of the existing channels giving the possibility to add new ones over the same optical bandwidth, and thus increasing the capacity of the network. Secondly, we discussed how this flexibility introduces additional complexity to control plane protocols, requiring new protocols extensions and path computation algorithm to deal with the high number of parameters to control. Finally, we presented the different types of network margins and cited some work in the literature that benefits from the flexibility to exploit these margins in order to increase network capacity. We have particularly focused on the unallocated margins and presented the different techniques that allow exploiting these margins.

Until now, all studies in the literature have considered only the optical spectrum as a limitation to the increase in network capacity. In this thesis, and unlike the current paradigm, we consider the optical power limitation over network links additionally to the spectrum one. Indeed, the reduction in spectrum occupation offered by the flexible technology increases the number of established channels over network links, increasing in turn their optical power level. In fact, these links where designed to support cer-

tain power levels (depending on the planned channel number) and thus the excess of optical power can possibly saturate the existing optical amplifiers deployed over links.

As one most important goal for operators is to increase the capacity of their networks while reducing their costs, in this thesis, we deal with migration from fixed-grid to flex-grid networks when keeping in use the existing infrastructures (i.e., optical fibers and amplifiers). More specifically, we study this migration by evaluating the optical power levels over network links that could possible saturate some optical amplifiers. We propose a solution to this problem, by taking benefits from the unallocated margins to reduce the optical power levels, while at the same time increasing network capacity. The practical feasibility of this solution is addressed by proposing protocol extensions and new path computation algorithms that take into account the power information. Our goal is to demonstrate that the migration to flexible networks is possible without the need to re-design or to replace the existing network infrastructures.

CHAPTER 3

OPTICAL POWER CONTROL IN GMPLS CONTROL PLANE

INTERNET services (e.g., video conferencing, cloud services, and video streaming) and consequently traffic demands are continually increasing, leading to huge traffic growth in the core optical network. Therefore, increasing optical networks capacities is a permanent need for operators to follow this traffic growth. However, since the deployment of new optical fibers is still expensive, network operators are pushing to exploit the totality of their network capacity by optimizing their optical resources and thus postponing the deployment of new optical infrastructures. This exploitation requires new technologies and flexible equipment that are able to handle different types of optical channels, from small to extremely high data rates.

In contrast, the fixed-grid technology is no longer qualified to handle the increasing data rates of optical channels. At the same time, the 50 GHz ITU-T grid, due to its fixed-spectrum spacing, leads to spectrum inefficient usage when the spectral bandwidth of the optical channels is smaller than the size of the allocated 50 GHz slot. The recently proposed ITU-T recommendation G.694.1 for the flex-grid optical network has defined a new spectral grid standard for WDM applications, bringing the solution to this spectrum wastage. This flexible spectral grid has a smaller slot granularity of 12.5 GHz, with nominal central frequency on a grid of 6.25 GHz spacing, allowing better spectrum efficiency compared with the current 50 GHz fixed-grid.

This recommendation has transformed the flex-grid into a promising technology that is capable of following traffic growth and various traffic demands. Flex-grid efficiently uses available spectrum resources, especially when associated with novel coherent transmission technologies and advanced modulation formats. Moreover, since flex-grid technology allows the reduction of channel spacing, it offers the possibility to

create new optical channels over the saved spectrum. However, increasing the number of optical channels increases the optical power injected in optical links, which may not be acceptable in some of the already deployed amplifiers.

Indeed, this increase in optical power, when switching from fixed-grid to flex-grid technology, has an impact on the legacy optical amplifiers. It could cause amplifier saturation and dramatic performance degradation for the already established channels (probably leading to transmission failure). Therefore, there is a need to replace the existing amplifiers with new ones that have bigger output powers. However, the deployment of such amplifiers require the re-design and service interruption of optical links generating a high cost for operators, in addition to the cost of purchasing new optical amplifiers.

In this respect, we demonstrated in [117] that, if we control the power of the optical channels, it is possible to keep the existing amplifiers when migrating to flex-grid technology. Moreover, this power control allows 10% of cost reduction with respect to a conventional fixed-grid, without mentioning the saved cost through avoiding the purchase and deployment of new amplifiers and the service interruption of the optical links.

3.1 Related works

In the literature, several studies have focused on developing accurate physical impairment models over uncompensated links [118–121]. These studies have demonstrated the existence of an optimal optical channel power that leads to minimum impairment generation and thus achieves better transmission performance (i.e., maximum reach/maximum OSNR). Figure 3.1, shows an illustration of this optimal channel power, where the variation of channel OSNR is plotted as a function of its optical power.

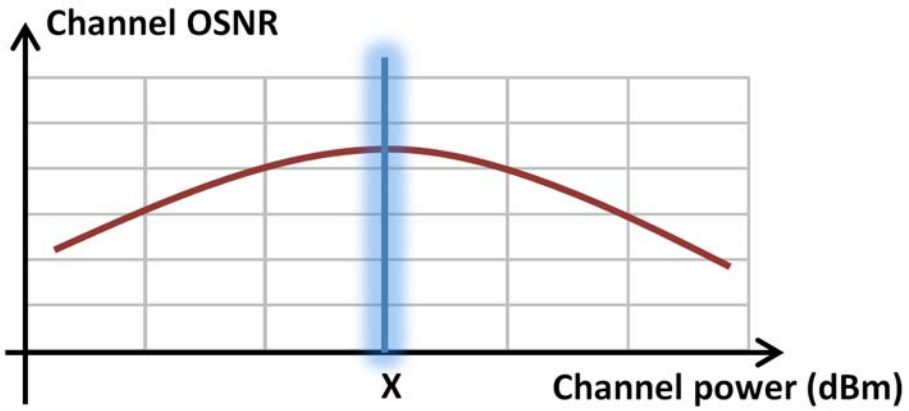

Figure 3.1: Channel OSNR versus channel power

In general, during the offline system design, every physical link between two ad-

jacent optical nodes is designed to support a maximum capacity while maximizing the optical reach for all channels through the use of this optimal power per channel (usually different optimal power per link, which depends on the length and the attenuation of the optical spans constituting the link). However, the resources provisioning for the worst case (i.e., full capacity and maximum transmission reach) consequently leads to power resource over-dimensioning with considerable unallocated margins on some links, due to the non-uniform distribution of traffic demands and their required reaches. Indeed, during network operation optical channels usually traverse different distances depending on the crossed optical path (i.e., depending on the number of crossed links). Therefore, they do not need the maximum optical performance, especially the short reach ones since they undergo less degradation.

In this respect, many recent studies focused on improving link performances (i.e., minimizing the nonlinear interference effect) and thus increasing network throughput by adjusting channel launch power and optimizing spectral resources using several modulation formats [97,99,114]. Others in [122,123] focused on adapting launch powers depending on required data rates and the reach in order to reduce overall network cost and saving the number of signal regeneration.

In fact, the practical feasibility of such adaptation has not yet been proposed, more precisely from a control plane point of view. All these studies, in addition to those dealing with the control plane of flex-grid networks [95, 124], have only considered the spectral resources as a limitation without taking into account the power resource limits of optical links (which depend on the deployed amplifiers). They proposed a control plane algorithm that only takes into account the transparent spectrum assignment and the physical feasibility of the optical channels. However, despite the demonstrated benefits from controlling the power of optical channels, there is no routing algorithm suggested until now with suitable control plane architecture, in order to allow the practical implementation of such channel power adaptation.

3.2 Contributions

For all these mentioned reasons, in this chapter, we take into account optical power resources limits in addition to the spectral ones. Moreover, we propose the practical feasibility of such power control through developing a power and impairment aware routing algorithm, in addition to protocol extensions making the relationship between planning and control plane (in operational phase). The proposed control process adapts the power of optical channels to their minimum required performances (adaptation to the real physical reach). This adaptation enables optical power margins to be used for overcoming the power limitations of amplifiers when increasing the number of channels over network links.

In fact, to study the power increase over optical links, a link design method is first proposed in order to evaluate the acceptable power levels in optical amplifiers. Then, a new path computation algorithm is developed for a distributed GMPLS-based con-

trol plane. Original protocol extensions are proposed to RSVP-TE and OSPF-TE to collect new physical parameters and to enable the use of the power control process. The performance of the novel scheme is demonstrated with simulations by evaluating the cumulative blocking ratio (CBR) and network throughput. Moreover, we produce additional performance evaluations (for instance, the effect of the number of shortest paths) and enrich the work with a deeper analysis of the blocking reasons for the simulated scenarios.

This chapter is organized as follows. Section 3.3 presents an overview of optical link design issues, briefly presents our link design method, and introduces the link power margin. Section 3.4 presents our power control process. Section 3.5 presents our new path computation algorithm. Section 3.6 presents our OSPF-TE and RSVP-TE protocol extensions required to implement the power control process in a GMPLS control plane. It also presents the signaling mechanism through a channel connection establishment example. Section 3.7 presents simulated scenarios and results, in addition to blocking reasons analysis. The conclusion and future works are presented in Section 3.8.

3.3 Optical link design and power limitations

We consider a set of successive optical spans constituting an optical link l between two optical nodes (e.g., reconfigurable optical add-drop multiplexers [ROADMs]), as shown in Figure 3.2. The optical link design consists in choosing a set of optical amplifiers that can compensate for span losses and simultaneously support the aggregated optical power of all the channels planned for that link, while seeking maximum optical performance. The link design has the objective of maximizing OSNR, through minimizing linear and nonlinear effects. The complexity of the process arises in particular because of the contradictory objectives of amplifiers; they must compensate for link span losses, satisfy the aggregate optical power for all optical channels sharing the fiber, and simultaneously minimize the amount of generated noise.

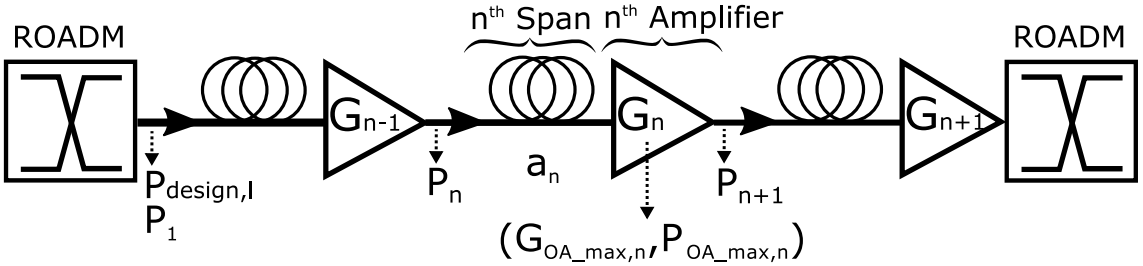

Figure 3.2: Simplified representation of an amplified link (succession of a fiber span and optical amplifier) between two ROADMs.

In general, optical links in fixed-grid WDM networks are designed to support a given number of channels $N_{channel\_max}$ (e.g., 80 channels with 50 GHz of spectral occupation for 4 THz of optical bandwidth). This $N_{channel\_max}$ is equivalent to an aggre-

gated optical power that, in turn, depends on the computed per channel optimal power during the design step. Usually, each link l in the network has the same $N_{channel\_max}$, except when the network operator has a particular need over certain links. However, to ease our study, without any loss of generality, we assume that these numbers are identical all over the network. It is important to note that we do not necessarily have for every link l the same channel optimal power because it depends on the physical characteristics of each link (i.e., span attenuation, amplifier configuration).

The use of flex-grid technology over these optical infrastructures may increase the number of channels in some links and thus their optical power levels (e.g., up to 106 channels with 37.5 GHz of spectral occupation in 4 THz of bandwidth and up to 128 channels in 4.8 THz of bandwidth). In fact, if the number of channels (i.e., the aggregated optical power for the $N_{channel\_max}$ channels) is not controlled and limited, there may be some risks of power saturation in the amplifiers that are already close to their maximum output power (i.e., power saturation limit) leading to strong performance degradation on these links.

Inversely, if the number of channels is limited to $N_{channel\_max}$, the spectrum gain enabled by flex-grid technology cannot be exploited. However, replacing optical amplifiers with new ones having bigger output power is a potential solution, although it is costly because it requires full redesign of the links and possible purchase of new amplifiers as well as interruption of the link to set up the new amplifier configuration.

In this chapter, we propose making the information of optical power available to the control plane to benefit from the flex-grid spectrum gain promises, while keeping the in-place amplifiers. However, this requires fine knowledge of the maximum power allowed in each link, which, in turn, requires understanding the link design step and the limitations of optical links.

3.3.1 Design method

In order to evaluate our power control process, we must precisely model the link design step. The design of optical links (i.e., selection/configuration of optical amplifiers) is an important phase to determine optical resource limits over every optical link. To this end, we have developed a link design method, which we presented in [117, 125, 126], taking advantage of the optimization strategy presented in [21]. Surely, any other design method could be used instead to determine these power resources. In this case, the estimator of the physical feasibility used in the control plane will be different because it depends on the design method.

The LOGON strategy proposed in [21] consists in performing local optimization of the OSNR and nonlinear impairments at the span level, leading to a global OSNR optimization over all the links of the network. It proposes applying an optimal power spectral density (PSD) on every channel at the input of every span to guarantee maximum transmission performance over the channels. This power is computed using span and amplifier characteristics by applying Equation (6) in [21]. Eq.(3.1) represents the aggregated optical power that corresponds to this power spectral density at the n^{th} span

input for $N_{channel\_max}$ channels having R_s spectrum width each, where h, μ, F_n, and $\rho_{NLI,n}$ stand for Planck's constant, the electromagnetic wave frequency, the NF of the n^{th} amplifier, and non-linear effect contribution respectively [21].

$$P_n = \left(\frac{h\mu F_n}{2\rho_{NLI,n}}\right)^{\frac{1}{3}} \tag{3.1}$$

$$F_n = F_{1,n} + \frac{F_{2,n} D_n G_{OA\_max,n}}{G_n^2} \tag{3.2}$$

$$G_n = a_n \frac{P_{n+1}}{P_n} \tag{3.3}$$

Our link design method consists in choosing the optical amplifier that satisfies the link design constraints (maximize OSNR, minimize non-linear effect, satisfy $N_{channel\_max}$ power, and compensate for span loss). Each amplifier NF is computed using Eq. (3.2), and varies according to the adjusted gain G_n. We use variable gain dual-stage amplifiers without mid-stage access where $F_{1,n}$ and $F_{2,n}$ are the NF for the first and the second stage, respectively, and D_n denotes the power ratio for both stages to account for the difference between preamp and booster performance. Eq. (3.3) computes the desired amplifier gain (G_n) to compensate for span loss, where a_n is the attenuation of the n^{th} span, P_n is the power at the input of the n^{th} span, and P_{n+1} is the power at the output of the G_n optical amplifier as shown in Figure 3.2.

We replace F_n in Eq. (3.1) by its value in Eq. (3.2), and then the P_n in Eq. (3.1) by its value of Eq. (3.3) to attain a third degree polynomial equation represented by Eq. (3.4), which we solved analytically. The solution of this equation in Eq. (3.5) gives us the value of the gain that should be adjusted in the n^{th} amplifier in order to obtain minimum linear and non-linear impairment generation.

$$h\mu F_{1,n} G_n^3 + h\mu F_{2,n} D_n G_{OA\_max,n} G_n - 2\rho_{NLI,n} a_n^3 P_{n+1}^3 = 0 \tag{3.4}$$

$$G_n = \sqrt{\frac{4F_{2,n} D_n G_{OA\_max,n}}{3F_{1,n}}} \times sinh\left(\frac{1}{3} asinh\left(\frac{\rho_{NLI,n}(a_n P_{n+1})^3 \sqrt{\frac{27F_{1,n}}{(F_{2,n} D_n G_{OA\_max,n})^3}}}{h\mu}\right)\right) \tag{3.5}$$

Our link design is performed from the last span to the first one; the amplifier that can satisfy both required gain (G_n) and optimum power (P_{n+1}), while achieving the smallest NF is selected. If none of the amplifiers can satisfy these requirements, the one with the closest maximum power (P_{OA_max}) is chosen. The difference of the required power is subsequently recovered by re-tuning the gain(s) of the following (downstream) amplifier(s).

In summary, this link design method computes amplifier gains while respecting optimal powers to be set at the input of optical spans, thus leading to link OSNR optimization. After this link design phase (or any other design phase), every link has its own

set of amplifier types with various power and gain settings, which subsequently determines the power resource limits and the quality parameter of the link (i.e., OSNR).

It is important to note that amplifiers are used in a fixed gain mode, which means that, once the design phase is finished, amplifier gain settings are never changed. Furthermore, to efficiently manage optical power resources, many essential parameters should be available to the control plane of the network. Therefore, in order to understand these parameters, we study the existing power resources available over the optical links after the application of our design method.

3.3.2 Link power margin

Let $N_{channel\_max}$ be the maximum number of channels per link. Let $P_{design,l}$ (by definition equal to P_1), as shown in Figure 3.2 be the input optical power designed for the link l having $N_{channel\_max}$. The difference of characteristics between all spans in terms of the losses, non-linearity coefficient, and length leads to the use of various types of amplifiers having different characteristics in terms of maximum gain (G_{OA_max}), maximum power (P_{OA_max}), and NF. This difference results in different $P_{design,l}$ and thus $P^{opt}_{channel,l}$ (individual optimum channel power over link l) over every link l and in different span optimum input powers (i.e., amplifier output powers). This power variation is given by Eq. (3.3). Therefore, there may remain a power margin ($P_{OA\_margin,n}$) over the n^{th} amplifier such that

$$P_{OA\_margin,n} = P_{OA\_max,n} - P_{n+1}, \tag{3.6}$$

where $P_{OA\_max,n}$ is the maximum power of the n^{th} amplifier. Figure 3.3 shows an example of power levels (P_{OA_max},P_{OA_margin}) over link l amplifiers, where different P_{OA_margin} values exist in the different amplifiers.

We define as link power margin $P_{margin,l}$, the minimum power margin (minimum P_{OA_margin}) that exists over the amplifiers of the link l:

$$P_{margin,l} = min_{n\in\aleph_l}\{P_{OA\_margin,n}\} \tag{3.7}$$

where $\aleph_l$ is the set of amplifiers of the link l. Therefore, the maximum optical power that can be applied at the input of link l without saturating any amplifier is

$$P_{max,l} = P_{design,l} + P_{margin,l} \tag{3.8}$$

In case there is no $P_{OA\_margin,n}$ in one of the amplifiers of the link l, the $P_{margin,l}$ is then equal to zero, and no additional power can be used over that link.

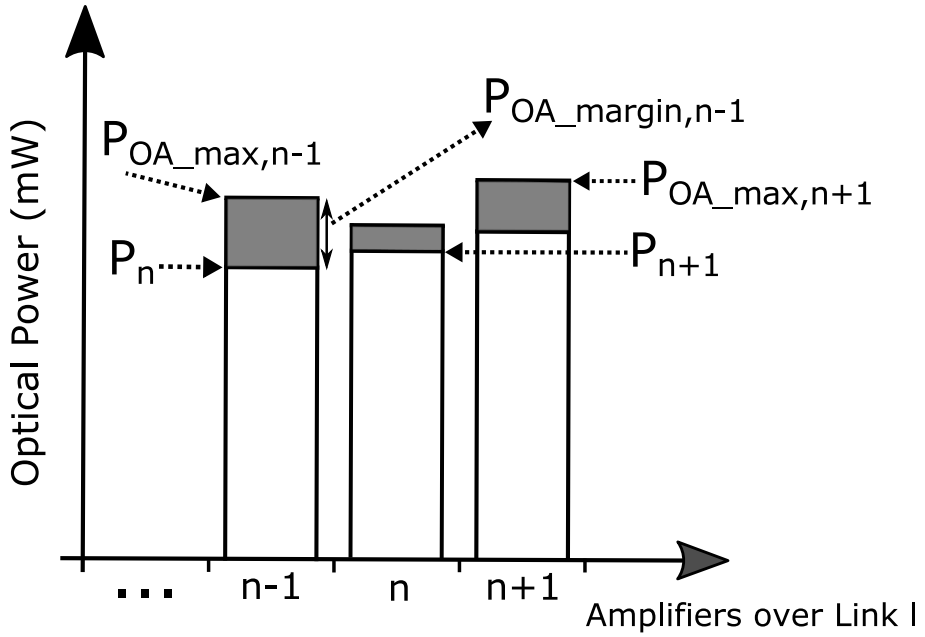

Figure 3.3: A simplified representation of optical power at amplifier level.

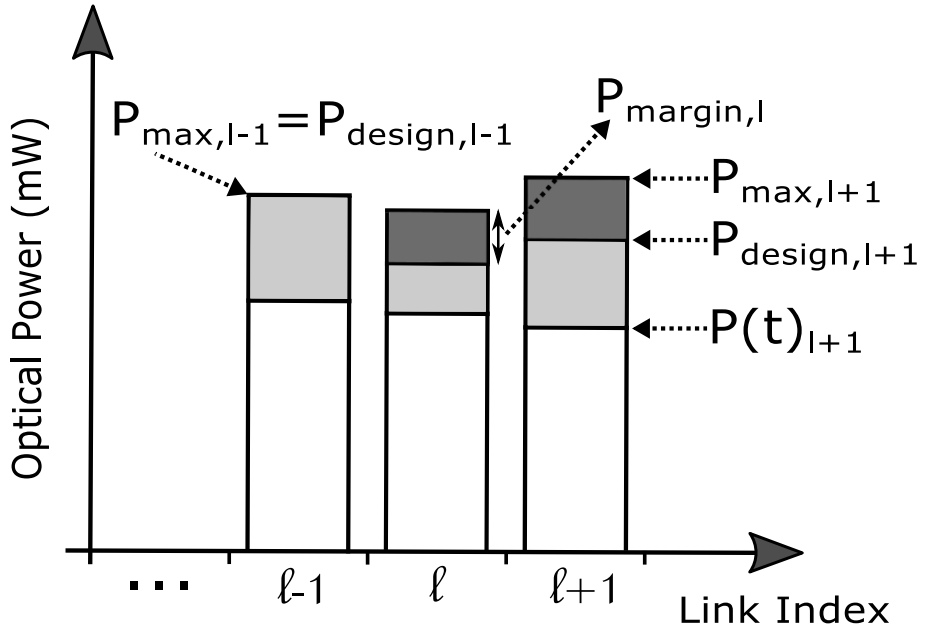

Figure 3.4: Simplified representation of power levels over optical links.

We define $P_l(t)$ as the current power at a moment t over the link l. It is a function of time t because it depends on the number and on the power of the established channels at time t. Figure 3.4 illustrates the different power levels that can exist over the optical links of a network, where l is the link index. For every link a $P_{max,l}$ power is supported, where $P_{max,l}$ is greater than $P_{design,l}$ of the link (by construction). It is exactly equal

to $P_{design,l}$ when no power margin exists. As shown in Figure 3.4, the links l and $l+1$ have strictly positive margins; therefore, additional optical resources may be used over these links. Inversely, the link $l-1$ does not have power margin; therefore, no additional power can be used over this link. Our utilization of power margin complements recent works on design margins and system margins, as in [96, 127, 128]. In these works, the power control aspect was neglected. Here, we specifically focus on the control of the optical power.

3.4 Optical power control

Optical networks are made of optical nodes (ROADMs) interconnected with optical links. In order to achieve maximum network performance, every optical link between two ROADMs is usually designed to support optimum performance independently from other links. With this design method, every link has its own set of optimum span powers and amplifier settings. The maximum performance is ensured by setting the optimum power for any new optical channel (i.e., $P^{opt}_{channel,l}$ [21]). This kind of policy does not consider that channels may require variable reaches; thus, some channels may not always need the maximum performance (e.g., the power of the channel with the shortest path does not need to be set to its optimal value to reach the destination). As a result, some transmission margins are wasted.

Channel performance and its optical power are tightly linked. Reducing the optical power from its optimum value to a lower value reduces the performance and thus adapts the channel to the required reach. This appears as an interesting method to save some optical power in a flex-grid network and to avoid wasting the transmission margin. More precisely, we expect that this power adaptation will allow the use of the transmission margin to increase link capacity in terms of channel numbers.

To perform the power control, we now propose exploiting the performance estimator of Eq. (3.9) of the LOGON strategy in [21]. This equation estimates the OSNR (including nonlinear effects in the form of nonlinear interference) of a lightpath p at the receiver side. The $OSNR_{est,p}$ value of the lightpath p, which is made of m successive links, is the inverse of the sum of the inverse OSNR of each link [21]. If the estimated OSNR ($OSNR_{est,p}$) is bigger than that required ($OSNR_{est,p}$), then the channel power can be adapted. We define the $OSNR_{margin,p}$ as the difference between the estimated and required OSNR:

$$OSNR_{margin,p}[dB] = OSNR_{est,p}[dB] - OSNR_{req,p}[dB] \tag{3.9}$$

It is noteworthy that LOGON assumes the worst case in terms of nonlinear effects (i.e., OSNR overestimation assuming full spectrum load), which means that the establishment of any new channel will not require the re-computation (i.e., re-estimation) of the OSNR for the already established ones because its effect is already considered.

The OSNR of an optical channel varies as a function of its optical power at the transmitter side: $OSNR = f(P_{channel})$. The function f is monotonically increasing on the interval $[0, P^{opt}_{channel,p}]$ [129], where $P^{opt}_{channel,p}$ is the channel transmit power for optimal

reception of light at the destination of the path p (i.e., the channel optimum power on the first link constituting the path p).

In order to translate power reduction into OSNR reduction, we have considered that every 1 dBm of optical power reduction corresponds to 1 dB of OSNR reduction. This is an overestimation to ensure a working channel. Indeed, 1 dBm of power reduction leads to less than 1 dB OSNR reduction, as explained in [129]. Therefore, we can consider that the OSNR margin in dB corresponds to the amount of power that can be saved for the related optical channel. Moreover, because optical amplifiers have fixed gains (adjusted according to the method explained earlier in Section 3.3.1), this OSNR reduction is obtained by tuning the power at the transmitter side. An x dBm of optical power attenuation at the transmitter side corresponds exactly to x dBm of power attenuation at the receiver side, when passing though the set of spans and amplifiers constituting the optical link. With this method, we obtain the adapted channel power:

$$P^{adapted}_{channel,p} = P^{opt}_{channel,p} \times \frac{OSNR_{req,p}}{OSNR_{est,p}} \tag{3.10}$$

We define the channel power adaptation value as $C_{adaptation}$:

$$C_{adaptation,p}[dB] = \beta \times OSNR_{margin,p}[dB] \tag{3.11}$$

where $\beta \in [0,1]$ and $C_{adaptation,p}$ represent the quantity of OSNR degradation to apply over the lightpath p. In our work, we use $\beta = 1$. However, β can be used to introduce flexibility to the channel power adaptation process. It offers the possibility for the control plane to efficiently manage its transmission power margins.

Estimation of the power that can be saved is a simple computation that can be easily integrated into a control plane. Other methods relying on more complex computation or monitoring mechanisms can be used to estimate the OSNR. However, this is beyond the scope of this chapter.

To illustrate the power control process, we assume that two optical channels having the same spectral occupation of 50 GHz (i.e., four slots of 12.5 GHz) are established over the same path p. The first channel is established without power adaptation and the second with power adaptation. Figure 3.5 shows an example of the optical power level at the transmitter side for the two established channels. In this example, the first channel (in yellow) uses its optimal power $P^{opt}_{channel,p}$. The second channel (in blue) is adapted to minimum acceptable performance $OSNR_{req}$, and its power value is computed using Eq. (3.10).

3.5 Routing algorithm

To find an optical path between a node pair, we propose a new path computation algorithm that considers spectral and power resources and performs a power adaptation process. Figure 3.6 shows the algorithm, which is executed at the ingress node during path computation.

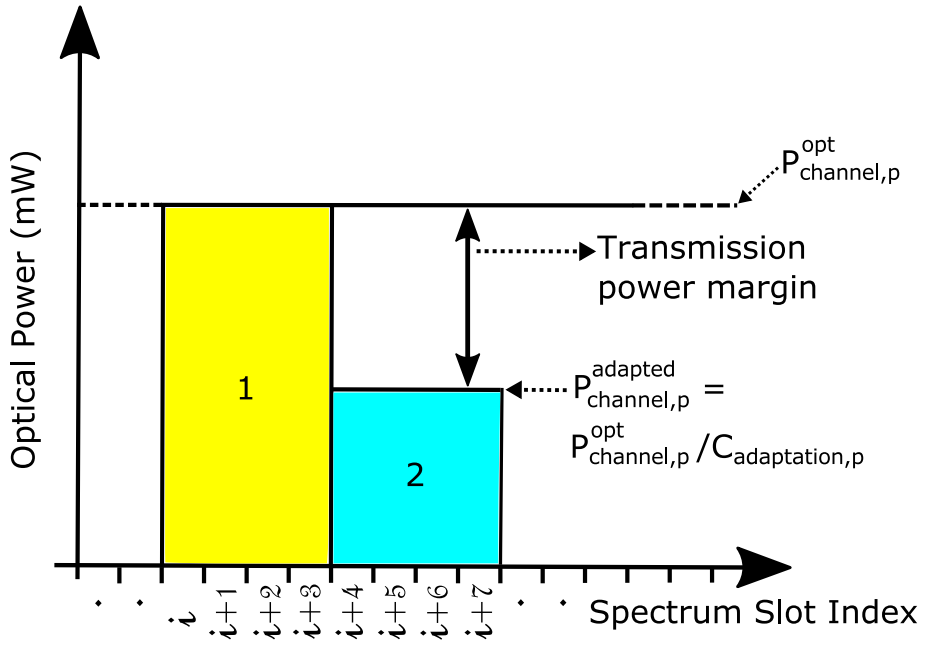

Figure 3.5: Optical channels with and without power adaptation.

For every optical connection request (i.e., lightpath establishment request) of T Gbit/s rate between a pair of source and destination nodes, it computes the shortest path using Dijkstra's algorithm. Then, it tries to find a group of S continuous and contiguous available slots of 12.5 GHz that satisfies the request T using the first-fit algorithm. The S slots are computed with respect to minimum spectrum occupation, supposing the same modulation format and baud rate for each request in this study. The request is blocked when no available slots are found to satisfy the connection request. However, once this set of available and successive optical slots over a path p is found, three other tests are performed: the physical feasibility, power adaptation (PA), and power verification (PV) tests. The physical feasibility test checks whether $OSNR_{est,p} > OSNR_{req,p}$. If the path is physically feasible, then $OSNR_{margin,p}$ is computed. If $OSNR_{margin,p} > 0$, then the channel optical power is adapted to minimum acceptable performance $OSNR_{req,p}$. Therefore, the channel OSNR degradation value is $C_{adaptation,p}$, and the target channel optical power is expressed as $P^{adapted}_{channel,p} = P^{opt}_{channel,p}/C_{adaptation,p}$.

Regardless of the adapted channel power value, a last power verification test is performed to ensure that this channel, if added, will not cause any saturation problems over the m links constituting the optical path p. This test consists in comparing, for every link of the optical path p, the link aggregate power $P_l(t)$ after adding the power of the new channel (either $P^{opt}_{channel,l}$ if no power adaptation is performed or $P^{adapted}_{channel,l}$ if power adaptation is performed) with the maximum allowed power ($P_{max,l}$). It is important to note that these power parameters ($P_{design,l}$, $P_{margin,l}$, $P_{channel,l}$, and $P_l(t)$)

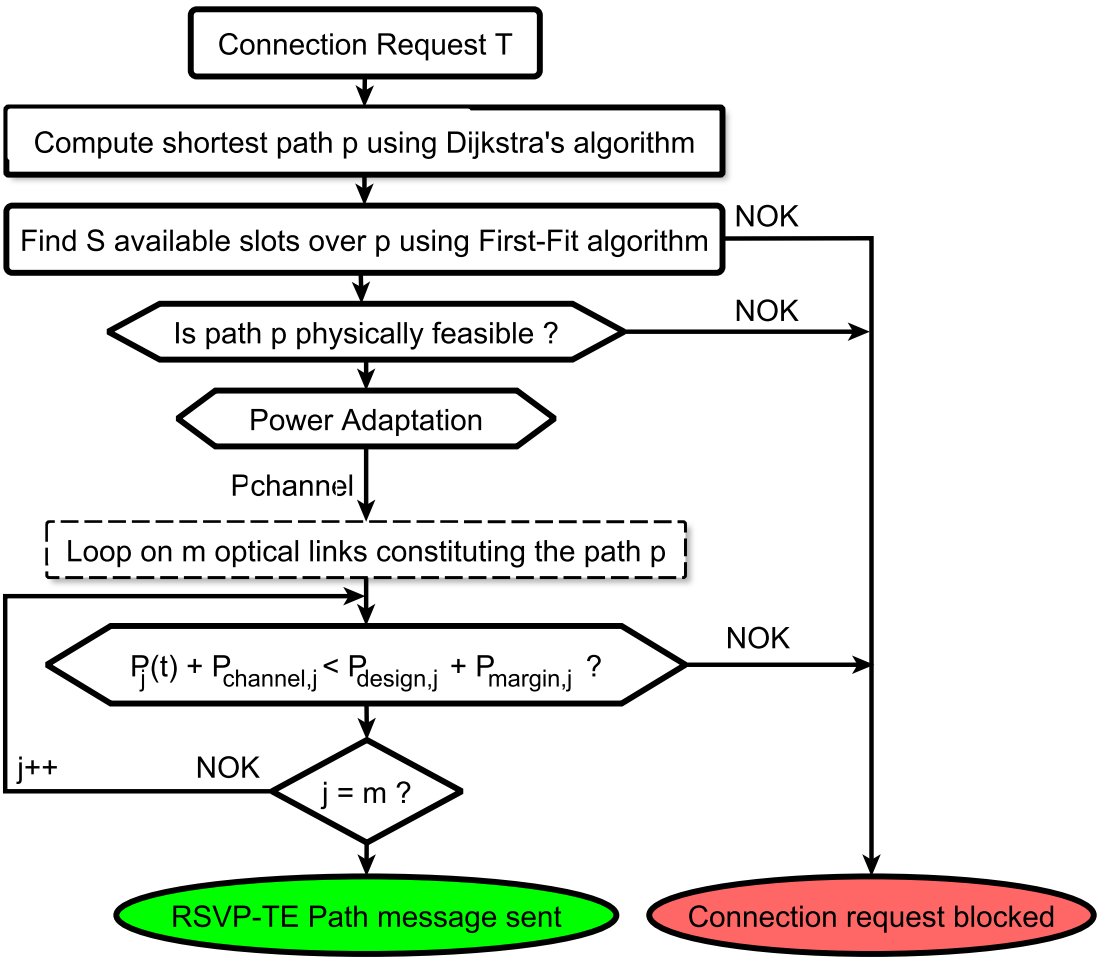

Figure 3.6: Path Computation Algorithm.

are made available at each node thanks to the extension that we propose for the OSPF-TE link state distribution process. Once these tests are done at the ingress node, the signaling is triggered on the chosen path (i.e., an extended RSVP-TE $Path$ message containing the power adaptation information is sent downstream in order to set up the optical channel). If any of these tests fail, the connection request is rejected.

Last, at each hop, during the signaling process, the aggregate power using the recommended channel power setting is checked in order to verify that it does not exceed the $P_{max,l}$ of each crossed link. Indeed, if the requests are frequent, some signaling process may simultaneously compete for the same optical resources in terms of optical power (race condition), and the signaling should avoid any over-provisioning due to the not-yet-updated link database.

3.6 GMPLS protocol extensions

The GMPLS is a network protocol suite for setting up connectivity services upon different switching type equipment [130]. GMPLS is used here because it is one of the most deployed control planes and because it is widely used to manage the optical network technologies. Moreover, it is a well-defined and stable protocol suite involving signaling, routing, and link management protocols to automatically provision end-to-end traffic-engineered connections.

In this section, we mainly focus on the OSPF-TE topology distribution and RSVP-TE signaling protocols, which are the main required bricks of our optical power control process. Despite recent efforts of IETF to enrich the GMPLS control plane with extensions for flex-grid networks [131, 132] and with physical layer awareness [133], neither the parameters that we need for the optical power control process nor the process itself are defined. Therefore, in this work, we propose adding several extensions for OSPF-TE and RSVP-TE protocols. Subsequently, we provide the detailed description of these extensions and present the routing and signaling mechanisms used to exploit them.

3.6.1 OSPF-TE extensions

At the end of the design phase, every optical link has its own set of characteristics, which are$P^{opt}_{channel,l}$, $P_{design,l}$, $P_{margin,l}$, and link $OSNR_l$. We assume that, in the initialization phase of the network, these physical parameters are recorded for each link in the neighboring nodes upon link commissioning. Then, they are collected via OSPF-TE flooding control messages and placed in a local database in each node.

As described in Section 3.5, in order to realize the power verification test, another parameter is needed, which is $P_l(t)$. It is added in the local database, with a value that corresponds to 0 mW during the initialization phase of the network because no channel has been established yet.

In this respect, we propose five new sub-TLVs to OSPF-TE link TLV:

- $P_{channel,l}$ (dBm): The input optimum power for the reference channel spacing (50 GHz) over the link l. It is used when no power adaptation is applied.

- $P_{design,l}$ (dBm): The total aggregated input power designed for the $N_{channel\_max,l}$ of the link l. This parameter is required by the control plane to determine the aggregated optical power allowed over the link l.

- $P_{margin,l}$ (dBm): The link optical power margin. This parameter represents the remaining power margin over the link l.

- $OSNR_l$ (dB): The OSNR of the link l as defined in Eq. (3.9) of [21]. This parameter is needed to estimate path feasibility during the path computation process. Note that this parameter is slightly different from the one proposed in [54, 134] because it includes a nonlinear effects contribution.

- $P_l(t)$ (dBm): The link power of link l at time t. This parameter is used by the power verification test.

We propose to include the first four sub-TLVs into the Opaque LSA type 8 ("OSPFv2 Extended Link Opaque LSA"). The $P_l(t)$ sub-TLV is included as part of the Opaque LSA type 1 ("Traffic Engineering LSA").We propose to encode every one of these five sub-TLVs over 8 bytes, where the first 2 bytes are used to indicate the type of sub-TLV, and the second 2 bytes are used to indicate the length of the sub-TLV (which is equal to 4 here). The last 4 bytes are used to encode the value field of the sub-TLV with respect to the 32 bit IEEE floating point format. In addition to the proposed sub-TLVs, we also rely on an additional sub-TLV to take into account the spectrum slot availability. Many coding formats were proposed for the slot availability sub-TLV in the IETF draft [131, 135]. We adopted the bitmap format in this work.

During the creation of the local databases, we separated the record for the static ($P^{opt}_{channel,l}$, $P_{design,l}$, $P_{margin,l}$, $OSNR_l$.) and dynamic ($P_l(t)$, spectrum slot availability bitmap) parameters [136]. The proposed static parameters are never changed during network operation except in the case where link design or equipment (amplifier or link) was changed (e.g., in the case of fiber repair). The dynamic parameter values change every time an optical channel is established or released. This separation allows the reduction of the amount of flooded information through OSPF-TE protocol.

It is noteworthy that additional parameters may be added to enrich the physical layer awareness, such as CD or PMD of the optical links, as proposed in [137]. However, these parameters are beyond the scope of our study because they have no direct relationship with our power control process. They may be included to improve the exactness of the physical feasibility evaluation of the lightpath.

3.6.2 RSVP-TE extensions

In the GMPLS protocol suite, the RSVP-TE protocol is used as the signaling process between optical nodes of the computed path to establish the requested connection. We adopted the already proposed RSVP-TE extensions by the IETF in [132] for the flex-grid optical networks.

These extensions are used to represent slot width (i.e., bandwidth occupation of the channel) and the frequency slot information. The slot width extension is used to represent how many spectrum resources are requested for a LSP. The frequency extension is used to identify the location of the channel in the spectrum of the optical link.

After the path computation procedure, the ingress node sends an RSVP-TE $Path$ message to the next node of the computed path. This $Path$ message contains information on connection to setup: the central frequency, the channel width (i.e., number of slots), and the $C_{adaptation,p}$ value. When a node receives a $Path$ message (or $Resv$ message), two tests are performed over its outgoing links: the slots' availability verification and the optical power verification.

The slots availability verification consists in verifying that the requested slots are not occupied by any other optical channel. The power verification tests whether the requested power does not exceed the link maximum power. Therefore, it uses the $C_{adaptation,p}$ value conveyed through $Path$ and $Resv$ messages in combination with the $P^{opt}_{channel,l}$ value recorded in its local database to compute the requested power of the connection. Then, it determines if the power respects the following constraint:

$$P_l(t) + (P^{opt}_{channel,l}/C_{adaptation,p}) \leq P_{design,l} + P_{margin,l} \tag{3.12}$$

The $C_{adaptation}$ parameter is conveyed through $Path$ and $Resv$ messages because it is only known by the ingress node (during path computation) and is not distributed by OSPF-TE. To this end, we propose to create new 8 bytes sub-TLVs (2 bytes for type, 2 bytes for length, 2 bytes to encode the value of β, and 2 bytes to encode the value of $C_{adaptation}$) in each of the $SENDER\_TSPEC$ (class number 12) and $FLOWSPEC$ (class number 9) objects of the $Path$ and $Resv$ messages, respectively. These sub-TLVs contain the value of the channel OSNR degradation $C_{adaptation,p}$ (in dB) and β for a path p, which are encoded respecting the 16 bit IEEE half-precision floating-point format.

It is important to note that, during the RSVP-TE signaling process, each node of the optical path stores channel information contained in the $Path$ and $Resv$ messages in a local database (referred to as "*Path State Block/Reservation State Block*" in the standard). Therefore, when an optical channel is removed, optical nodes use the stored information to release the optical resources of the channel i.e., occupied slots). Simultaneously, it also updates the values of $P_l(t)$ for the concerned links, using $C_{adaptation,p}$ parameter combined with $P^{opt}_{channel,l}$ to compute the value of the optical power to be subtracted from $P_l(t)$.

In the same context, the integration of the power verification test requires the addition of a new type of error in case the test fails. Therefore, we propose to define a new error code for the $ERROR\_SPEC$ (class number 6) object of the RSVP-TE $PathErr$ message [138]. This allows identification of the error by the ingress node in order to indicate that the link power resource is fully used.

3.6.3 Connection establishment example

To explain the control mechanism used in our work, we consider here, as an example, an optical network with six optical nodes (i.e., ROADMs). Figure 3.7 shows the six interconnected nodes (A, B, C, D, E, and F).

We assume that network optical links are already designed and that the nodes database is filled with essential information ($P^{opt}_{channel,l}$, $P_{design,l}$, $P_{margin,l}$, $OSNR_l$, and $P_l(t)$). Moreover, we suppose, in this example, that a connection request between ROADMs A and C is sent from the network operator to Node A. Figure 3.8 shows the signaling mechanism and the RSVP-TE message flow triggered to establish the optical channel.

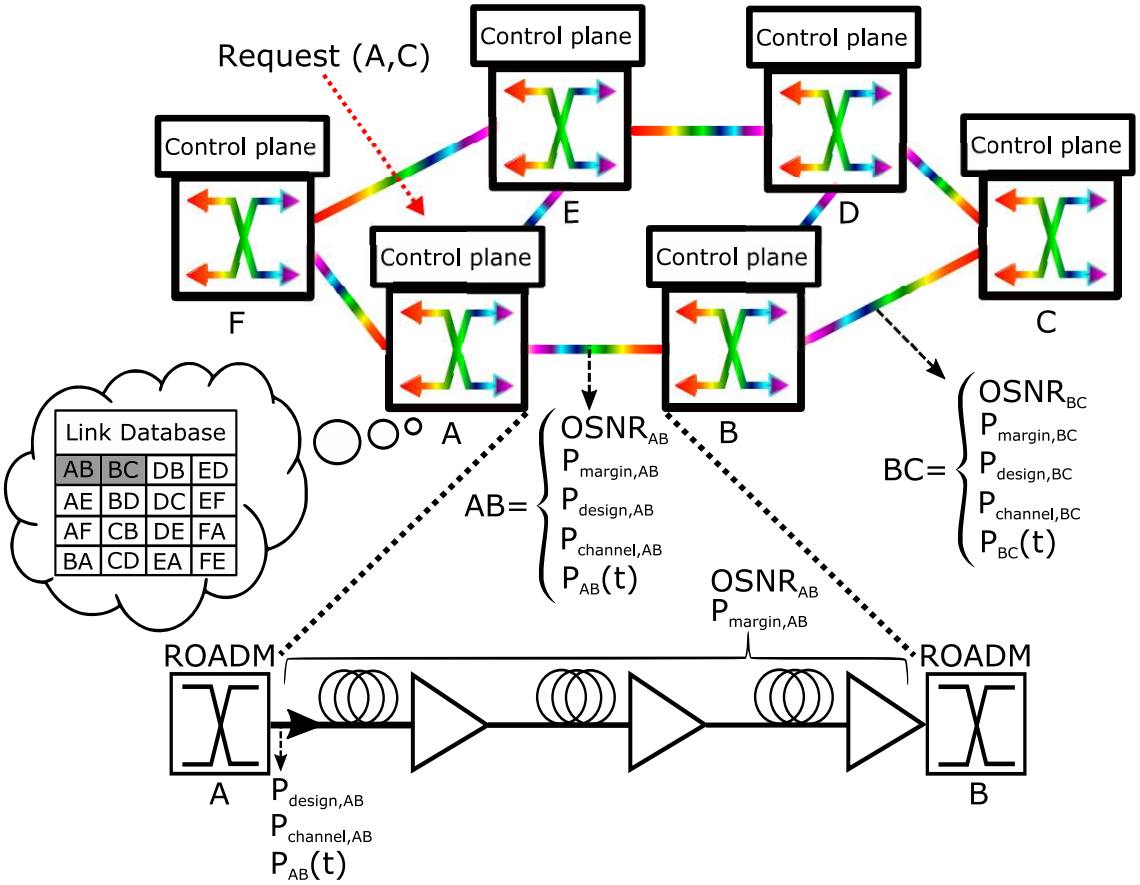

Figure 3.7: Network example.

Upon receipt of the connection request by Node A, the path computation algorithm is triggered. We assume that, after performing the algorithm, the selected path p is A-B-C (shortest path) and S free available slots are found. We suppose also that the $OSNR_{est,ABC}$ of the path is bigger than $OSNR_{req,ABC}$. Therefore, the optical channel for the path p is power adaptable, and a $C_{adaptation,ABC}$ parameter is computed.

Before triggering the RSVP-TE signaling process, Node A performs the slot and power verification tests over its outgoing link (i.e., AB). These tests are executed to ensure that optical spectrum resources are still available and no power saturation will occur after adding the new optical channel over link AB ($P_{AB}(t) + (P^{opt}_{channel,AB}/C_{adaptation,ABC}) \leq P_{design,AB} + P_{margin,AB}$). Once verification is done, Node A sends an RSVP-TE $Path$ message to Node B with the same information on the selected path p (A-B-C), the S slots, and the $C_{adaption,ABC}$ value. Upon reception of the $Path$ message by Node B, the same tests are performed over its outgoing link, BC (it checks that S is still available over the link BC and that $P_{BC}(t) + (P^{opt}_{channel,BC}/C_{adaptation,ABC}) \leq P_{design,BC} + P_{margin,BC}$). Then, it sends a $Path$ message to Node C, once the verification is done.

Once the $Path$ message arrives at the egress Node C, a hardware configuration is

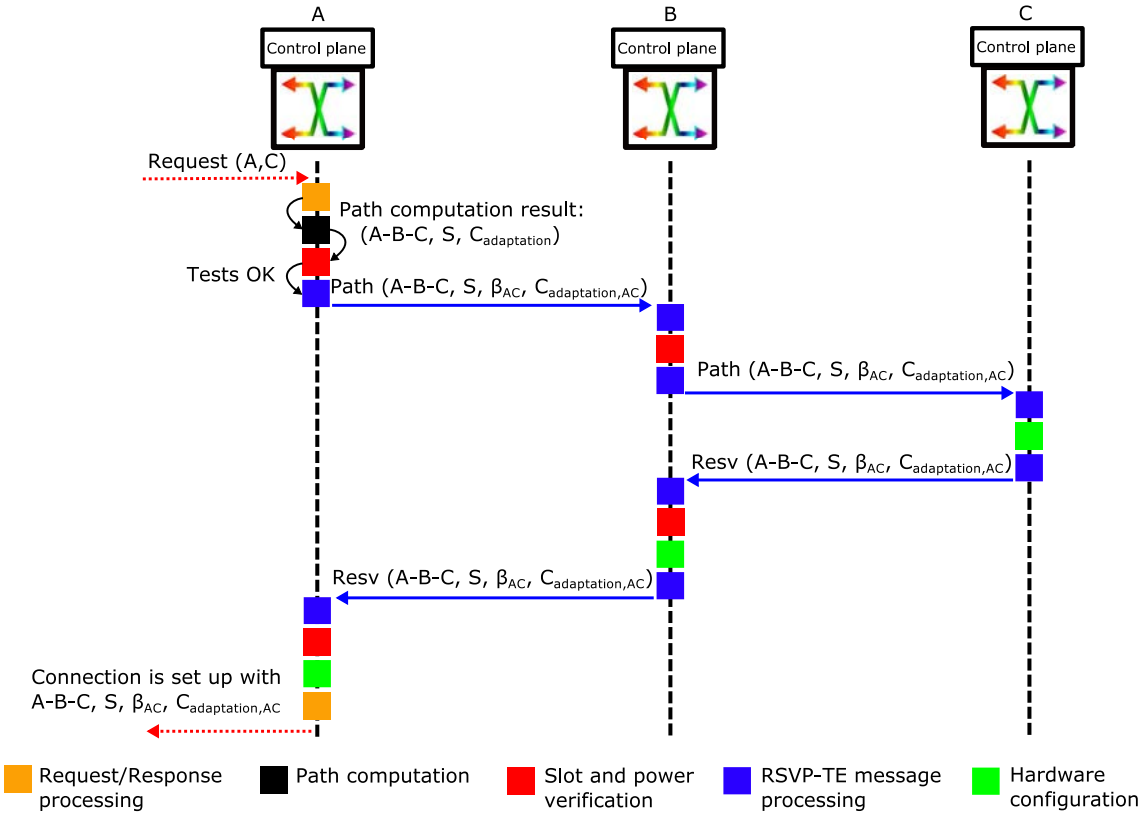

Figure 3.8: Flow diagram in A, B, and C controller during the connection provisioning process.

performed for its $Drop$ port (in order to receive the optical channel). Moreover, the spectrum bitmap and the power value of the link BC are updated ($P_{BC}(t) = P_{BC}(t) + P^{opt}_{channel,BC}/C_{adaptation,ABC}$) in its local database. Then, an $Resv$ message is sent to Node B. On receipt of the $Resv$ message by Node B, slot availability and power verification tests are performed again over link BC. Then, a hardware configuration is made to ensure the switching of the requested channel. Moreover, the spectrum bitmap and the power value of link BC are also updated in its local database, and a $Resv$ message is sent to Node A. In turn, Node A executes the same tests over link AB after the receipt of the $Resv$ message. Once verified, the hardware configuration is performed to its Add port in addition to channel power adaptation. Moreover, the spectrum bitmap and the power value of link AB ($P_{AB}(t) = P_{AB}(t) + (P^{opt}_{channel,AB}/C_{adaptation,ABC})$ are updated in its local database. Finally, the optical channel is established, and a connection setup confirmation is sent back to the network operator.

It is important to note that every optical node sends its neighboring nodes a set of OSPF-TE LSAs messages. This regular update will naturally flood the changes over its outgoing links after the end of any signaling phase.

3.7 Simulation scenarios and results

3.7.1 Simulation setup and scenarios

In order to evaluate our proposed power control process, we developed a distributed GMPLS-based network simulator over OMNET++. It simulates OSPF-TE and RSVP-TE protocol messages and mechanisms, as explained in Section 3.6. Moreover, it takes as input a network topology (links, spans, and amplifier types) and designs its optical links using our design method detailed in [125]. Finally, it fills in the OSPF-TE database with the essential needed parameters ($P^{opt}_{channel,l}$, $P_{design,l}$, $P_{margin,l}$, $OSNR_l$, $P_l(t)$, etc.). Simulations are performed over the 32 optical nodes and 42 optical links of the European backbone network, as shown in Figure 3.9. Single mode fiber spans are assumed to be used (chromatic dispersion = 17 ps.nm^{-1}.km^{-1}, fiber attenuation = 0.22 dB/km, non-linearity coefficient = 1 W^{-1}.km^{-1}).

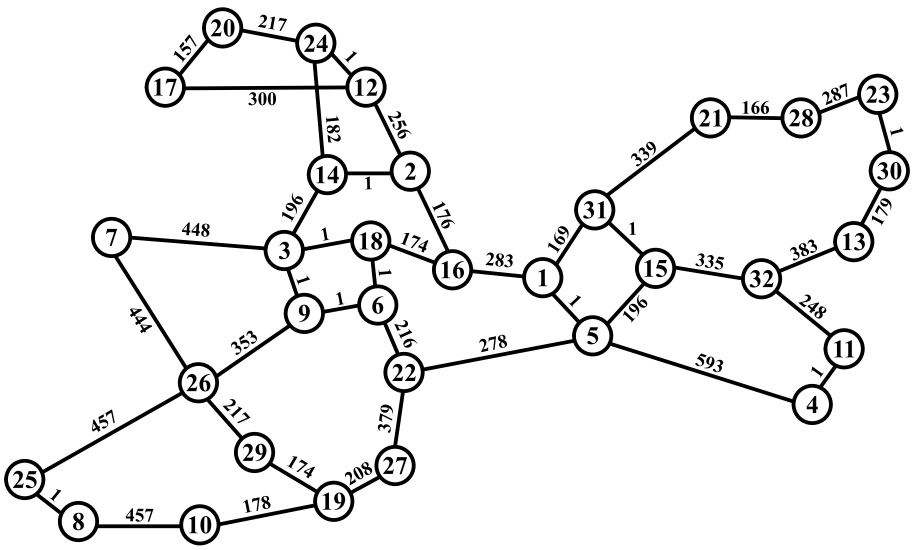

Figure 3.9: European Backbone Network Topology.

Links are designed using the three amplifier types presented in Table 3.1, assuming nonidentical span lengths that are randomly drawn according to a Gaussian distribution $\mathcal{N}(\mu = 100\text{km}, \sigma = 27\text{km})$. Table 3.1 shows the amplifier portfolio used (several variable gain dual-stage amplifiers without midstage access), where F_1 and F_2 are the NF for the first and second stages, respectively, and D denotes the power ratio for both stages to account for the difference between preamp and booster performance. Filtering penalties induced by transit across one optical node are 0.05 dB for the 50 GHz (four slots of 12.5 GHz) channel spacing and 0.64 dB for the 37.5 GHz (three slots of 12.5 GHz) [139].

In order to simplify the results analysis, only 100 Gbit/s optical channels are established in all scenarios (T = 100 Gbit/s). The minimum accepted OSNR at the receiver side, using 0.1 nm noise reference bandwidth, including operational margins, is set to

Type	P_{OA_max}(dBm)	G_{OA_max}(dB)	F_1(dB)	F_2(dB)	Power ratio: D(dB)
A1	17	30	5	6.5	3
A2	19	25	5.5	7	5
A3	20	23	6	7.5	7

Table 3.1: Amplifier Models

15 dB for 100 Gbit/s quadrature phase-shift keying (QPSK) modulation format with coherent detection and soft decision forward error correction, whatever the channel bandwidth (three or four slots of 12.5 GHz). Six scenarios are studied:

- Fixed-grid (FG): This scenario represents today's core optical networks where no power information is communicated in the control plane. The power control is not activated in the path computation algorithm or in the protocol. The number of channels that can be set up on a given link is limited to 80, where each channel occupies four contiguous slots (4 × 12.5 GHz = 50 GHz).

- Fixed-grid with power margins (FG4S_PV): In this scenario, the control plane is power aware and thus benefits from the extra power margin of every link ($P_{margin,l}$) to set up channels in the limit of the 4.8 THz bandwidth (C bandwidth). The power adaptation is set to off, but the power verification is set to on, and each channel occupies four contiguous slots.

- Fixed-grid with power control and power margins (FG4S_PAPV): In this scenario, both power adaptation and power verification are allowed. Each individual channel power is tuned to the power satisfying the minimum acceptable OSNR value ($OSNR_{req}$). Each channel occupies four contiguous slots.

- Flex-grid (FX): This scenario is the same as FG but with channels occupying only three contiguous slots (filtering penalty is bigger than for FG scenario).

- Flex-grid with power control and power margins (FX3S_PAPV): This scenario is the same as FG4S_PAPV, but each channel occupies three contiguous slots.

- Flex-grid with power control and power margins (FX3-4S_PAPV): This is the same as the previous scenario, but with the possibility to choose three or four slots of 12.5 GHz for each 100 Gbit/s channel. The path computation algorithm first tries three slots of 12.5 GHz for the channel setup. If the path is not physically feasible (probably due to its filtering penalty because it is higher for three-slot channels), the algorithm tries to establish the optical channel using four slots.

In this work, several fixed-grid and flex-grid scenarios are simulated. Therefore, in order to fairly compare them, we perform the same link design for eighty 100 Gbit/s

QPSK channels over a 50 GHz grid (80 × 50 GHz = 4 THz per link) for all scenarios. However, the full usable bandwidth of each link is set to 4.8 THz (optical amplifier usable bandwidth) as defined by the ITU-T. Table 3.2 summarizes the six simulated scenarios.

Simulated scenarios	Power adaptation	Power margin	Channel Spacing (GHz)	Filtering penalty (dB)
FG	No	No	50	0.05
FG4S_PV	No	Yes	50	0.05
FG4S_PAPV	Yes	Yes	50	0.05
FX	No	No	37.5	0.64
FX3S_PAPV	Yes	Yes	37.5	0.64
FX3-4S_PAPV	Yes	Yes	37.5 or 50	0.05 or 0.64

Table 3.2: Simulated scenarios

The path computation algorithm presented in Section 3.5 is modified to enable the simulation of the different scenarios. We summarize in Figure 3.10 the set of spectrum and power control tests applied during the execution of the path computation algorithm. Depending on the scenario, some tests are activated or deactivated. In this algorithm, the K shortest paths can be computed for any request between any node pairs (s,d). Therefore, when the K paths have been computed, the ingress node executing the algorithm tries to establish the first path. If it is not possible, the second path is tested and so on. The connection request is blocked if no path from the K computed paths can pass the set of tests. The K paths are ordered in increasing length order. The algorithm selects the first path from K that satisfies all the constraints (continuity, contiguity,physical feasibility, and, if needed, power feasibility). If one of the K paths passes all the tests, the provisioning process is triggered with a set of channel parameters (path, slots, $C_{adaptation}$). The connection request is blocked if no path among the K passes all the tests.

Note that, in all scenarios, paths that exceed maximum reach (i.e., with OSNR below $OSNR_{req}$) are rejected, and our optical network does not implement regeneration (left for further study). Fifty simulation runs (each run with a different seed) are performed for each of the six scenarios. We simulate an incremental channel setup, where channels are established and never released (i.e., channel establishment until the network is fully loaded). It is important to note that, for every scenario, the same 50 seeds are used in order to exactly simulate the same sequence of optical connection requests. The results depicted in Figures 3.11 and 3.12 are given by averaging the 50 simulation runs with a confidence interval of 95% (too small to be displayed on the figures). The connection request inter-arrival time at each node follows an exponential law with a value of 0.4 for its parameter. The source-destination pair of each request is randomly chosen among all network nodes according to a uniform distribution.

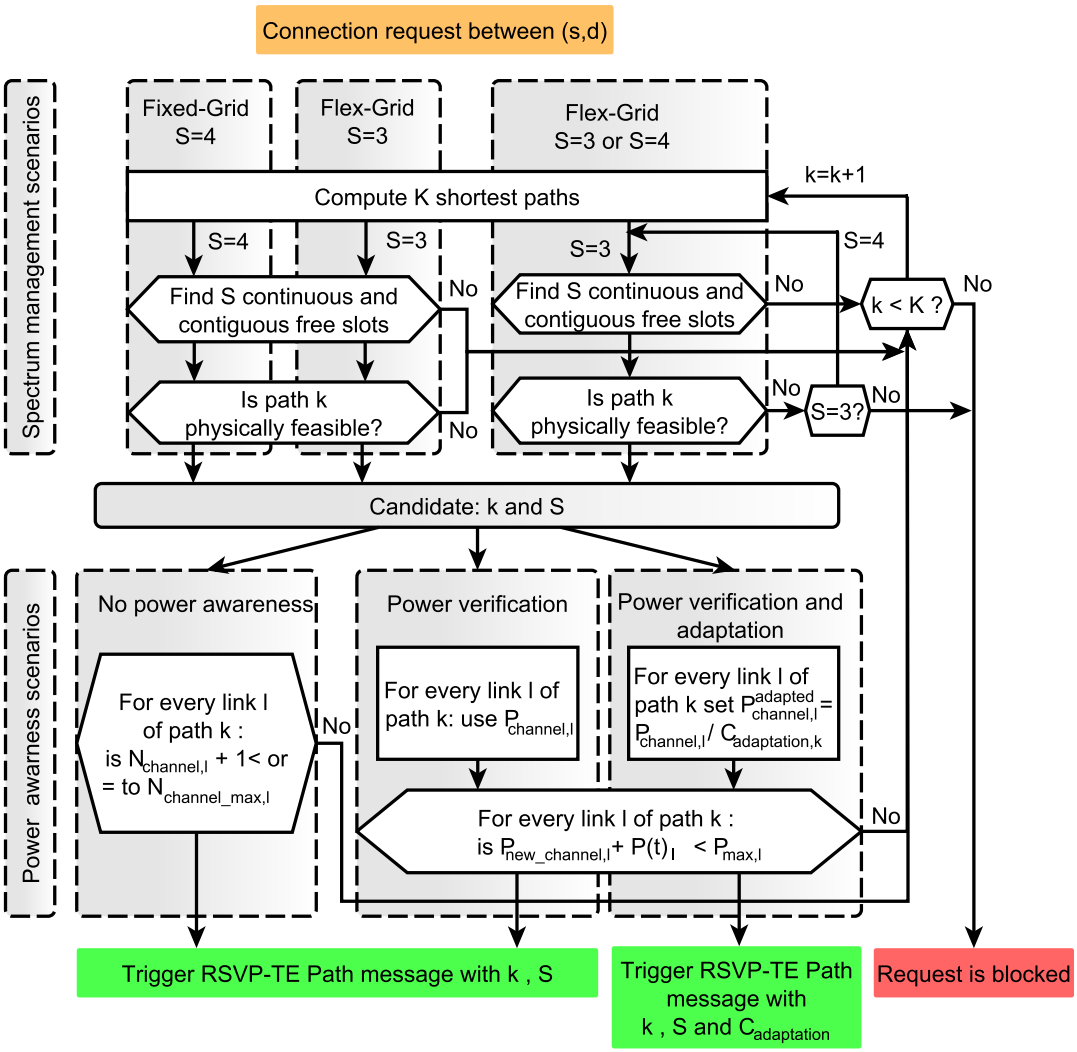

Figure 3.10: Path computation algorithm of the simulated scenarios.

3.7.2 Simulation results

We consider the CBR a first evaluation criterion, which is the ratio of the total number of blocked requests over the total number of generated requests until a time t. Figure 3.11 shows the CBR of the six scenarios as a function of the normalized spectrum occupation of the network, which is the ratio of the total occupied spectrum of all the links of the optical network until a time t over the total spectrum of all the links. Note that, on each link, the spectrum occupation corresponds to the number of reserved slots of all channels, each one having three- or four-slot occupations depending on the scenario.

For all scenarios, the CBR at low occupation is not zero because of the rejected demands due to physical feasibility (paths longer than maximum reach). Not surprisingly,

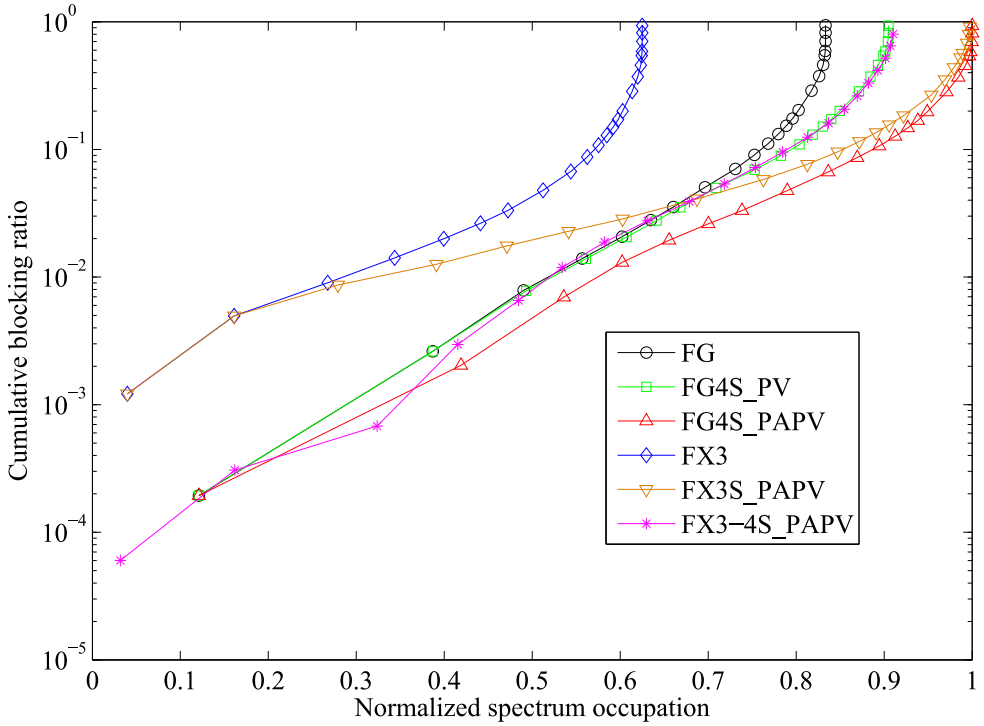

Figure 3.11: Cumulative blocking ratio vs. normalized spectrum occupation.

because FX and FX3S_PAPV have a larger filtering penalty, they block more demands at low occupation than the other scenarios. The CBR of the FX scenario increases rapidly with the spectrum occupation not only because of the physical feasibility blocking but also because of the limited number of channels over every link. When comparing FX and FG scenarios in terms of spectrum occupation, we notice that, when the network is fully loaded (i.e., when no optical channel can be established), the FX spectrum occupation represents 75% of that of FG. This result confirms the gain brought by flex-grid technology in terms of spectrum occupation. Moreover, FG and FG4S_PV have the same CBR until approximately 65% of spectrum occupation. Over 65% occupation, the CBR of FG4S_PV is smaller because the network benefits from power awareness; it can accept more than 80 channels relying on the remaining power margins over the links.

Furthermore, FG4S_PAPV has a smaller CBR than FG and FG4S_PV because it can benefit not only from the power margin, but it also can create some reduction in power with our channel power adaptation process. The CBR of FG4S_PAPV stays below the CBR of FG and FG4S_PV starting from approximately 26% of spectrum occupation. This means that, even at low load, the power reduction enabled by our proposed power control mechanism can be useful.

Moreover, when investigating the optical power levels, we noticed that the FG4S_PAPV scenario is not limited by the optical power resource availability. In fact,

the blocking was only due to physical feasibility and bandwidth availability, even at a high load. As explained earlier, the FX and FX3S_PAPV scenarios have bigger CBR at a low occupation ratio because they use only 37.5 GHz spacing for establishing the 100 Gbit/s channels; the filtering penalty (0.64 dB) then reduces the number of feasible paths in the whole network. However, when network load increases, the FX3S_PAPV CBR is lower than the CBR of FG and FG4S_PV. This is explained first because, with three slots per channel, the network can accept more channels than with four slots. In addition, the optical power control process is able to sufficiently save power that is required for these additional channels (despite the fact that the filtering penalty limits the performance and thus the amount of optical power reduction).

This analysis is confirmed by the FX3-4S_PAPV scenario. It has a CBR smaller than FX3S_PAPV for spectrum occupation lower than 0.65. This is because paths that were rejected due to their nonphysical feasibility with 37.5 GHz are established here with 50 GHz. Nonetheless, this is paid with lower spectrum efficiency; the spectrum fragmentation caused by the mixing of 37.5 and 50 GHz channels (no spectrum fragmentation awareness is used) prevents using the whole spectrum bandwidth, unlike FG4S_PAPV and FX3S_PAPV. This also is confirmed in Figure 3.12.

It is important to note that the spectrum efficiency of the FX3S_PAPV is slightly smaller than FG4S_PAPV because some links still have spectrum resources, but their power resources are completely used at high loads. This is because setting up only three-slot channels not only increases the number of channels but also decreases the potential for power reduction over links. Power adaptation produces less power margins because of the higher filtering penalty (0.64 dB).

We notice that the amount of $P_{margin,l}$ over the links is too small to satisfy more than 80 channels with this network design (link power margins represent approximately 2.5% of the available power over the network). This means that, when switching to flex-grid networks, the $P_{margin,l}$ will not be sufficient to handle the increase in the number of optical channels. In this situation, the power adaptation process is essential to save enough power to cancel the blocking for power reasons.

Moreover, we remarked that, when the network is fully loaded (i.e., spectrally saturated), the remaining power over the entire network (sum of the remaining power over all network links) is high. We have 52%, 25%, and 35% of remaining power for FG4S_PAPV, FX3S_PAPV, and FX3-4S_PAPV scenarios, respectively. The value of the remaining power is high because all the $OSNR_{margin,p}$ of the established channels have been used to save optical power (i.e., reduce transmitted power). Therefore, for some channels, it is possible to use the existing $OSNR_{margin,p}$ for other purposes such as using a higher-order modulation format to reduce the spectral occupation of the channel and thus increase link capacity. However, this increases the decision complexity in the control plane because it should decide when to use the $OSNR_{margin,p}$ for power attenuation and when to use it to change the modulation format. This alternate decision policy is not addressed in this chapter and is left for future work.

Figure 3.12 shows the network capacity (amount of 100 Gbit/s requests accepted and established) as a function of the normalized spectrum occupancy. Note that a four-

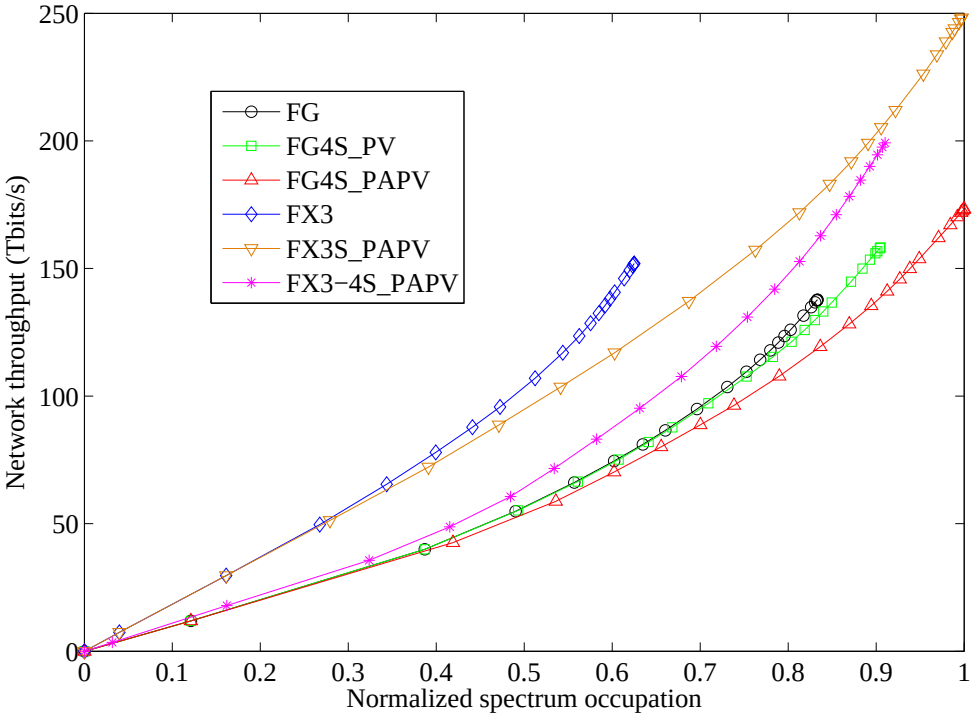

Figure 3.12: Network throughput vs. normalized spectrum occupation.

slot 100 Gbit/s request going through three optical links (three-hop path), for example, will count as 100 Gbit/s on the y axis and 3 × 4 slots (3 × 50 GHz) on the x axis. This explains why the FG4S_PV and FG4S_PAPV curves are below that of FG; both scenarios accept additional long path requests (i.e., paths with bigger number of hops) at high load because they can use more spectrum than FG (limited to 80 channels per link) thanks to the power control. This explanation also holds for the FX3S_PAPV scenario, which has much shorter paths on average than all the other scenarios (the FX3S_PAPV curve is above that of FG).

The FX scenario carries approximately 152 Tbit/s of data traffic, which is more than the traffic carried with the FG scenario (137.8 Tbit/s). This result is expected because established connections in the FX scenario have shorter reaches and therefore occupy less bandwidth and slightly reduce the blocking due to the exceeded maximum channel number per link. The FG, FG4S_PV, and FG4S_PAPV reach at most 137.8, 158.2, and 173.3 Tbit/s, respectively, of carried traffic. Therefore, the power control has increased the capacity of the fixed-grid network by approximately 25%.

As expected, the power control coupled with the use of the flex-grid in FX3S_PAPV greatly increases the network capacity to 248 Tbit/s. This represents 80% of the capacity increase compared with FG (i.e., accounting for the 0.8 THz more total spectrum resources compared with the 4 THz of FG) and 45% when compared with FG4S_PAPV.

We also note that the FX3-4S_PAPV scenario has a larger capacity than FG4S_PAPV, despite the fact that it can occupy less bandwidth because of spectrum fragmentation.

All these results mean that channel power adaptation is an efficient mechanism to benefit from the link total spectrum bandwidth, without the need to redesign the existing optical network.

3.7.3 Blocking reasons

To understand exactly what is happening during simulations, we plotted the reasons for request blocking for each scenario in bar charts and evaluated the effect of the number of shortest paths on the request blocking.

In our study, there are four blocking reasons:

- No available spectrum (No Spec): This type of blocking arises when no available continuous and contiguous slots are found over a path p.
- No sufficient OSNR (No OSNR): This type of blocking arises when the $OSNR_{est,p}$ of the computed path is smaller than $OSNR_{req,p}$.
- No available power (No Pow): This type of blocking arises when no power resource is available in one link constituting the chosen optical path p.
- Maximum channel number exceeded (MXCE): This blocking reason is considered for FG and FX scenarios, where no power awareness exists in the control plane. Therefore, blocking arises when the channel number exceeds the maximum allowed (which is 80 here) over a link l over the requested path p (whatever the real remaining power or spectrum).

The blocking counting method is described as follows: for each connection request and its computed path p, if there are no available continuous and contiguous slots (over the path p), the blocking reason is counted as No Spec. However, if there are available slots, but the $OSNR_{est,p}$ for the path p is smaller than $OSNR_{req,p}$, the No OSNR blocking reason is counted. In the case where spectrum resources are available and the path is physically feasible ($OSNR_{est,p} > OSNR_{req,p}$), but there is no power resource available in one of the links constituting the computed path p (i.e., a link saturation may have occurred after adding the new optical channel), the No Pow blocking reason is counted. For FG and FX scenarios, because no power control is performed, the MXCE blocking reason is considered when the number of channels established over any link exceeds the maximum allowed. Therefore, No Spec is counted first, then No OSNR, and finally MXCE.

To fairly compare the different scenarios, we recorded the results of simulation after 2000 connection requests were generated (same request sequence, same traffic, and same set of source and destination node pairs for all scenarios). Then, we plotted (in bar charts) the number of blocked requests per reason for blocking for each of the six scenarios. This is shown in Figures 3.13 and 3.15 for fixed-grid and flex-grid scenarios,

respectively, to ease visualization. In addition, these blocked requests per scenario are plotted as a function of the number of hops per channel, as shown in Figures 3.14 and 3.16. Simulations are performed for one shortest path ($K = 1$) and for three shortest paths ($K = 3$).

3.7.3.1 One shortest path

Figure 3.13 shows that, in the FG scenario, the MXCE reason is dominant. Indeed, no power information is available for the control plane, and the number of channels is the first blocking reason encountered when computing the path. Note that this does not mean that paths blocked due to the MXCE reason are otherwise feasible with respect to the continuity constraint or the physical feasibility constraint.

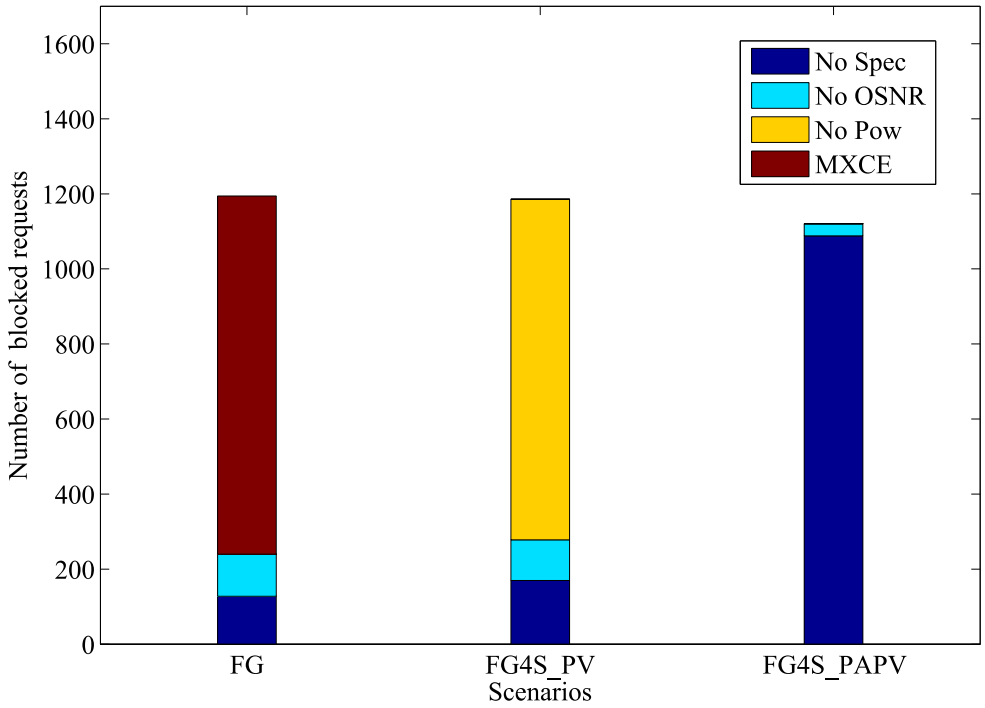

Figure 3.13: Blocking reasons in FG scenarios.

In the FG4S_PV scenario, because the link power margin can be used, the amount of accepted requests is increased, and the number of blocked requests is reduced (from 1194.4 to 1185.5 requests on average). Moreover, the No Pow reason is the main reason for blocking. This means that most of the requests have passed the continuity, the contiguity, and the physical feasibility tests but failed because the amount of power margin is not sufficient for a large number of them. This result confirms our first analysis that link power margin is not sufficient to avoid amplifier saturation. However, some additional channels are accepted due to the use of power margins, leading to a bit more

spectrum occupancy than in the FG (this explains the increase of the No Spec blocking reason from 128 to 170 requests). This is also clear in Figure 3.14, and it is independent from the number of hops.

Figure 3.13 shows that, with the power control process in FG4S_PAPV, the blocking occurs for two reasons: No OSNR and No Spec. This is explained by the fact that the power control process is capable of reducing link power; therefore, link power saturation is no longer occurring. Power adaptation frees more optical power resources than required by the requests. Power is no longer a limitation in this case. As a result, more connections are accepted and less are blocked, as shown in Figure 3.14. Therefore, network links are more spectrally occupied.

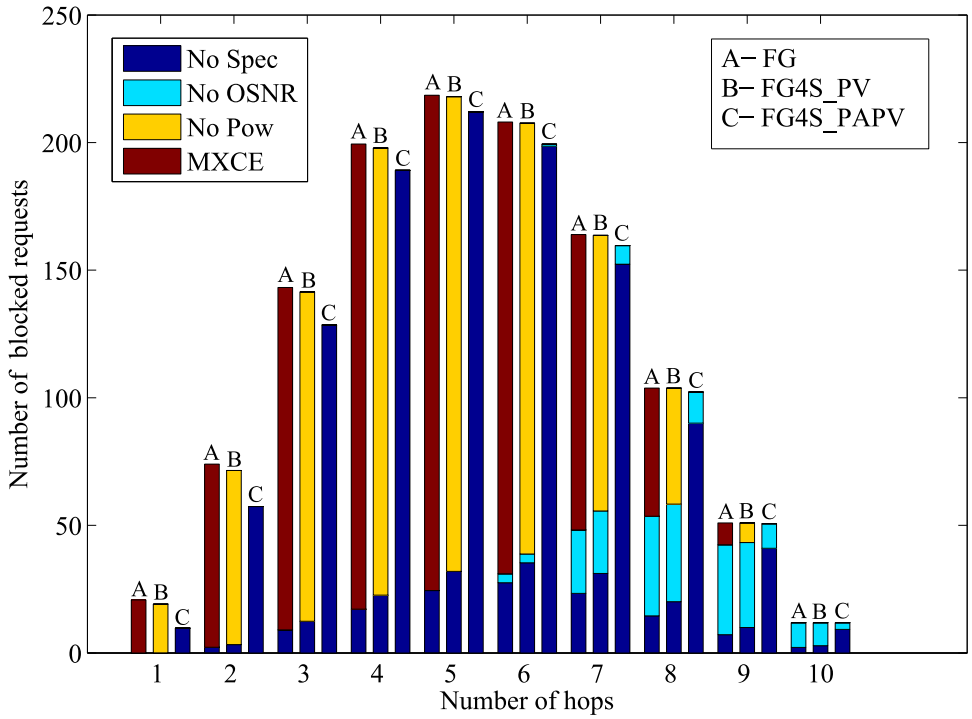

Figure 3.14: Blocking reasons per number of hops in FG scenarios.

This explains why the number of No OSNR blocking in the FG4S_PAPV scenario is smaller than the No OSNR blocking number in the FG and FG4S_PV scenarios: more requests are counted as blocked due to spectrum resources first, even if these requests do not pass the physical feasibility test. This somehow masks part of the No OSNR blocking reason in the FG4S_PV scenario (because of the blocking counting method).

Figure 3.15 shows that, in the FX scenario, there is no blocking due to No Spec because the use of three slots for each 100 Gbit/s channel has reduced the spectrum used in the network; therefore, there is sufficient available spectrum for all requests. This confirms the spectral gain promises when using the flex-grid technology. However, the

blocking reasons are instead due to No OSNR because the filtering penalty is bigger than that of the FG scenarios. Of course, similarly to the FG scenario, there is always some blocking due to MXCE because power information is not available to the control plane.

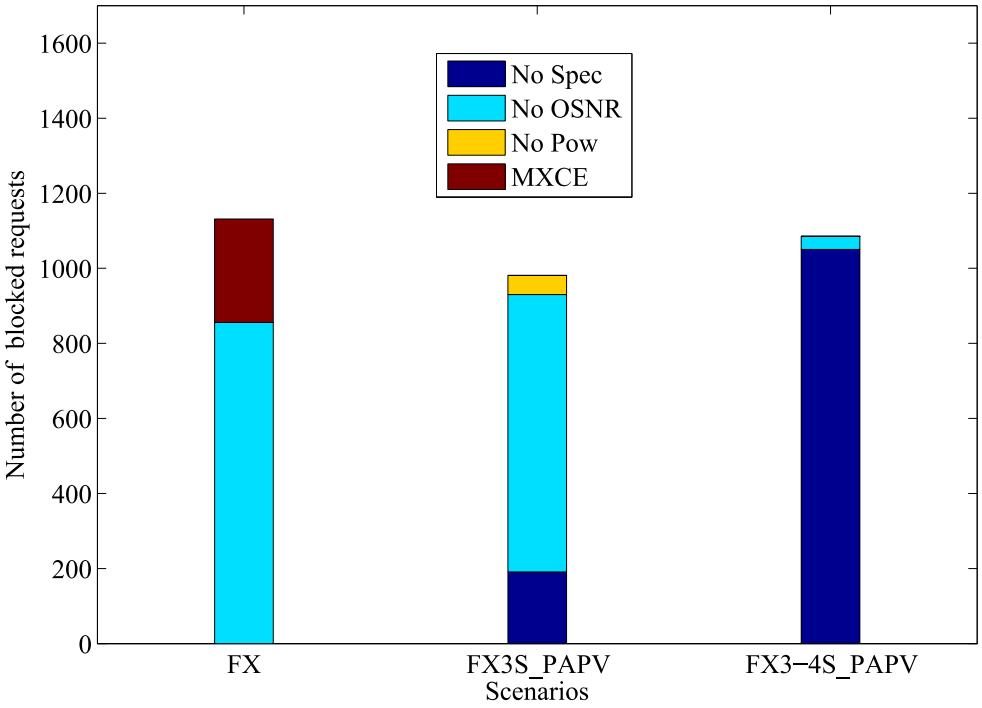

Figure 3.15: Blocking reasons in FX scenarios.

We notice that, in the FX3S_PAPV scenario, the dominant blocking reason also is No OSNR because of the high filtering penalty but with a smaller number (739.2 requests) in comparison with that of FX (855.7 requests). The reason behind that is the same as explained in the previous paragraph when comparing the number of No OSNR blockings in the FG and FG4S_PAPV scenarios. In this scenario (FX3S_PAPV), the activation of the power control process increases the number of established channels, as shown in Figures 3.15 and 3.16; therefore, some optical links are fully occupied (up to 128 channels rather than 80 in the FX scenario). This explains the appearance of No Spec blockings.

At the same time, we can see in Figure 3.15 that No Pow blocking arises in the FX3S_PAPV scenario. Moreover, this blocking reason is limited to requests with a small number of hops, as shown in Figure 3.16. In fact, the high filtering penalty reduces channel performance and the quantity of power that can be saved through the power control process because less $OSNR_{margin,p}$ is saved per channel, and more power resources are consumed. Thus, the amount of freed optical power resources is not

enough to cope with the available spectrum resources and requests.We also can notice that the requests with long paths are more likely to be blocked due to the OSNR limit, and their blocking reason is considered No OSNR, even if there is a lack of power resources (due to the counting method).

It is noteworthy that, because the traffic is uniformly distributed among all fibers, this lack of power resources (and the lack of spectral resources) will appear, especially on links such as the one between Node 1 and Node 16 and between Node 5 and Node 22 of Figure 3.9. This is because these links interconnect two parts of the network. Therefore, special attention should be dedicated to these links, which will be discussed in one of our future works.

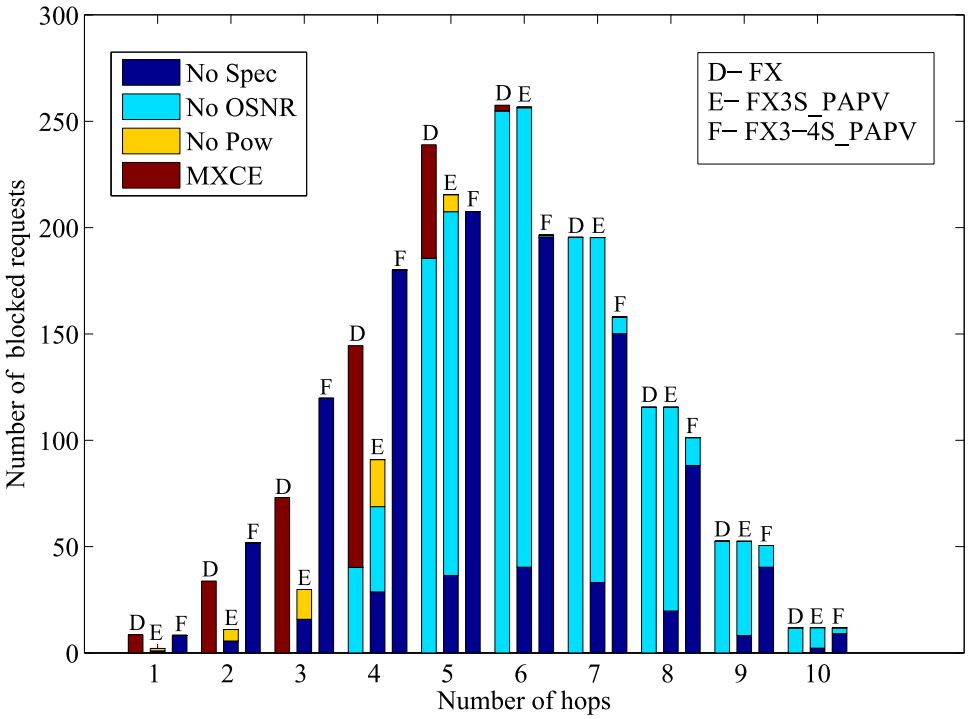

Figure 3.16: Blocking reasons per number of hops in FX scenarios.

Last, the FX3-4S_PAPV scenario suffers from spectrum limitation. This is due to spectrum fragmentation because a mix of three- and four-slot channels is used; thus, network links cannot be fully occupied. In addition, four-slot channels occupy more spectrum and have a bigger number of hops. Therefore, No Spec blocking is dominant, and the No Pow blocking reason never arises. This is in line with the effort made in the literature to reduce spectrum fragmentation.

Figure 3.16 shows that the FX and FX3S_PAPV scenarios accept more requests with a small number of hops (less blocking for paths with a small number of hops) because of the freed spectrum. Instead, in FX3-4S_PAPV, a higher number of blockings appears

for requests with hop counts lower than five because more requests with a large number of hops are accepted. Moreover, in FX3-4S_PAPV, the number of No OSNR blocking is reduced. This is explained by the fact that connection requests that are not physically feasible with three slots (because of the high filtering penalty) are established with four slots.

We can deduce from these results that the strategies used for channel establishment (i.e., selection of the transponder type, channel power, modulation format, spectral occupation, and baud rate) are important in order to exploit the capacity of network links. Therefore, a more intelligent routing algorithm is needed in order to benefit from the flex-grid technology gain promises.

3.7.3.2 Three shortest paths

To complete the evaluation of our power control process, the path computation algorithm is improved by introducing path diversity (i.e., K shortest path computation) and simulations are repeated with $K = 3$ shortest paths.

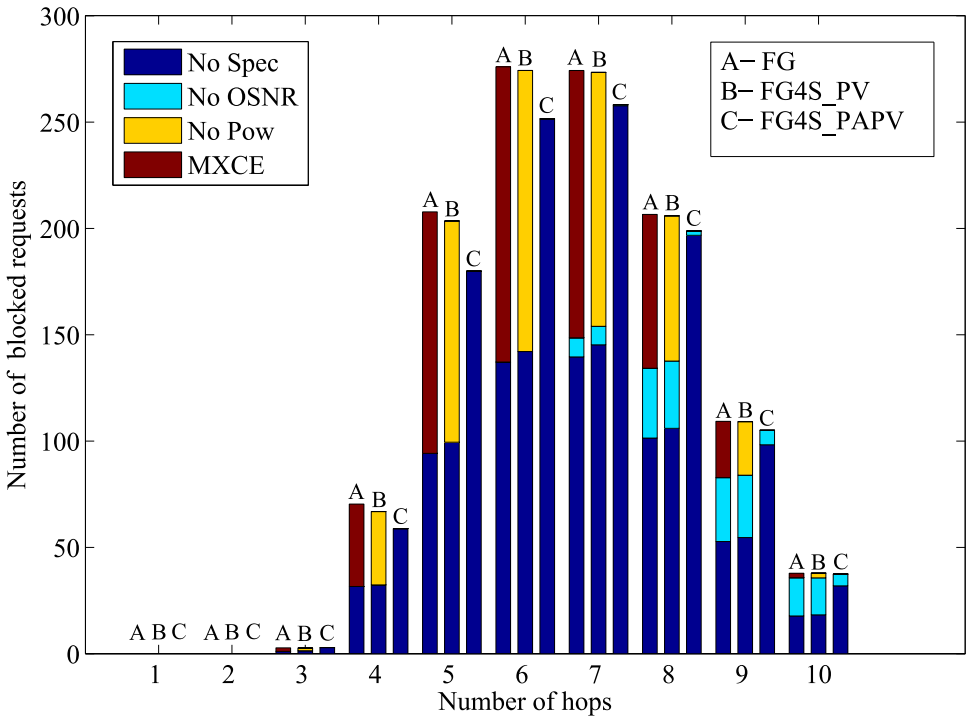

Figure 3.17: Blocking reasons per number of hops in FG scenarios with K=3.

Figures 3.17 and 3.18 plot in bar charts the number of blocked requests as a function of the number of hops per channel. In these simulations, the blocking reason is recorded for the last tested path. This is why no blocking is recorded for one- and two-hop paths, as shown in Figures 3.17 and 3.18. This is expected because the established

connections have longer reaches on average with $K = 3$. Accordingly, connection requests occupy more spectrum; therefore, network throughput for all scenarios is reduced, and the No Spec blocking number increases are compared with $K = 1$.

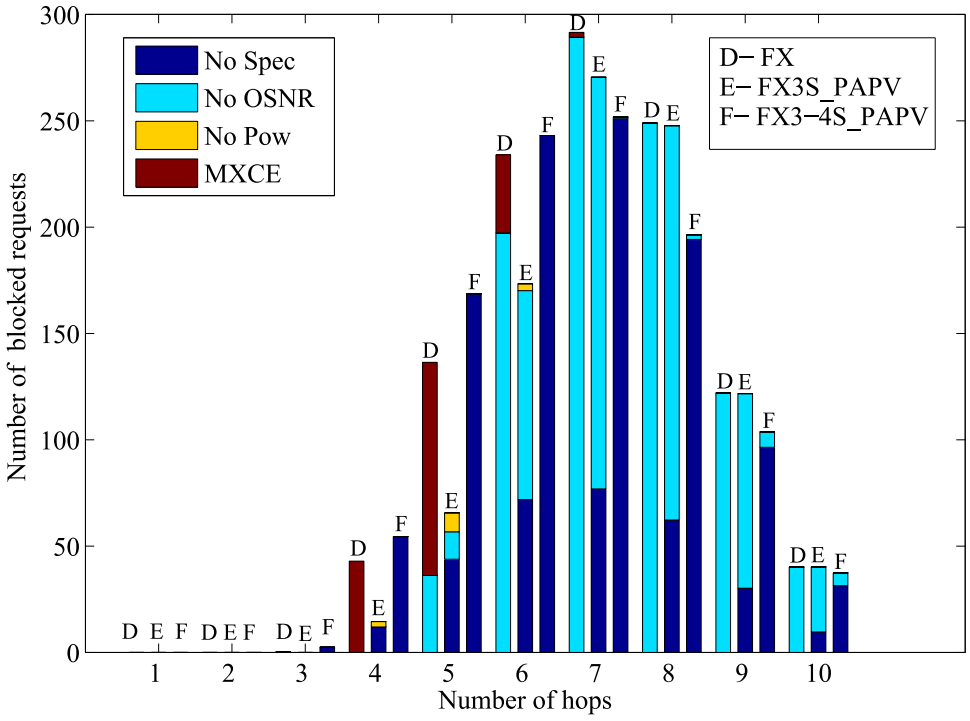

Figure 3.18: Blocking reasons per number of hops in FX scenarios with K=3.

We note that the CBR values when $K = 3$ are slightly reduced for all scenarios in comparison with the shortest path $K = 1$. However, we obtain approximately the same behavior and shape for $K = 1$ and $K = 3$ (the cumulative blocking ratio is divided by two).

It is interesting to increase the number of computed shortest paths in order to avoid blocking in case there is a lack of spectrum and power resources over optical links. Indeed, this reduces the network blocking, but, at the same time, more resources are consumed on average. However, Figure 3.18 shows that the No Pow blocking reason in FX3S_PAPV is not avoided even for just 2000 generated requests.

This result shows that, even with a routing algorithm, which takes advantage of path diversity, No Pow blocking could not be avoided. Thus, as previously explained, the links interconnecting different parts of the network will always be problematic. This is why it is important to include power information in the control plane to efficiently manage network resources and therefore define strategies to avoid this kind of blocking.

3.8 Conclusion

In this chapter, we addressed the optical amplifier power limitation issue that an optical network operator will face when migrating networks from fixed-grid to flex-grid networks. We presented our link design method that allows specifying the power information of optical links that are essential for the control plane. A channel power control process is proposed in addition to a path computation algorithm that integrates power verification and power adaptation tests. We show how the whole power control process can be implemented into a distributed GMPLS-based control plane and propose new extensions for OSPF-TE and RSVP-TE protocols to include power information and to integrate power awareness. Simulation results reveal that the power control process is an efficient way to benefit from flex-grid capacity promises while maintaining the use of legacy amplifiers without the need to redesign any link in the network. In addition, it helps us to efficiently manage link power resources and to avoid power saturation, which is certainly unacceptable during network operation.

It is important to emphasize that our power control process is completely independent from link design, OSNR estimator, or control plane protocol. Any other link design method associated with any OSNR estimator could be used to perform the power control. In addition, this process could be used for an already deployed network, where established channels are adjusted to fit operator requirements while monitoring their error rates. At the same time, it also could be considered for new flex-grid networks under construction, where we anticipate the deployment of power controlled channels to liberate margins and thus increase network throughput.

Finally, it is noteworthy that the developed power control process and path computation algorithm are completely compatible with the software defined network (SDN) paradigm. In fact, they can be implemented and executed by any SDN controller if the same collected information through OSPF-TE was stored in the controller database.

CHAPTER 4

OPTICAL POWER CONTROL WITH REGENERATION

THE evolution to translucent optical networks was driven by the scalability problem of transparent networks where optical impairments limit the reaches of optical connections. This is usually the case for large networks where optical channels suffer from the accumulation of optical impairments when undergoing a high number of optical links. Indeed, the deployment of optical regenerators allow overcoming signal degradation experienced over network links and thus guaranteeing a feasible channel between any two optical nodes. However, the use of optical regenerators increases the complexity of channel provisioning, where additional information is required by the path computation algorithm in order to assign regeneration sites for the unfeasible channels. In fact, establishing an optical channel in translucent network will require extensions to control plane protocols to take into account regeneration information during path computation and signaling phase.

In Chapter 3, the migration from fixed-grid to flex-grid networks have been studied only for transparent networks with an incremental traffic pattern. The proposed power adaptation process and protocols extensions have considered channels provisioning without regeneration information. In the continuity of what have been studied, we address in this chapter the migration from fixed-grid to flex-grid for the case of translucent networks that are representative of nowadays networks. Furthermore, as the next generation of optical networks is intended to be flexible and dynamic, we consider in this work dynamic traffic scenarios, where optical channels are dynamically established and removed, without a prior knowledge of the traffic requests. In this respect, the impact of the power saturation problem is evaluated considering this kind of traffic pattern.

4.1 State of the art

In the literature, several works [124, 140–142] addressed the establishment of optical channels in translucent optical networks, where signaling mechanisms and protocols extensions were proposed to handle the optical regeneration in GMPLS control plane. Indeed, as with the optical impairments [10], different approaches (i.e., routing-based or signaling-based) can be developed to take into account the optical regeneration information in the control plane. These approaches are usually based on OSPF-TE and RSVP-TE protocols, by adding new extensions to include the required information such as regenerator availability and regenerator reservation information.

The works in [124, 140] have proposed a novel extensions to OSPF-TE protocol to enable the dissemination of optical regeneration information (e.g., regenerators modules availabilities, regeneration types: 1R, 2R, 3R [92]). These extensions allow for optical nodes to be aware of the number and the location of available regenerators in the network. Moreover, the authors proposed adding a new sub-object called "Regenerator sub-object" in the explicit route object (ERO) of the RSVP-TE $Path$ message. This extension was added in order to specify the optical regenerators that should be used during the signaling phase when establishing an optical channel.

In [141], the authors proposed several extensions to RSVP-TE and OSPF-TE protocols to take into account optical regeneration in GMPLS control plane. The OSPF-TE extensions were proposed to advertise the information on regenerator availability and capability (i.e., number of regenerator per node and regeneration types). The RSVP-TE extensions were used to collect regenerator information and assign regenerators along the connection path. In this respect, the authors proposed three extensions to the RSVP-TE protocol: Regenerator object (RO), Regenerator flag (RF), Regenerator availability object (RAO). In brief, the RO extension was used to assign the regenerator to be used (i.e., by handling the regenerator ID). The RF extension was used to specify the optical node where regeneration should be performed. Finally, the RAO extension was used to collect the set of available regenerator in each intermediate node along the optical path. Therefore, depending on the information stored in the optical nodes, the information disseminated by OSPF-TE and the ones to be collected by RSVP-TE (i.e., depending on the extensions used between the three proposed), different provisioning strategies were proposed [141]. Some are based only on RSVP-TE [143, 144] in order to avoid the advertisement of a large amount of information in the control plane. Others are based on both protocols (i.e., RSVP-TE and OSPF-TE) [145].

Alternatively, in [142], a bit is appended in the wavelength label ERO sub-object, where it is used to indicate for intermediate nodes that an optical regeneration is required locally. This proposition considers that regenerator per node availability is already disseminated through OSPF-TE protocol.

4.2 Contributions

In fact, the RSVP-TE extensions proposed in [141, 142] does not respect the RFC standard of the RSVP-TE protocol, since non-standardized objects (e.g., RAO, RO) were defined and used to convey regeneration information rather than using standardized objects. On the contrary, the extensions proposed in [124, 140] to RSVP-TE and OSPF-TE, respect the RFC standards of these protocols. However, these extensions were proposed before the apparition of the RFC7581 and RFC7689 standard [146, 147] in June and November 2015 respectively. Therefore, some of the encoding formats of these extensions should be adapted to the proposed standard.

Indeed, the RFC standard in [146] proposes a specific encoding formats for a set of information fields described in [148]. These encoding formats concerns information needed by the Routing and Wavelength Assignment algorithm and used to disseminate four categories of information: Node Information, Link Information, Dynamic Node Information, and Dynamic Link Information. The goal is to facilitate the path computation and the establishment of LSPs in translucent optical networks.

In this chapter, we focus on the Node Information that concerns optical regeneration modules and the connectivity matrix in optical nodes. However, we assume that there are no connectivity constraints in the optical nodes. Therefore, we consider only the information related to the optical regeneration modules to allow the assignment of the optical regeneration modules during the signaling of an optical channel. In this respect, we propose new routing algorithm, signaling mechanism and protocols extensions for the GMPLS control plane, to allow performing the power adaptation process in translucent networks. In particular, we propose new extensions to RSVP-TE and OSPF-TE protocols to take into account for regeneration and power information during the establishment of a regenerated optical channel. The performance of the novel scheme is demonstrated with simulations considering dynamic traffic patterns. The simulated scenarios are evaluated through their blocking probability as a function of the network load considering three network topologies.

The rest of this chapter is organized as follows. Section 4.3 presents the method used to assign regeneration sites and the one used to compute the power adaptation coefficients for a regenerated optical path in translucent network. Section 4.4 presents the developed path computation algorithm that takes into account optical regeneration. Section 4.5 is dedicated to the proposed extensions for OSPF-TE and RSVP-TE protocols. The novel signaling mechanism is explained through an example of channel establishment. Section 4.6 presents simulated scenarios and performance results over the network topologies considered. Finally, the conclusion is presented in Section 4.7.

4.3 Optical power control with regeneration

4.3.1 Optical regeneration assignment method

In translucent network, when the optical channel is not physically feasible, an optical regeneration (for our purposes, OEO conversion) is performed in one or several nodes along the path, to get an acceptable quality of transmission (e.g., OSNR, Q or BER) at the receiver side. Usually, the strategy of operators is to reduce the cost of the network by minimizing the number of regenerators used. This minimum cost is ensured by exploiting the maximum reach of the optical transceivers. In this chapter, we consider this regeneration strategy which we call hereafter "default regeneration algorithm".

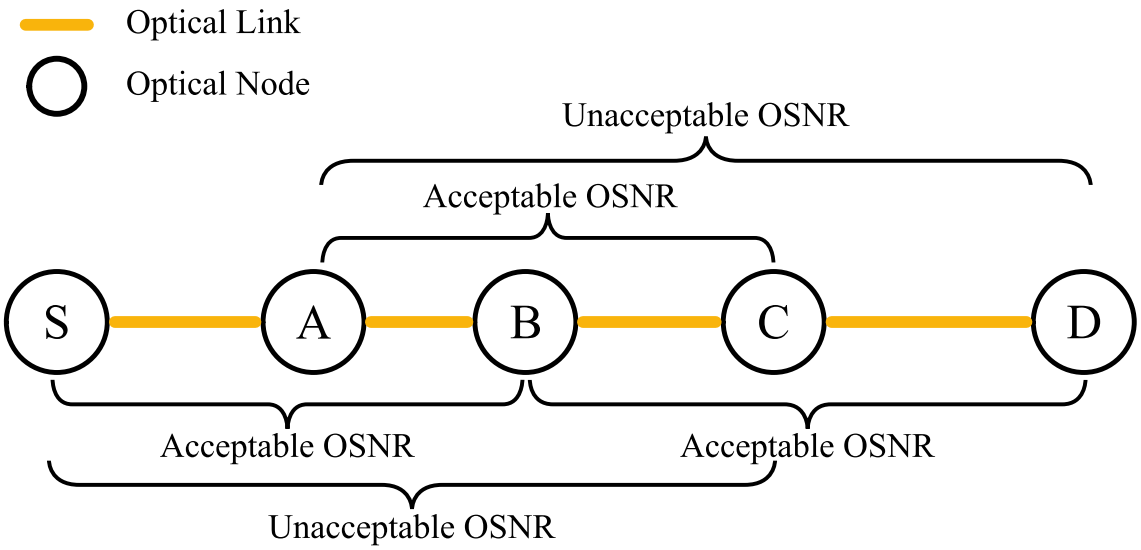

Figure 4.1: Example of an unfeasible optical path

Figure 4.1, shows an example of connection establishment over an unfeasible optical path. In fact, since the optical path is physically unfeasible between the source and destination nodes, regeneration sites should be assigned at intermediate nodes to get a working channel (i.e., an acceptable OSNR at the receiver side). In this example, several regeneration sites combination are possible, however, only one combination guarantees minimum cost. Indeed, regeneration combinations such as regeneration in node A and C, or regeneration in node A, B and C are possible, but they are not the best solution in terms of cost. Therefore, if the default regeneration algorithm is applied, only the node B is assigned to perform the optical regeneration, since it allows exploiting the maximum reach of the transceiver and thus minimizing the number of regenerators used.

4.3.2 Power adaptation with optical regeneration

Once the regeneration sites are identified with any regeneration algorithm (e.g., the default regeneration algorithm or others), the optical path is then decomposed into a set of feasible transparent segments. Therefore, in order to perform the power adaptation process over the regenerated optical path, the power adaptation coefficient should be computed for every transparent segment. In this respect, OSNR estimation is performed over each segment to compute the $OSNR_{margin}$ per segment and thus deduce the applicable $C_{adaptation}$ coefficient.

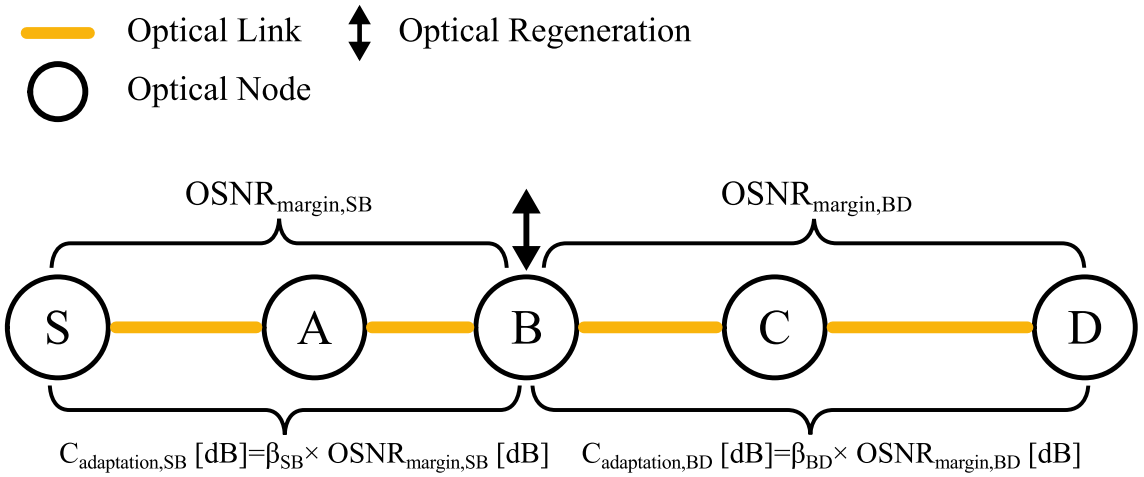

Figure 4.2: Regeneration assignment using the default regeneration algorithm

We consider the example of Figure 4.1, where an optical regeneration is performed in Node B (as shown in Figure 4.2). In this example the optical path is decomposed into two transparent segments SB and BD. Therefore, two $C_{adaptation}$ coefficients are required, in order to adapt channel optical power. Figure 4.2, shows the two $OSNR_{margin}$ computed over the two segments: $OSNR_{margin,SB}$ and $OSNR_{margin,BD}$. From these two $OSNR_{margin}$, we can deduce the value of $C_{adaptation}$ coefficients and thus adapt channel optical power at the transmitter side of each segment.

4.4 Routing algorithm with regeneration

To provision an optical channel in translucent optical network, we propose a new path computation algorithm that considers spectral and power resources, physical feasibility of the optical channel and assignment of regeneration, in addition to channel power adaptation. Figure 4.3 shows a simplified representation of the algorithm (the essential blocks constituting the algorithm). In our work, the connection request is always sent to the ingress node, on which the path computation algorithm is always executed. Therefore, similarly to the path computation algorithm in the case of transparent optical networks, the algorithm tries to find an optical path that satisfies the request.

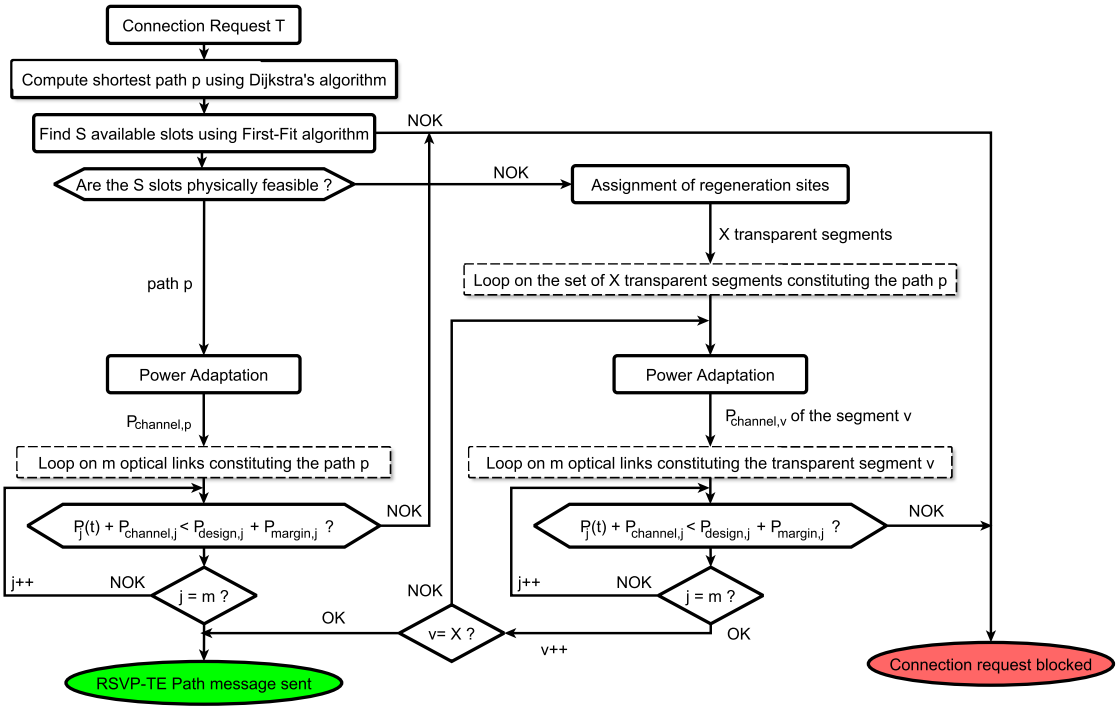

Figure 4.3: Path computation algorithm with regeneration

In this respect, the algorithm computes first the shortest path using Dijkstra's algorithm, for every optical connection request of T Gbit/s capacity, between a pair of source and destination nodes. Then, using the first-fit algorithm, it tries to find a group of S available slots of 12.5 GHz that are continuous, contiguous and satisfies the capacity T of the request. For any request, the S slots are computed to get minimum spectrum occupation, supposing a fixed modulation format and baud rate. If no available slots are found the connection request is blocked.

Furthermore, once the S available and successive spectrum slots over the shortest path p are found, the physical feasibility test is performed. This test checks whether an optical channel can be established transparently (without optical regeneration) over the path p (i.e., $OSNR_{est,p} > OSNR_{req,p}$). If it is the case (i.e., the path p is physically feasible without regeneration), then a transparent segment can be established and just one $C_{adaptation}$ coefficient is required to adapt the power of the channel. In contrast, if the path is not physically feasible, one or several optical regeneration are to be performed to get a working channel. The number of the performed regeneration depends on the accumulated impairments over the path and on the regeneration assignment strategy used (i.e., minimum regeneration or other strategies [149]). As a result, depending on the number of regeneration sites, the path p is decomposed into a set of X transparent segments. Therefore, an $OSNR_{margin}$ is to be computed per segment to get the applicable $C_{adaptation}$ value (i.e., applicable power attenuation) over every segment of the path p.

After the computation of the $C_{adaptation}$ coefficients, a power verification test is performed to ensure that the newly added channel will not cause any saturation problem over the links constituting the path p. Similarly to the case of transparent network, this test consists in comparing, for every link of the path p, its aggregate power $P(t)$ (after adding the power of the new channel $P^{adapted}_{channel,l}$) with its maximum allowed power ($P_{max,l}$).

In the case where no optical regeneration is performed, the channel power value per link l is $P^{adapted}_{channel,l} = P^{opt}_{channel,l}/C_{adaptation,p}$. Contrariwise, in the case where optical regeneration is performed, a different $C_{adaptation}$ coefficient is applied per transparent segment. Therefore, the channel power value per link l is $P^{adapted}_{channel,l} = P^{opt}_{channel,l}/C_{adaptation,v}$ where v is the index of the transparent segments of the path p. Once these tests are done, the signaling process can be triggered over the chosen path. In that case, an extended RSVP-TE $Path$ message containing power and regeneration information is sent downstream in order to set up the optical channel. If any of these tests fail, the connection request is rejected.

Finally, in each crossed hop during the signaling process, the power verification test is performed to check if the aggregated power over the outgoing link does not exceed the $P_{max,l}$. Indeed, if connection requests are frequent, some signaling process may simultaneously compete for the same optical resources in terms of optical power (race condition). This is why the signaling should avoid any over-provisioning due to the not-yet-updated link database. The same phenomenon (i.e., resources competition) could arise for the optical regeneration modules. Therefore, a last verification test is performed in the regenerating nodes to ensure that the requested regenerator modules are still available.

Besides, to perform such path computation algorithm a set of information is required. In the following section, we propose several GMPLS protocol extensions to allow the execution of such an algorithm in the control plane and thus making possible the provisioning of optical channels in translucent networks.

4.5 GMPLS protocol extensions with regeneration

In Chapter 3, GMPLS protocol extensions was proposed to include routing ($P_{design,l}$, $P_{margin,l}$, $P_{channel,l}$, and $P_l(t)$, $OSNR_l$) and signaling information (i.e., β, $C_{adaptation}$) allowing the execution of the path computation algorithm in transparent networks. However, in the case of translucent networks, additional extensions are required to take into account for the regeneration information and to facilitate the application of the power adaptation process. These extensions are essential to be able to use the path computation algorithm developed in Section 4.4. Therefore, in this section, we propose new extensions to OSPF-TE and RSVP-TE protocols. Subsequently, we provide the detailed description of these extensions, their encoding formats and present through an example the routing and signaling mechanisms used to exploit them.

4.5.1 OSPF-TE

During path computation, optical regeneration sites are usually assigned when the path is not physically feasible. However, this assignment process requires a prior knowledge of the regeneration modules sites (i.e., in which node), their capabilities (e.g., acceptable bit rates, modulation formats, etc.) and availability, and lastly their connectivity in the optical nodes (i.e., input/output ports connectivity). In this respect, the RFC standard in [146] proposed several encoding formats to facilitate the dissemination of node information and particularly the regeneration information.

In fact, the OSPF-TE protocol allows the dissemination of two types of information: Node and link information. Usually, these two kinds of information are disseminated using two top-level TLVs: Optical Node Property TLV and Link TLV. The information concerning the optical node can be separated into two categories [150]: node devices (e.g., optical regenerators) and switching capabilities of the node (i.e., connectivity matrix) [151]. Indeed, depending on the control plane implementation being used and on the switching capability of the ROADMs, the Connectivity Matrix information may be optional. In this work, we suppose that the ROADMs support symmetric switching (complete port-to-port connectivity) and thus there is no need to advertise their internal connectivity. Therefore, we consider only the information concerning optical devices in the ROADMs. The Optical Node Property TLV includes node properties and signal compatibility constraints. The RFC standards in [152] defined five sub-TLVs to describe these properties and constraints:

1. Resource Block Information,
2. Resource Accessibility,
3. Resource Wavelength Constraints,
4. Resource Block Pool State,
5. Resource Block Shared Access Wavelength Availability.

These five sub-TLVs represent respectively, the resource signal constraints and processing capabilities of a node, the structure of the resource pool (i.e., optical regenerator pool) in relation to the switching devices in the node, the input or output wavelength ranges (for wavelength converter devices), the usage state of a resource (i.e., the availability of an optical regenerator), and lastly the accessibility via shared fibers. For simplification reason, we suppose that there are sufficient optical ports and switching modules to handle all wavelength signals. Therefore, only the Resource Block information and the Resource Block Pool State are required and there is no need to advertise the rest of the proposed sub-TLVs.

On one hand, the Resource Block information sub-TLV allows to list optical regenerators existing in the optical nodes and enables the description of their processing capabilities (e.g., acceptable bit rates, modulation formats, types of regenerator: 1R, 2R, 3R, etc.). On the other hand, the Resource Block Pool State allows having updated

information on the available regenerators in each node after the establishment of any LSP. Hence, to take into account this information, we propose here to add two new sub-TLVs to the Opaque LSA type 1 (”Traffic Engineering LSA”) in the TE Node Attribute TLV (type 6). The encoding of these sub-TLVs is presented in [146].

In this work, we consider only the 3R regeneration (signal amplification, pulse shaping and timing regeneration). Therefore, the first sub-TLV which is called ”RB Set Field” includes the identifiers range for the 3R regeneration modules in every node. Its encoding description is presented in [146]. In our case, we suppose that there is only one range defined per node, and thus the sub-TLV can be encoded on 8 bytes: the first 4 bytes encode the identifier for the start of the range, and the last 4 bytes encode the identifier of the end of the range. Moreover, 4 additional bytes are used to indicate the processing capabilities of the regeneration modules (i.e., to indicate that the regeneration type is 3R). The encoding description is also presented in [146].

The second sub-TLV includes the state of regenerator modules in form of bitmap formats to allow identifying if the requested regenerator module is available or used. This sub-TLV has a variable length since it depends on the number of regeneration modules in the node, but it must be a multiple of 4 bytes (with padding bits if required). Each bit from the sub-TLV indicates the usage status for a regeneration module (0 for available and 1 for used). The sequence of the bitmap is ordered according to the identifiers sequence defined in the ”RB Set Field” (i.e., the first bit of the bitmap sub-TLV corresponds to the first regeneration module in the regenerators list of the ”RB Set Field” sub-TLV). These OSPF-TE extensions, in addition to the previously proposed in Chapter 3 for link parameters, represents the total information required by any node to execute the path computation algorithm proposed in Section 4.4.

4.5.2 RSVP-TE extensions

In Chapter 3, we have conveyed through RSVP-TE $Path$ message the required connection information to establish a transparent optical channel. This RSVP-TE $Path$ message included information on: the central frequency (i.e., channel label), the channel width, and the $C_{adaptation,p}$ parameters. These parameters were valid for an end-to-end connection in a transparent optical network. However, in translucent networks, since optical regenerations are performed, the same information is required for every transparent segment constituting the optical path. Moreover, additional information is also required to indicate the need to regenerate the optical signal in intermediate nodes.

4.5.2.1 Label encoding

In this respect, we propose to use the Flexi-Grid Label in the Label ERO sub-object as in [153]. The encoding of the Flexi-Grid Label is presented in [154]. This label is used to encode the central frequency and the width (i.e., reserved spectrum bandwidth) of the optical channel. In this work, we suppose that the optical channel keeps the same

Flexi-Grid Label all over the path, even if the optical channel is regenerated in intermediate nodes (i.e., we do not take into account the use of wavelength converters). Therefore, the added labels in the ERO sub-object are the same before and after the identifiers of the regeneration nodes. Once the following extensions are specified under these assumptions, the move to wavelength conversion will be straightforward.

4.5.2.2 Extension for $C_{adaptation}$

After the execution of the path computation algorithm in the ingress node, the required Beta and $C_{adaptation}$ parameters are available to be applied over the set of segments constituting the regenerated optical path. Therefore, as in Chapter 3, we propose to create 8 bytes sub-TLVs (2 bytes for type, 2 bytes for length, 2 bytes to encode the value of β and 2 bytes to encode the value of $C_{adaptation}$) in the ERO Hop Attributes sub-object (type 35) in the form of Hop Attributes TLVs [155]. Indeed, multiple Hop Attributes TLVs may be added, depending on the number of hops of the optical path (i.e., proportional to the number of nodes in the path). In fact, the added Hop Attributes TLVs should have the same values per transparent segment; in contrast, they can have different values between the different transparent segments.

4.5.2.3 Regeneration encoding

When the computed optical path is not physically feasible, the path computation algorithm tries to find available regeneration modules in intermediate nodes to regenerate the optical signal. This is possible thanks to the disseminated regeneration modules availability information by the OSPF-TE extensions proposed in Section 4.5.1. Once the optical regeneration modules are chosen through the regeneration algorithm (in our work, using the default regeneration algorithm), their identifiers should be conveyed through RSVP-TE $Path$ message in order to request their activation in the corresponding nodes.

Therefore, we propose to use the extension ResourceBlockInfo sub-TLV as defined in [147]. In our case, we encode this extension in form of 8 bytes sub-TLVs (1 byte for type, 1 byte for length, 4 bytes to encode the regenerator identifier and 2 bytes padded with zeros to ensure four-octet alignment of the sub-TLV) and we add it in the ERO Hop Attributes sub-object (type 35) in the form of Hop Attributes TLVs. The number of added ResourceBlockInfo sub-TLVs (which we call hereafter “Regeneration” extension) depends on the number of signal regeneration to be performed over the optical path. These extensions include the identifiers of the assigned optical regeneration modules, and they are proposed in respect to the recommendations of the RFC standard in [147].

4.5.3 Connection establishment example

To understand the provisioning process with power adaptation in translucent optical network, we consider here, as an example, an optical network with six optical nodes (i.e., ROADMs). Figure 4.4 shows the six interconnected nodes (A, B, C, D, E, and F).

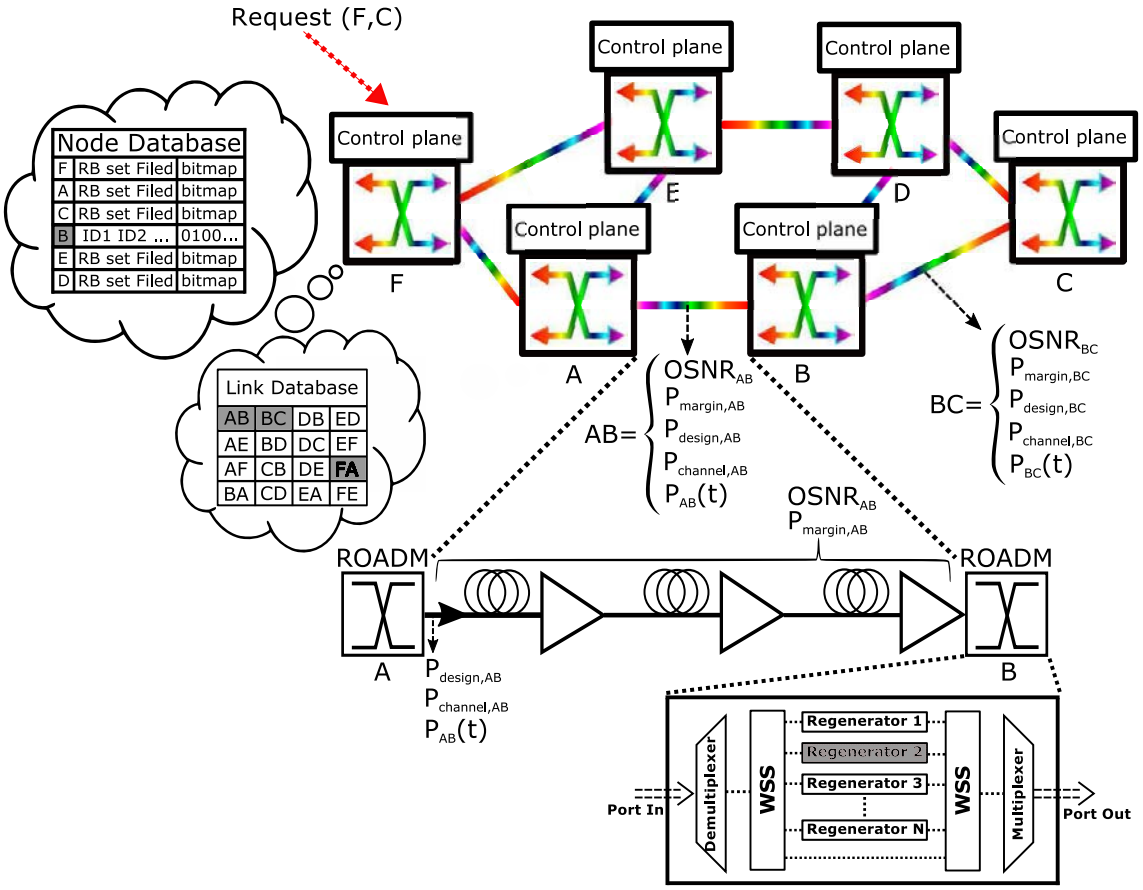

Figure 4.4: Network example

We assume that optical design has already been performed for all network links, and that every node database is filled with links (spectrum bitmap, $P^{opt}_{channel,l}$, $P_{design,l}$, $P_{margin,l}$, $OSNR_l$, and $P_l(t)$) and nodes (RB Set Field, regenerator availability bitmap) information. Moreover, we suppose, in this example, that a connection request between the ROADMs F and C is sent to Node F. Figure 4.5 shows the signaling mechanism and the RSVP-TE message flow triggered to establish the optical channel.

In fact, upon receipt of the connection request by Node F, the path computation algorithm is triggered. We assume that, after performing the algorithm, the selected path p is F-A-B-C (shortest path) and a set of S free available slots is found respecting the continuity and contiguity constraints. We suppose also that the path p is not transparently feasible, because its $OSNR_{est,FABC}$ is below the acceptable $OSNR_{min}$, and thus the Node B is assigned to perform signal regeneration. The regeneration in Node B was chosen in respect to the minimum regeneration strategy described in Section 4.3 (i.e., using the default regeneration algorithm). In this respect, the optical path is decomposed into two transparent segment F-A-B and B-C, where $OSNR_{est,FAB}$ and $OSNR_{est,BC}$ are higher than $OSNR_{min}$. In this case, the optical channel is power adaptable over the two segments and the $C_{adaptation}$ parameter is computed per segment

($C_{adaptation,FAB}$ and $C_{adaptation,BC}$).

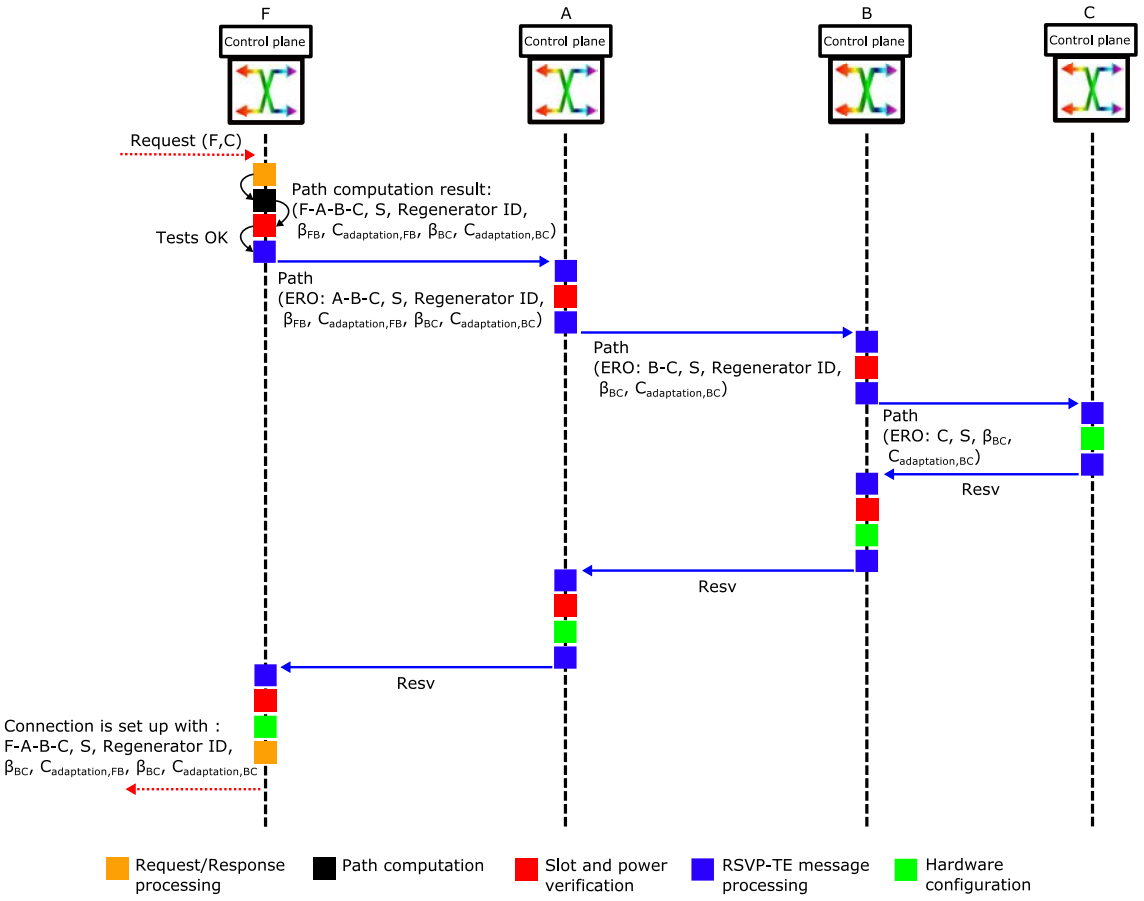

Figure 4.5: Flow diagram in F, A, B, and C controller during the connection provisioning process.

Before triggering the RSVP-TE signaling process, Node F performs the slot and power verification tests over its outgoing link (i.e., FA). These tests are executed to ensure that optical spectrum resources are still available and no power saturation will occur after adding the new optical channel over link AB ($(P_{FA}(t) + P^{opt}_{channel,FA}/C_{adaptation,FAB} \leq P_{design,FA} + P_{margin,FA})$).

Once verification is done, Node F sends an RSVP-TE $Path$ message to Node A including the information on the selected path p, the S slots used, the identifier of the regeneration module and the $C_{adaptation}$ parameters values (i.e., $C_{adaptation,FAB}$ and $C_{adaptation,BC}$). These channel parameters are added in ERO, in form of a list of sub-objects as proposed in Section 4.5.2 (in the section that talks about extensions) and respecting the processing of the ERO in [43]. Figure 4.5 shows some details of the RSVP-TE message sent to Node A.

Upon reception of the $Path$ message by Node A, the same tests are performed over its outgoing link, AB (it checks that S is still available over the link AB and that

$P_{AB}(t) + P^{opt}_{channel,AB}/C_{adaptation,FA} \leq P_{design,AB} + P_{margin,AB}$. Then, once this verification is done, Node A sends a $Path$ message to Node B after processing the ERO as specified in [43].

Once Node B receive the $Path$ message from Node A, it detects the "Regeneration" extension in the ERO sub-object and thus check whether the requested regenerator is still available or it has been used by another connection. If it is available, the slot and power verification tests are performed over its outgoing link BC (it checks that S is still available over the link BC and that $P_{BC}(t) + P^{opt}_{channel,BC}/C_{adaptation,BC} \leq P_{design,BC} + P_{margin,BC}$). At the end of this step, Node B sends a new $Path$ message to the Node C.

Once the $Path$ message arrives at the egress Node C, a hardware configuration is performed for its Drop port (in order to receive the optical channel). Moreover, the spectrum bitmap and the power value of the link BC are updated (($P_{BC}(t) = P_{BC}(t) + P^{opt}_{channel,BC}/C_{adaptation,BC}$)) in its local database, then a $Resv$ message is sent to Node B.

On receipt of the $Resv$ message by Node B, slot availability (not necessary in case local resource reservation was made during downstream signaling) and power verification tests are performed again over link BC. Then, a hardware configuration is made to the requested regenerator and the required power attenuation is applied at the input of the transmitter. Moreover, the spectrum bitmap, regeneration availability bitmap and the power value of link BC are updated in its local database, and a $Resv$ message is sent to Node A.

In turn, Node A executes the same tests over link AB after the receipt of the $Resv$ message and once verification is done, a last $Resv$ message is sent to Node F. These tests are repeated in Node F after the reception of the $Resv$ message. Then, a hardware configuration is performed to its Add port and a power adaptation is applied to the transmitter. Moreover, the spectrum bitmap, regenerator availability bitmap and the power value of link FA ($P_{FA}(t) = P_{FA}(t) + P^{opt}_{channel,FA}/C_{adaptation,FA}$) are updated in its local database. Finally, the optical channel is established, and a connection setup confirmation is sent back to the requester (e.g., network operator or client device).

It is important to note that every optical node sends to its neighboring nodes a set of OSPF-TE advertisements. These advertisements are sent to regularly update other nodes with the changes over its outgoing links, typically after the end of a signaling phase. In our case, additional advertisements are sent to update the changes in optical nodes (i.e., to update the availability of optical regeneration modules in each node).

4.6 Simulation and results

4.6.1 Simulation setup and scenarios

In order to evaluate the proposed power control process in translucent network, we improved our distributed GMPLS-based network simulator to take into account the optical regeneration. The simulator was extended by adding the newly proposed OSPF-TE

and RSVP-TE protocol extensions in Section 4.5. The novel path computation algorithm and the signaling mechanism are implemented as explained in Section 4.5.3 and 4.4. Moreover, the simulator takes as input a network topology (links, spans, and amplifier types) and designs its optical links using our design method presented in Section 3.3.1. Finally, it fills in the OSPF-TE database the essential needed parameters (link spectrum bitmap, $P^{opt}_{channel,l}$, $P_{design,l}$, $P_{margin,l}$, $OSNR_l$, $P_l(t)$, regenerator availability bitmap, RB set field).

Simulations are performed over the same network topology of chapter 3 (32 optical nodes and 42 optical links of the European backbone network) assuming same links parameters (CD, alfa, non-linearity coefficient, etc.) and same amplifiers portfolio. Moreover, in order to understand the impact of network topology on link power resources, additional simulations are performed over two other network topologies: German (with 17 nodes and 26 links) and NSF (with 14 nodes and 21 links).

However, in order to simplify the results analysis, only 100 Gbit/s optical channels are established in all scenarios (T = 100 Gbit/s). Filtering penalties induced by transiting across one optical node are 0.05 dB for the 50 GHz (four slots of 12.5 GHz) channel spacing and 0.64 dB for the 37.5 GHz (three slots of 12.5 GHz) [156]. The minimum accepted OSNR at the receiver side, using 0.1 nm noise reference bandwidth, including operational margins, is set to 15 dB for 100 Gbit/s QPSK modulation format with coherent detection and soft decision FEC, whatever the channel bandwidth (three or four slots of 12.5 GHz). Eight scenarios are considered. The first six scenarios are similar to the ones described in Chapter 3 (i.e., FG, FG4S_PAPV, FX, FX3S_PAPV and FX3-4S_PAPV) with the difference that they take into account optical regeneration:

- Fixed-grid with optical regeneration (FG_R): this scenario is the same as FG, but in the case of non-feasible channel, the path computation algorithm assigns an optical node to perform signal regeneration. The spectral occupation is four slots over each transparent segment.

- Fixed-grid with power control, power margins and optical regeneration (FG4S_PAPV_R): this scenario is the same as FG4S_PAPV but with optical regeneration capability. The channel power adaptation is performed over the transparent segments constituting the optical path (power adaptation to the minimum acceptable OSNR value).

- Flex-grid with optical regeneration (FX_R): this scenario is the same as FX but with optical regeneration capability. The regenerated channels occupy only three contiguous slots over every transparent segment.

- Flex-grid with power control, power margins and optical regeneration (FX3S_PAPV_R): This scenario is the same as FX3S_PAPV but with optical regeneration capability. The channel power adaptation is performed over the transparent segments constituting the optical path (power adaptation to the minimum acceptable OSNR value).

- Flex-grid with power control, power margins and optical regeneration (FX3-4S_PAPV_R4): This scenario is the same as FX3-4S_PAPV, but with optical regeneration capability. However, the path computation algorithm first tries three slots of 12.5 GHz for the channel setup. If the path is not physically feasible, the algorithm tries to establish the optical channel using four slots. If still unfeasible, a set of optical nodes is assigned for signal regeneration. This regeneration is performed using four slots channel. The channel power adaptation is performed over the all the transparent segments constituting the optical path (OSNR computation consider the filtering penalty for the 4 slots channel and the channel is adapted to the minimum acceptable OSNR value).

- Flex-grid with power control, power margins and optical regeneration (FX3-4S_PAPV_R3): This scenario is the same as FX3-4S_PAPV, but with optical regeneration capability. However, the path computation algorithm first tries three slots of 12.5 GHz for the channel setup. If the path is not physically feasible, the algorithm tries to establish the optical channel using four slots. If still unfeasible, a set of optical nodes is assigned for signal regeneration. Contrarily to the previous scenario, this regeneration is performed using 3 slots channel. The channel power adaptation is performed over the all the transparent segments constituting the optical path (OSNR computation consider the filtering penalty for the 3 slots channel and the channel is adapted to the minimum acceptable OSNR value).

The last two scenarios are:

- Flex-grid with optical regeneration (FX3-4S_R): This scenario is the same as FX3-4S, but with optical regeneration capability. The path computation algorithm first tries three slots of 12.5 GHz for the channel setup. If the path is not physically feasible, the algorithm tries to establish the optical channel using four slots. If the path is still unfeasible, the algorithm tries to establish the optical channel using four slots. If still unfeasible, an optical node is assigned for signal regeneration. This regeneration is performed considering a four slots channel.

- Flex-grid with unlimited link power resources and optical regeneration (FX3S_Full_R): This is a bench mark scenario. It is considered to evaluate the power saturation problem. In this scenarios, only three slots channels are established and the $P_{max,l}$ of every link l is supposed unlimited.

In this work, several fixed-grid and flex-grid scenarios are simulated. Therefore, in order to fairly compare them, we perform the same link design for eighty 100 Gbit/s QPSK channels over a 50 GHz grid (80 × 50 GHz = 4 THz per link) for all scenarios. However, the full usable bandwidth of each link is set to 4.8 THz (optical amplifier usable bandwidth) as defined by the ITU-T. Table 4.1 summarizes the eight simulated scenarios.

Simulated scenarios	Power adaptation	Power margin	Channel Spacing (GHz)	Filtering penalty (dB)	Channel spacing after regenration (GHz)
FG_R	No	No	50	0.05	50
FG4S_PAPV_R	Yes	Yes	50	0.05	50
FX_R	No	No	37.5	0.64	37.5
FX3S_PAPV_R	Yes	Yes	37.5	0.64	37.5
FX3-4S_R	No	No	37.5 or 50	0.05 or 0.64	50
FX3-4S_PAPV_R4	Yes	Yes	37.5 or 50	0.05 or 0.64	50
FX3-4S_PAPV_R3	Yes	Yes	37.5 or 50	0.05 or 0.64	37.5
FX3S_Full_R	Not required	Not required	37.5	0.64	37.5

Table 4.1: Simulated Scenarios

The path computation algorithm presented in Section 4.4 is modified to enable the simulation of the different scenarios. Depending on the scenario, some tests are activated or deactivated. In this algorithm, only one shortest path is computed for any request between any node pairs (s, d). The connection request is blocked if it cannot pass the set of tests (continuity, contiguity, physical feasibility, and, if needed, power feasibility). Once all the tests are passed (with or without signal regeneration), the provisioning process is triggered with a set of channel parameters (path, slots, one or multiple $C_{adaptation}$ coefficients, and one or multiple regenerator identifiers). The number of required parameters depends on the channel characteristics (i.e., if it can be established with or without signal regeneration).

4.6.2 Simulations configuration

Scenarios were simulated considering a dynamic connection establishment, where optical connections are established and released automatically. Connection requests are dynamically generated following a Poisson process, where every source-destination pair of each request is randomly chosen among all network nodes according to a uniform distribution. The inter-arrival and holding times for every request follow an exponential distribution with averages of $1/\lambda$, and $1/\mu$, respectively. The connection holding time $1/\mu$ is fixed to 100 s. The offered network load is obtained by varying $1/\lambda$. The processing time of the packets is considered negligible compared to the propagation delays.

For each network load (i.e., for every value of $1/\lambda$), thirty simulation runs (each run with a different seed) are performed for each of the eight scenarios. Simulation results are collected after the arrival of 35×10^4 requests in order to ensure that the network is in a stable state. The results depicted in the following figures are given by averaging the 30 simulation runs of each $1/\lambda$ with a confidence interval of 95% (too small to be displayed on the figures). It is important to note that, for every scenario, the same 30 seeds are used in order to exactly simulate the same sequence of optical connection

requests. Moreover, the number of 3R regeneration modules per node is considered as unlimited and thus no blocking could occur due to regenerator modules unavailability.

4.6.3 Simulation results

We consider the blocking probability (BP) as an evaluation criterion. It is expressed as the ratio between the number of blocked lightpaths and the number of requested lightpaths. Simulation results for blocking probability are plotted as a function of the total network load defined as $N \times \lambda/\mu$, where $N = 32$ is the number of network nodes and the load is expressed in Erlang.

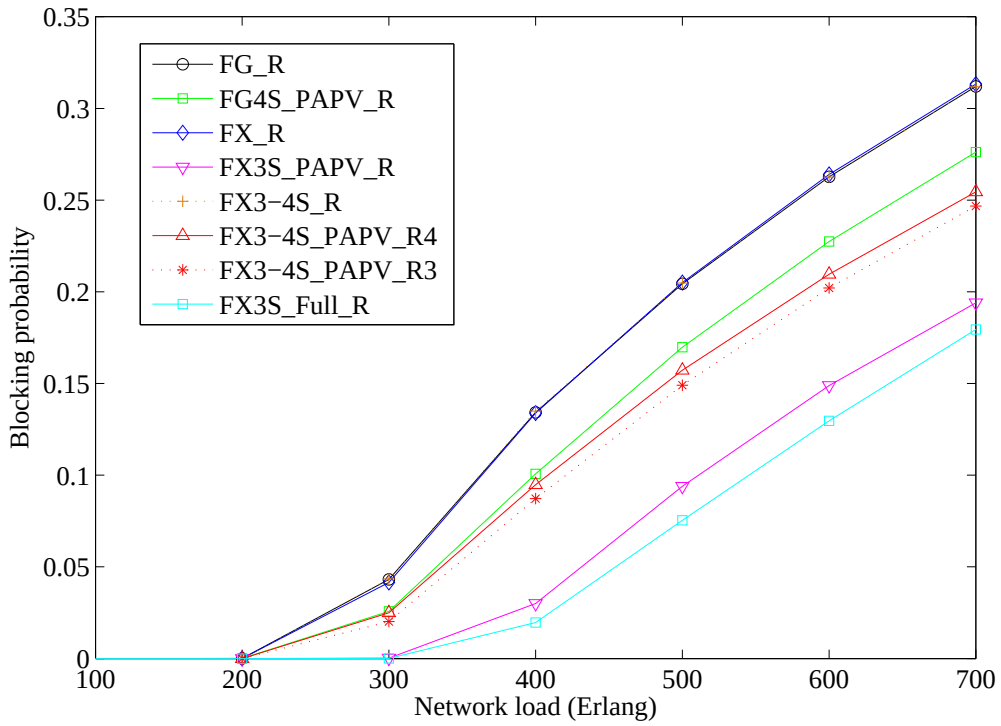

Figure 4.6: Blocking probability versus Network load

Figure 4.6 shows the blocking probability of the eight scenarios as a function of network load. The result is similar to the incremental scenarios without optical regeneration. Indeed, all scenarios with power adaptation (i.e., FG4S_PAPV_R, FX3S_PAPV_R, FX3-4S_PAPV_R4 and FX3-4S_PAPV_R3) have lower BP than the other scenarios (i.e., FG_R, FX_R, and FX3-4S_R). We can notice that, FG_R, FX_R and FX3-4S_R scenarios have approximately the same blocking probability. These scenarios are not limited anymore to physical feasibility and thus optical regeneration can be performed when required. Therefore, the blocking in these scenarios can occur only due to spectrum

unavailability or due to the limitation of channel number, which explains the difference with the case without optical regeneration in Chapter 3.

In fact, the use of flex-grid technology in FX_R and FX3-4S_R (3 slots channels) allow reducing the spectrum occupation in optical links. However, even if there is available spectrum slots to establish an optical channel, the blocking can arise from the limited channels number per link (channel number is limited to avoid power saturation since the control plane is not power aware). Accordingly, the blocking in FX_R is more likely to be due to channel number limitation, where channels number is limited to 80 per link. However, in FX3-4S_R the blocking occurs due to the spectrum fragmentation and to channels number limitation, since the mixing between three and four slots creates unusable spectrum slots. This analysis is confirmed in the next section when blocking reasons are analyzed.

In contrast, the performance of FG4S_PAPV_R, FX3S_PAPV_R, FX3-4S_PAPV_R4 and FX3-4S_PAPV_R3 scenarios is differently impacted. Indeed, in these scenarios, an additional type of blocking could arise which is the power saturation. The FG4S_PAPV_R in Figure 4.6 shows that, the use of the power adaptation process while conserving the fixed-grid technology helps increasing the performance of the network. This increase is realized through the power saving, allowing the establishment of more than 80 channels per link. However, this gain is directly limited by the spectrum occupation due to the use of four slots channels, promoting in this respect, more blocking due to spectrum unavailability.

We can notice also on Figure 4.6, that the use of flexible technology with power adaptation offers better performance in terms of blocking probability. Indeed, the FX3S_PAPV_R, FX3-4S_PAPV_R and FX3-4S_PAPV_R3 scenarios undergo less blocking due to the use of use of 3 slots channels reducing the spectrum occupation in optical links. These scenarios benefits at the same time from the spectrum occupation reduction and from power saving. However, the FX3_PAPV_R perform less blocking probability in comparison with FX3-4S_PAPV_R4 and FX3-4S_PAPV_R3, knowing that it was the inverse with the incremental channel establishment in chapter 3.

Indeed, FX3_PAPV_R4 and FX3_PAPV_R3 is no more suffering from physical feasibility problem, and thus the high filtering penalty that was severely affecting channel performance (i.e., affecting the reaches of the 3 slots channels) is no anymore a serious problem due to optical regeneration. Contrariwise, the FX3-4S_PAPV_R4 and FX3-4S_PAPV_R3 scenarios, due to the dynamic traffic establishment and to the mixing between three and four slots channels, undergo more severe spectrum fragmentation. Therefore, even if there is sufficient available power, the blocking will occur due to fragmented spectrum of network links. However, FX3-4S_PAPV_R3 perform less blocking than FX3-4S_PAPV_R4 since the regenerated channels in FX3-4S_PAPV_R3 use 3 slots rather than 4 slots, which reduces the spectrum occupation.

Not surprisingly, the FX3S_Full_R benchmark scenario has the lowest blocking probability and thus the best performance. This was expected since the spectrum unavailability is the only type of blocking that could occur, because link power resources are supposed unlimited. Therefore, the performance difference between the

FX3_PAPV_R and FX3S_Full_R is totally due to the effect of link power saturation.

4.6.4 Blocking reasons analysis

As in Chapter 3, we complete our study with a deep analysis of the blocking reasons in each scenario. To this end, we plotted the reasons of request blocking for each scenario in bar charts. The same four blocking reasons presented in Chapter 3 (No Spec, No OSNR, No Pow and MXCE) are considered in this evaluation. However, the No OSNR blocking does not exist anymore since optical regeneration can be performed when the path is not feasible.

The blocking counting method is described as follows: for each connection request and its computed path p, if there are no available continuous and contiguous slots that satisfy the connection request, the blocking reason is counted as No Spec. Contrariwise, in the case spectrum resources are available; the blocking reason is counted as No Pow or as MXCE depending on the scenario. For FG_R, FX_R and FX3-4S_R scenarios, because no power control is performed, the MXCE blocking reason is considered when the number of channels established over any link exceeds the maximum allowed (i.e., number of channels > 80). For the other scenarios with power awareness, the blocking reason is counted as No Pow. In summary, the priority is given to the No Spec blocking and then to the No Pow and MXCE. This counting method allows avoiding confusion on the No Pow blocking.

To fairly compare the different scenarios, we recorded for each scenario the blocking reasons for the 10000 connection requests generated after the first 35×10^4 requests (same request sequence, same traffic, and same set of source and destination node pairs for all scenarios). Then, we plotted (in bar charts) the number of blocked requests per blocking reason for each of the eight scenarios. Figure 4.7 shows the number of blocked requests in every scenario at a network load of 600 Erlang (where BP > 0.1).

We can notice that at this load (i.e., 600 Erlang) the scenarios without power adaptation, like FG_R, FX_R and FX34_R, have approximately the same number of blocked requests. In FG_R and FX3-4S_R, two reasons of blocking are occurring: No Spec and MXCE. However, in FX_R scenario, the blocking is only due to MXCE since the use of 3 slots channels reduces the spectrum occupation in every link and thus the spectrum is no more a serious limitation. This shows the impact of not considering link power resources (high number of blocked requests due to MXCE).

In FG4S_PAPV_R, FX3-4S_PAPV_R4 and FX3-4S_PAPV_R3 the blocking is due only to No Spec because of two reasons: there is no longer limitation to the number of channels per link and the power adaptation process was able to save sufficiently the required power for the additional channels (low filtering penalty for the 4-slot channels in FG4S_PAPV_R). However, even if the quantity of saved power is reduced due to the use of 3 slots channels in FX3-4S_PAPV_R4 and FG3-4S_PAPV_R3, only No Spec blocking is arising since the mixing of 3 and 4-slot channels increase the fragmentation of optical spectrum.

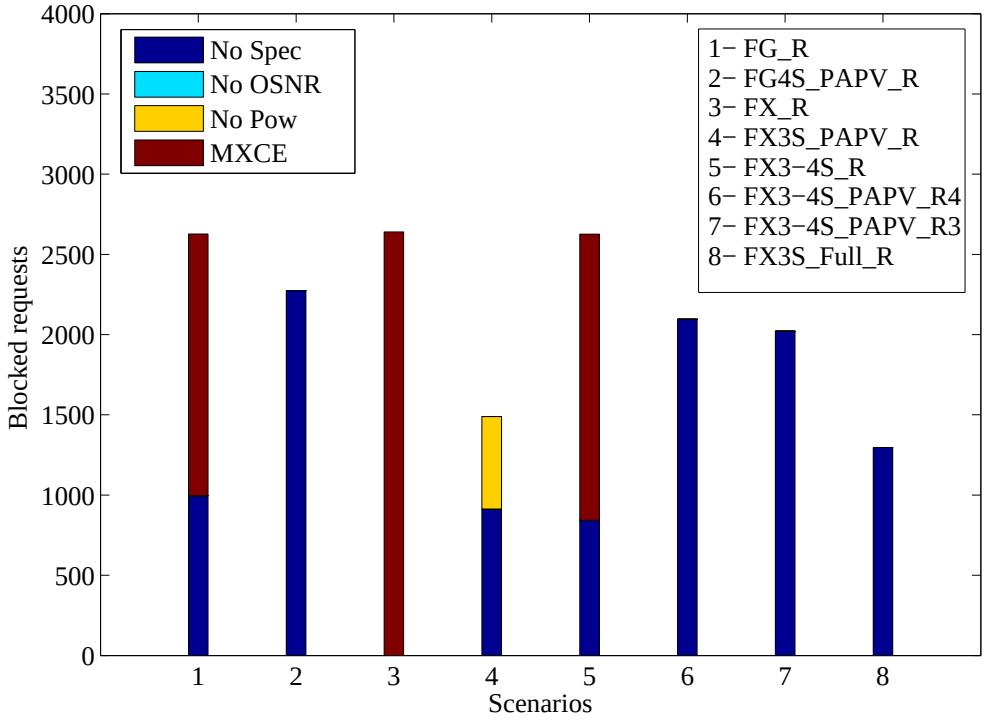

Figure 4.7: Blocking reasons per simulated scenario

Contrariwise, the FX3S_PAPV_R scenario is more impacted due to the use of 3 slots channels (which reduced the quantity of saved optical power because of the high filtering penalty). Therefore, the No Pow blocking appears in addition to the No Spec, because link spectrum is less fragmented (i.e., only horizontal fragmentation exists) and thus optical links can be more loaded. Finally, as expected in FX3S_Full_R, only No Spec blocking is arising because link power resources are supposed unlimited. These results demonstrate that the use of the power adaptation process allows reducing the number of blocked requests and thus increases network capacity and performance.

In summary, the results in Figures 4.6 and 4.7, demonstrate that upgrading the network with flex-grid technology without adapting channels power prevent benefiting from the reduction in spectrum occupation (as it was shown with FX_R and FX3-4S_R). Therefore, a power aware control plane with power adaptation process helps to increase network capacity and thus reduce the blocking probability as in FG4S_PAPV_R. Indeed, when flexibility is associated with power adaptation as in FX3S_PAPV_R, FX3-4S_PAPV_R4 and FX3-4S_PAPV_R3, we can get better network performance and an important increase in network capacity.

4.6.5 Performance in terms of optical regeneration

In terms of regeneration, each scenario performs more or less optical regeneration depending on the regeneration strategy used in the path computation algorithm. Figure 4.8 shows the number of optical regeneration modules used in the eight scenarios as a function of network load. We can notice that the scenarios using 4-slot channels (such as FG_R, FG4S_PAPV_R, FX3-4S_R, FX3-4S_PAPV_R4 and FX3-4S_PAPV_R3) use less optical regeneration modules compared with the scenarios using only 3 slots channels. Indeed, the 3 slots channels suffers from high filtering penalty and thus long reach channels are more likely to be regenerated in intermediate nodes.

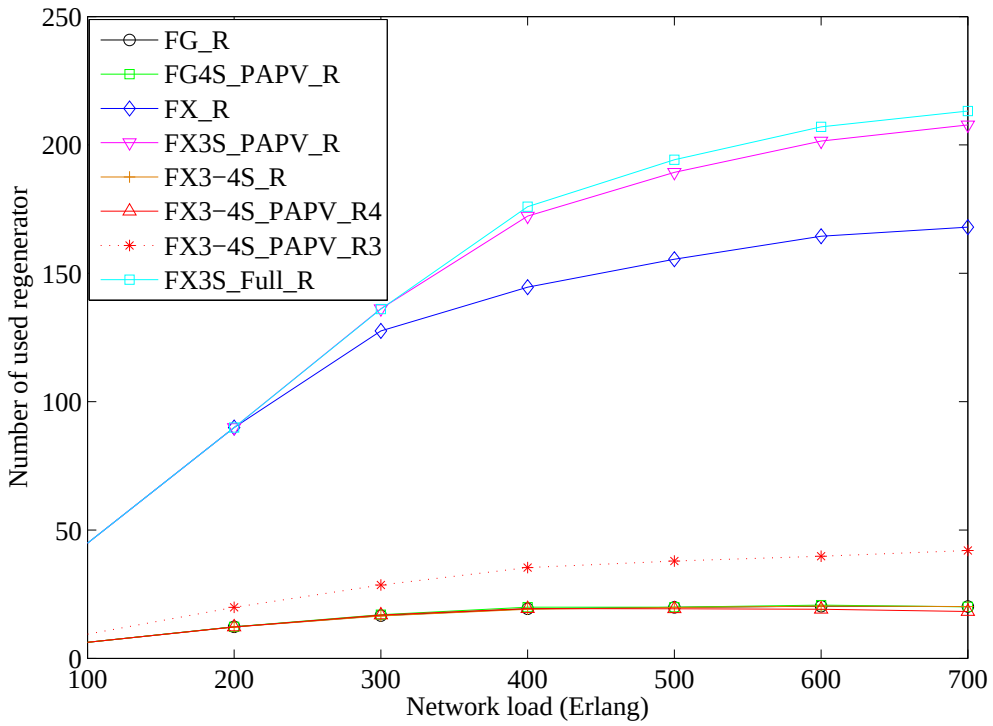

Figure 4.8: Number of regenerators used per scenario as a function of network load

Moreover, we can notice also on Figure 4.8 that these scenarios (FG_R, FG4S_PAPV_R, FX3-4S_R and FX3-4S_PAPV_R4 except FX3-4S_PAPV_R3) use on average the same number of regenerators. This result indicate that even with additional established channels in the scenarios using the power adaptation process (i.e., FG4S_PAPV_R and FX3-4S_PAPV_R4), the number of regenerators used is still the same in comparison with the scenarios without power adaptation process. This means that the use of power adaptation process allows increasing the capacity of the network for the same cost in terms of regeneration. This effect can be explained using Figure 4.9, where we plotted in bar charts the number of blocked requests per number of hops.

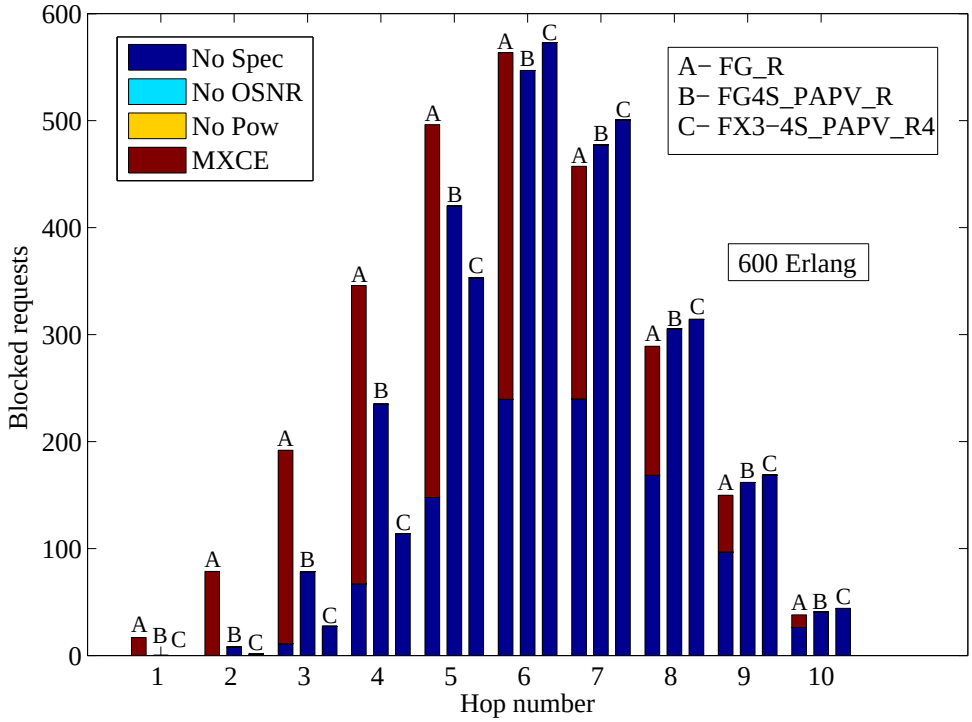

Figure 4.9: Blocked requests as a function of the number of hops

Figure 4.9 shows that the number of long reach requests in FG4S_PAPV_R and FX3-4S_PAPV_R4 are more likely to be blocked in comparison with the FG_R scenario. In fact, the possibility to use more than 80 channels per link increases the spectral occupation in optical links and thus long-reach channels are blocked due to the horizontal fragmentation. At the same time, when mixing 3 and 4-slot channels in FX3-4S_PAPV_R4 additional blocking could occur due to the vertical fragmentation. This is why the average number of regenerators used in FX3-4S_PAPV_R4 is slightly smaller than in FG4S_PAPV_R (long-reach channels are more blocked in FX3-4S_PAPV_R4 thus less regenerators are used).

However, Figure 4.8 shows that FX3-4S_PAPV_R3 scenario uses more optical regenerators compared to FX3-4S_PAPV_R4. In fact, two reasons are behind this result. The first one is because performing optical regeneration with 3 slots channels help to reduce spectrum occupation and thus more optical channels can be established in the network. The second one is because in FX3-4S_PAPV_R3 the non-feasible channels are regenerated using 3 slots and thus due to the high filtering penalty, more optical regeneration modules can be required along the regenerated path. This analysis is confirmed by Figure 4.10, where we plotted in bar charts the number of blocked requests per number of hops, for the FX3-4S_PAPV_R4 and FX3-4S_PAPV_R3 scenarios. We can notice that, long-reach channels (>6 hops) are more blocked in FX3-4S_PAPV_R4 compared

to FX3-4S_PAPV_R3 and thus more optical regenerators are used in FX3-4S_PAPV_R3.

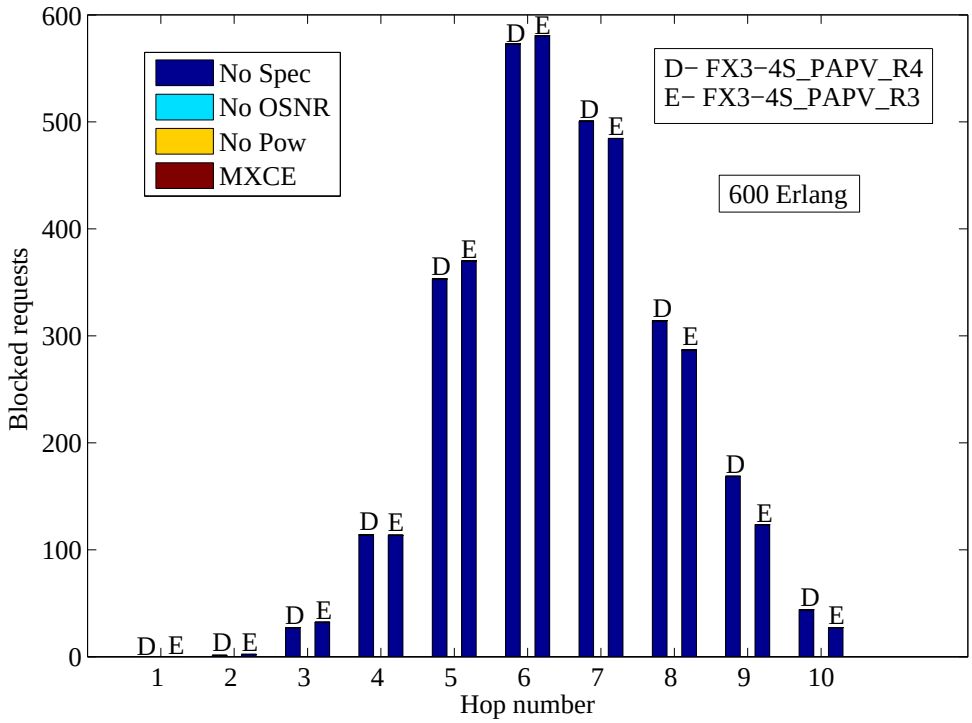

Figure 4.10: Blocked requests as a function of the number of hops

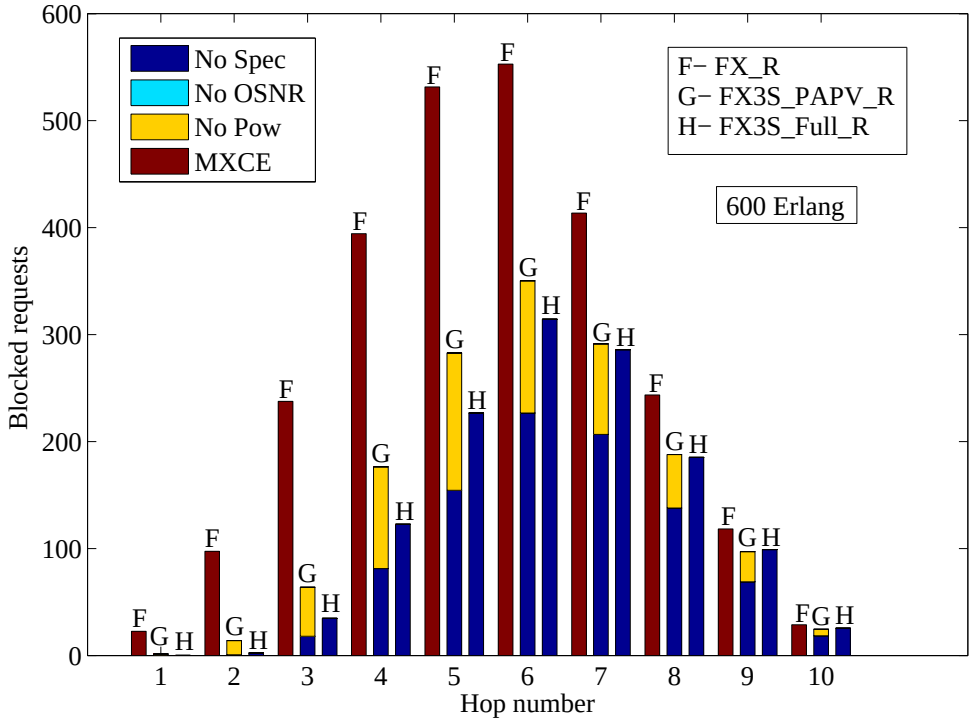

Figure 4.11: Blocked requests as a function of the number of hops

Another interesting result is shown in Figure 4.8, where FX3S_PAPV_R uses more optical regenerators in comparison to the FX_R. Indeed, the limitation on the number of channels per link in no more a limitation in the FX3S_PAPV_R scenario. Therefore, the saved optical spectrum due to the use of only 3 slots channels allows the establishment of higher number of channels when associated with the power adaptation process. This can be confirmed in Figure 4.11, where the number of blocked channels (short and long-reach channels) is reduced and thus more optical regeneration modules are used on average in FX3_PAPV_R.

In the final analysis, we can deduce from these results that the use of flexible technology without adapting the optical power prevent benefiting from the saved optical spectrum. Moreover, it increases network costs in terms of regenerators used (as with the FX_R in Figure 4.8), without any gain in terms of performance as for FX_R and FX3-4S_R in Figure 4.6.

4.6.6 Other networks topologies

Another dimension of analysis is added to identify the other parameters that could impact the occurrence of the power saturation problem. To this end, we repeated the simulations over the German and NSF networks as shown in Figures 4.12 and 4.13, using the same link design method and parameters (fiber parameters and amplifiers portfo-

lio) used for the European topology. The eight scenarios were considered with exactly the same number of simulation runs for the two networks. Table 4.2 summarizes the characteristics of the three considered network topologies.

	German network	European network	NSF network
Number of nodes N	17	32	14
Number of links l	26	42	21
Minimum node degree	2	2	2
Maximum node degree	6	4	4
Average node degree	3.05882	2.625	3
Minimum link length (km)	36	1	300
Maximum link length (km)	353	457	2800
Average link length (km)	170.5	206.09	1080.95
Maximum path length (hops)	6	10	3

Table 4.2: Characteristics of German, European and NSF networks

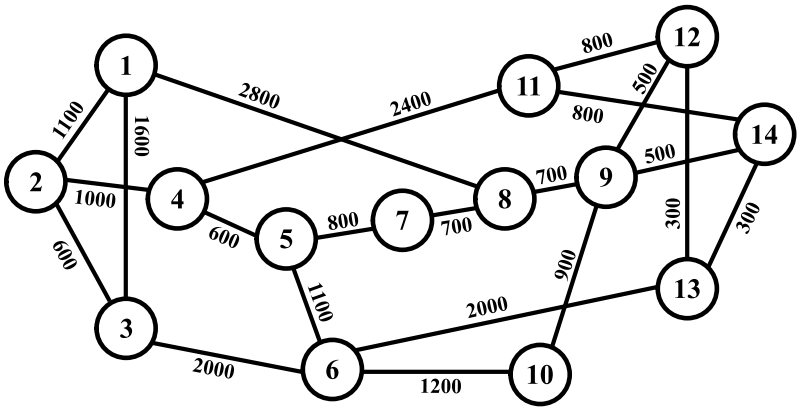

Figure 4.12: NSF network

4.6.6.1 NSF topology

The results on NSF topology are shown on Figures 4.14 and 4.15, where Figure 4.14 shows the blocking probability as a function of network load and Figure 4.15 shows the number of blocked requests per blocking reason for each simulated scenario. In terms of blocking probability, the eight scenarios show similar performance behavior in comparison with the European topology, where scenarios using power adaptation process have lower blocking probability. However, in NSF network the power saturation problem appears this time in the FX3_PAPV_R and FX3-4_PAPV_R3 scenarios. This saturation problem arises not really because of the high filtering penalty, but instead due to

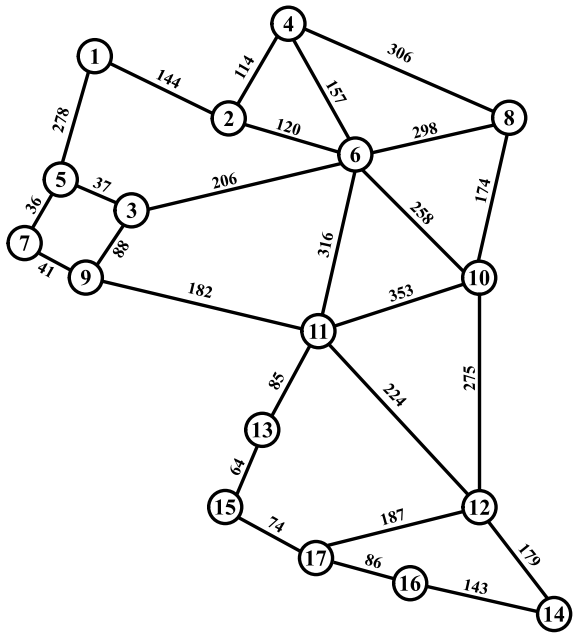

Figure 4.13: German network

the high OSNR degradation over network links (because the channel maximum hop is only three as shown in Figure 4.16).

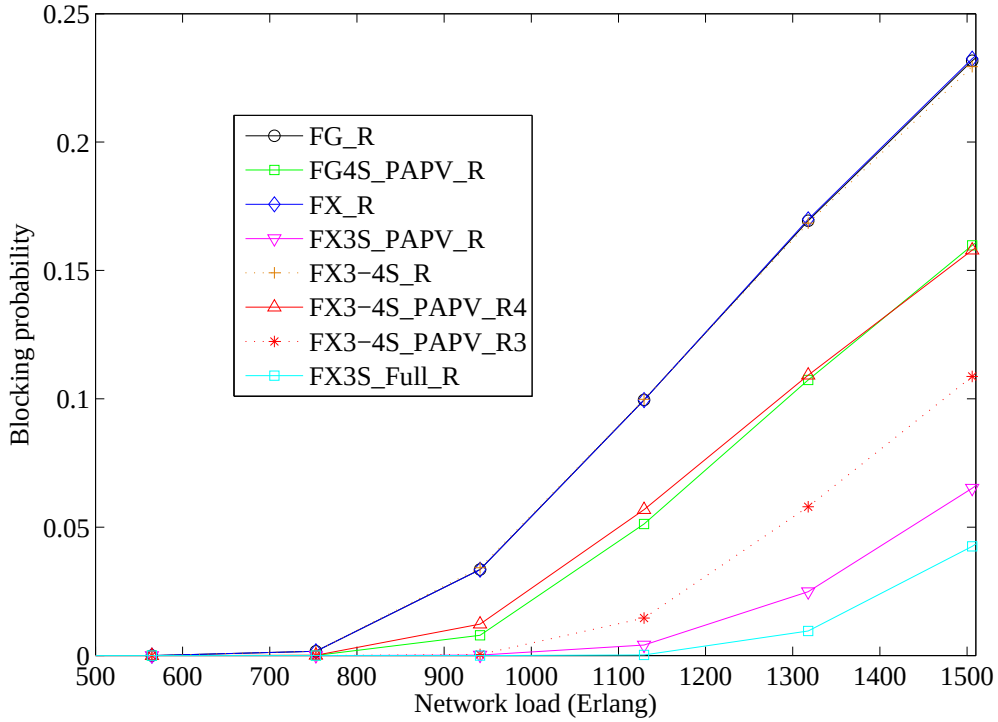

Figure 4.14: Blocking probability as a function of network load in the NSF network

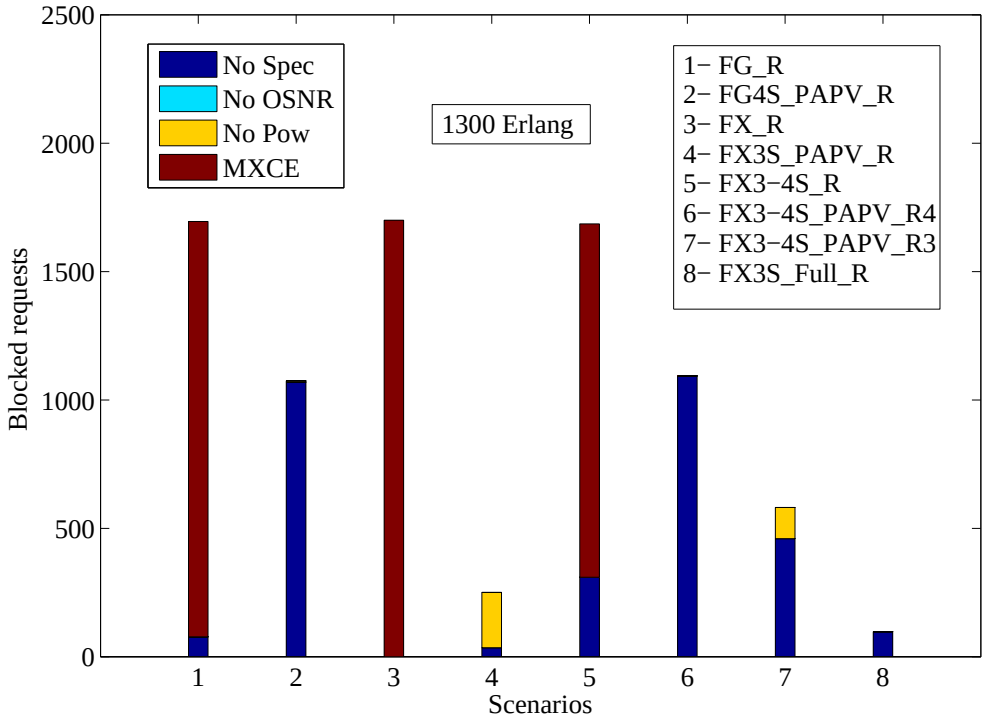

Figure 4.15: Blocking reasons per simulated scenario in NSF network

Indeed, the optical links in NSF networks are too long (as shown in Figure 4.12), reducing the power saving achieved by the power adaptation process and thus creating saturation problem.

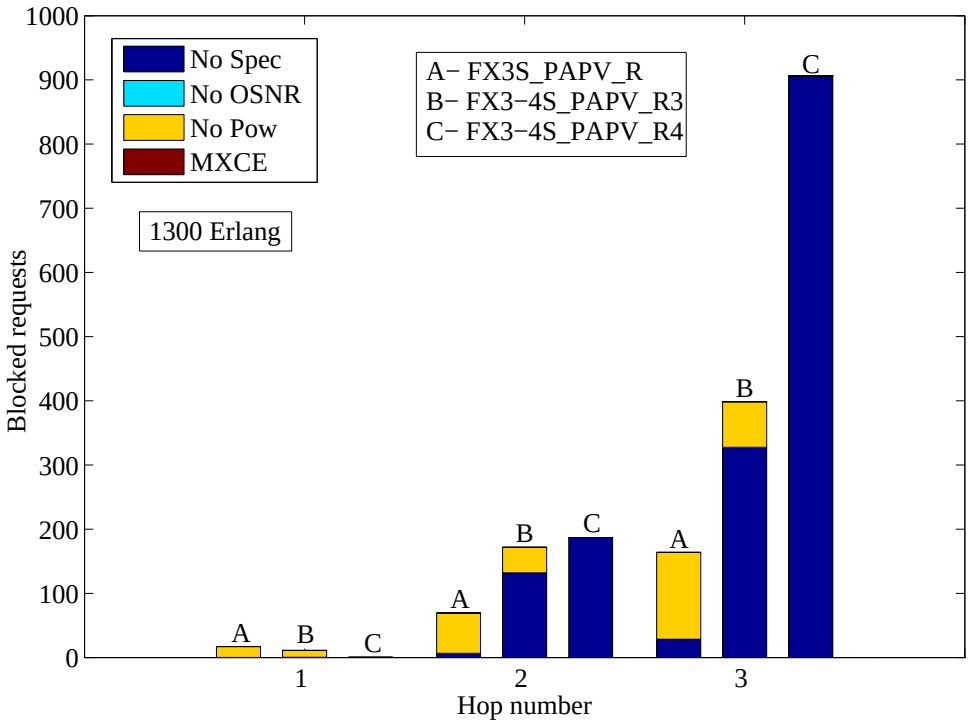

Figure 4.16: Blocked requests as a function of the number of hops in NSF network

From Figures 4.14 and 4.16, we can notice that the FX3-4_PAPV_R3 scenario has better performance compared to FX3-4_PAPV_R4, however, it uses more optical regenerators as shown on Figure 4.17. In this respect, higher number of optical channels is established in FX3-4_PAPV_R3 scenario leading to the apparition of No Pow blocking. This highlights the impacts of the adopted regeneration strategy on the performance of the scenario and on the blocking reasons.

4.6.6.2 German topology

Figures 4.18 and 4.19 shows the results of the simulations performed over the German network. We can notice from Figure 4.18 that, like for the previous topologies, the scenario that uses the power adaptation process performs lower blocking probability in comparison with the one not using power adaptation.

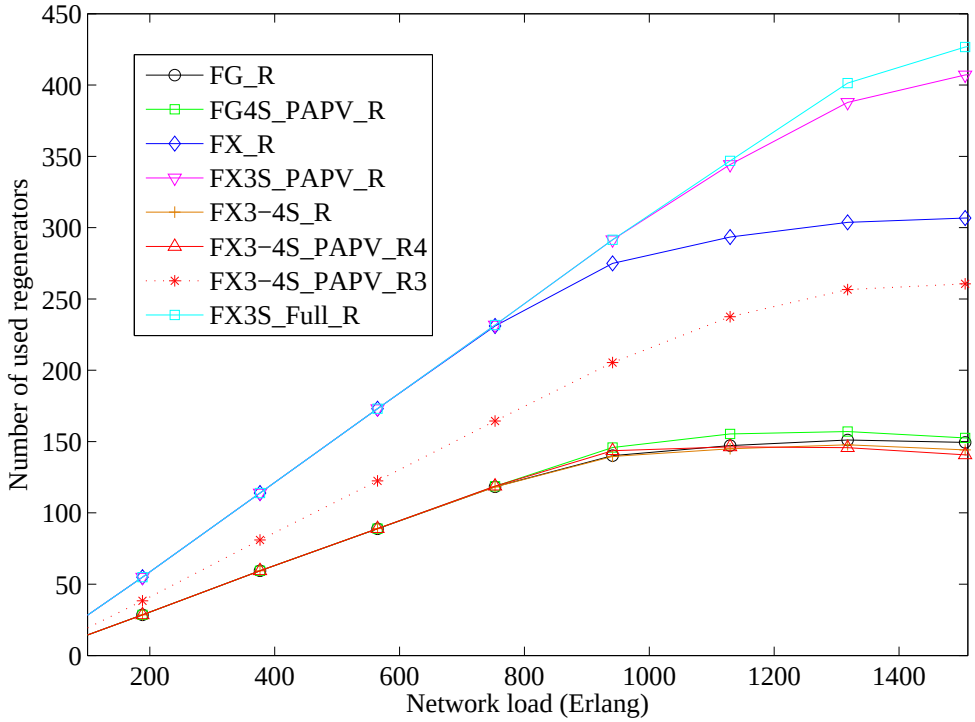

Figure 4.17: Number of regenerators used per scenario as a function of network load for NSF network

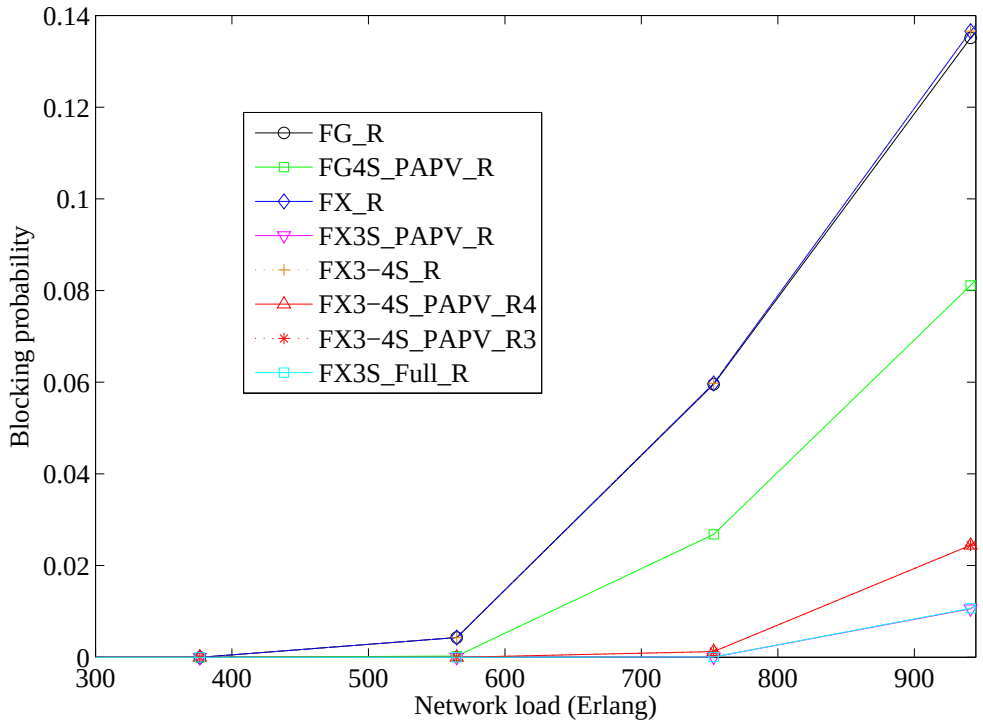

Figure 4.18: Blocking probability as a function of network load in the German network

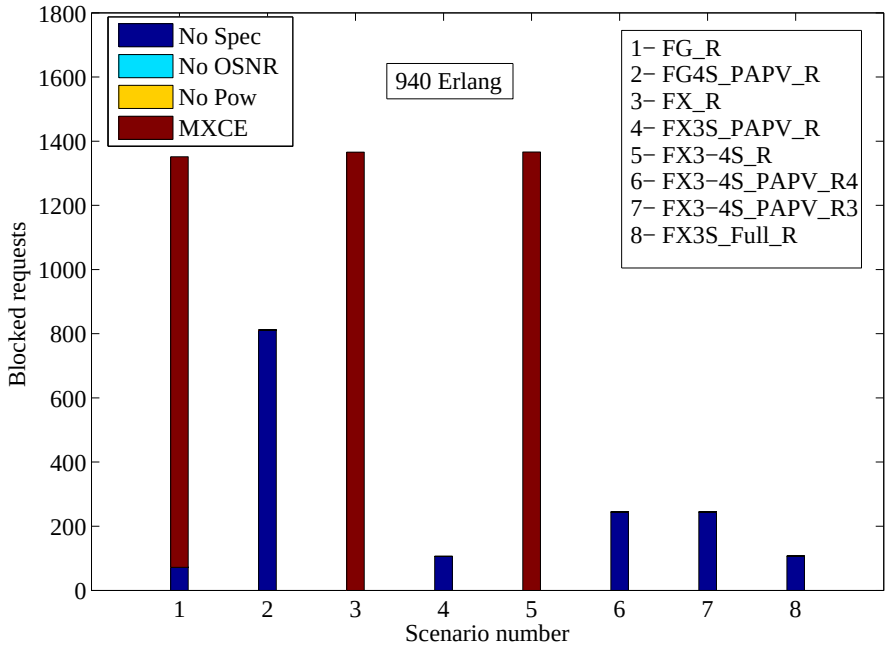

Figure 4.19: Blocking reasons per simulated scenario in German network

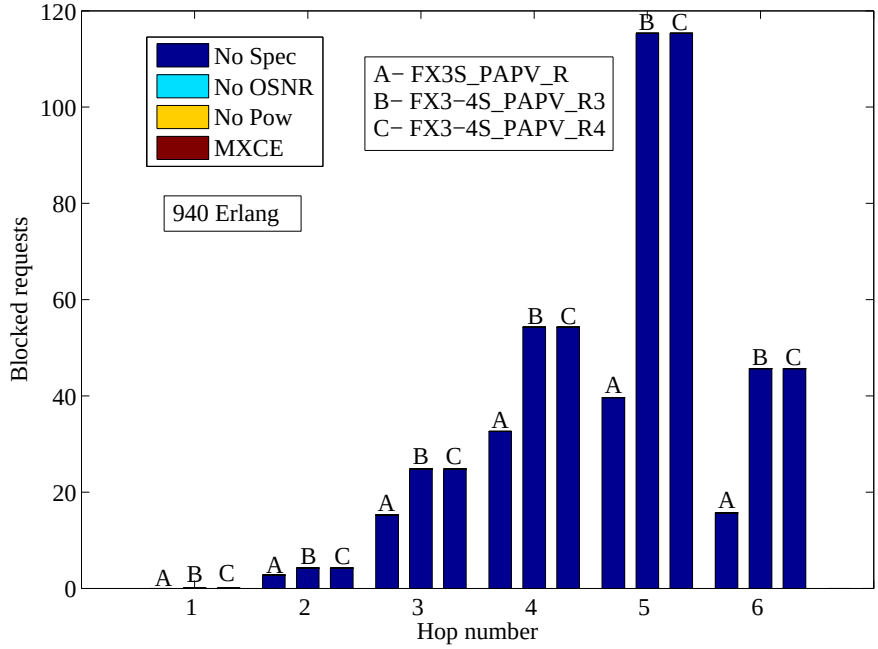

Figure 4.20: Blocked requests as a function of the number of hops in German network

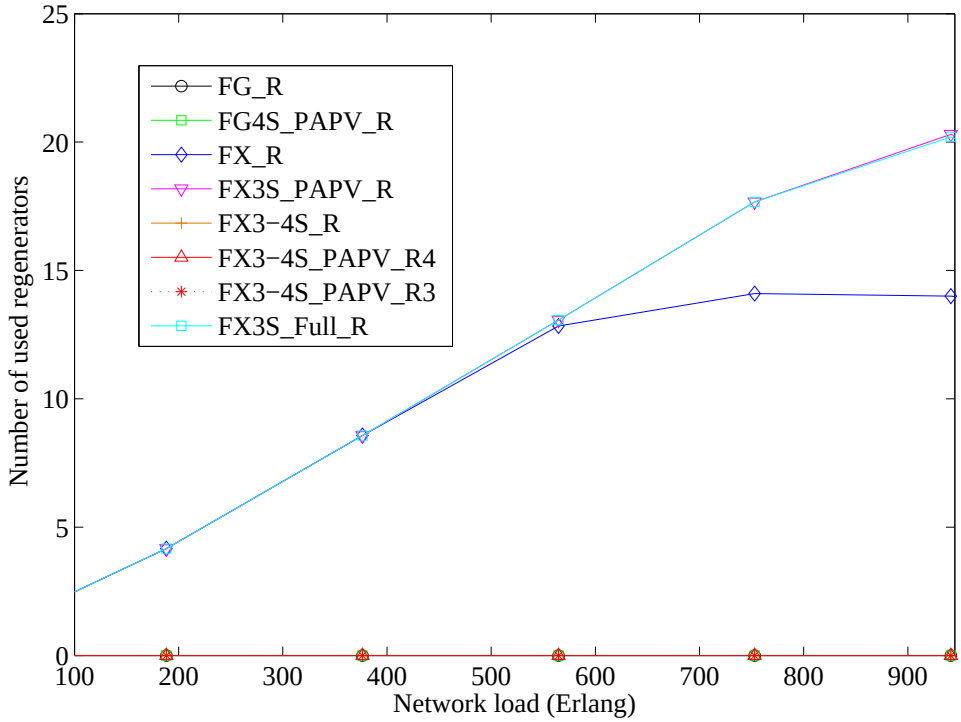

Figure 4.21: Number of regenerators used per scenario as a function of network load for German network

However, on the contrary to what happens in the NSF network, the power saturation problem did not arise in FX3S_PAPV_R neither in FX3-4S_PAPV_R3 as shown in Figure 4.19. In fact, the German topology has shorter links between nodes and these links are well designed in such a way the OSNR degradation over them is very small. Moreover, the established channels cross a small number of optical nodes (the maximum hop length of channels is six as shown in Figure 4.20), which reduces the impact of the high filtering penalty. Therefore, the power adaptation process was capable of saving sufficient power and thus avoiding the power saturation. This is why FX3S_PAPV_R and FX3S_Full_R have exactly the same BP.

Furthermore, contrarily to what happens in NSF network, the FX3-4S_PAPV_R3 and FX3-4S_PAPV_R4 scenarios have the same BP and blocking reasons. This is because the optical links have short length and introduce less impairments (links are well designed), and thus any channel that is not feasible with 3 slots can be established with 4 slots. Therefore, in these scenarios, there was no optical regeneration performed during simulations as it can be noticed on Figure 4.21.

These results show the dependency between network topology (in terms of link length), link design, and the quantity of saved power through the power adaptation process. In fact, a well-designed network with small distances between nodes allows

saving sufficient power when the power adaptation process is used and thus avoiding power saturation problem. In contrast, if the optical links are too long or suffer from high OSNR degradation, the power saturation problem will probably arise even if the power adaptation process is used.

4.7 Conclusion

In this chapter, we addressed the optical power adaptation in translucent optical networks. We extended the GMPLS protocol suite in order to support optical regeneration and power adaptation process. In this respect, a path computation algorithm with new protocols extensions and signaling mechanism were proposed to RSVP-TE and OSPF-TE protocols. These extensions allow taking into account the optical regenerator availability and assignment, and performing channel power adaptation. Moreover, the migration from fixed-grid to flex-grid networks was studied with dynamic traffic patterns, where it was demonstrated that the power saturation problem can arise independently from traffic pattern (i.e., incremental or dynamic).

Simulation results showed that upgrading network with flexible technology without adapting channels power prevent benefiting from spectrum saving and increases network cost. These results were confirmed by repeating simulations over two additional network topologies. A dependency has been noticed between network topology, the quantity of saved optical power (in other words, the arising of power saturation) and link design (i.e., OSNR of the links). Finally, the regeneration assignment strategy used in the path computation algorithm can also impact also the performance of the network and its cost.

CHAPTER 5

POWER AWARE REGENERATION ALGORITHM

In the previous chapter, we proposed a power adaptation process for translucent optical network to deal with the power saturation problem when migrating to flex-grid networks. This process was based on channel performance adaptation to save optical power and thus overcoming the link power saturation problem. However, even with this power adaptation process, the saturation problem still arises in flexible scenarios, especially, if the optical network is highly loaded. In fact, this power saturation problem arises usually over the highly loaded links (as it will be shown in the following sections). Therefore, in this chapter, we propose a power aware regeneration algorithm that allows avoiding this power saturating problem. The algorithm takes into account link power information to assign optical regeneration sites in such a way it reduces the power level over the highly loaded links.

In the following, we first begin by presenting some of the existing works on regenerator placement and assignment strategies. Then, through an ILP formulation, we model the objective of our power aware regeneration algorithm. Secondly, through an example, the execution result of the algorithm is compared with the default regeneration algorithm presented in Section 4.3. Then, the pseudo code and the functional description of the algorithm are presented. Finally, simulations are carried out to evaluate the performance of such a power aware regeneration algorithm.

5.1 State of the art

In general, two problems relative to optical regenerators are to be taken into account during the planning phase and during the operational phase of translucent optical

networks. The first one is the regenerator placement related to the planning phase, where network operators try to place a limited number of optical regenerator modules in strategical sites, in order to respond to a predefined (forecast) static traffic demands. This step is realized offline, with the aim to reduce the number of regenerators used and thus the cost of the network. The second one is the regenerator assignment problem related to the operational phase, where algorithms are developed to assign the placed regenerators to the incoming connection requests. It is an online problem, where the goal is to minimize (not in all the cases) the utilization of optical regenerators while minimizing the connection blocking under static or dynamic traffic patterns. It is desirable that the computation done during the planning phase (the number of placed regenerators and their sites) is coherent with the computation done during the operational phase (i.e., during the online path computation). This allows having the regenerators provisioned and available (with sufficient number) in the sites requested during the operational phase.

In the literature, several works in [157–160] have addressed the regeneration placement problem with linear programming formulation and heuristic solutions. Some of these solutions are based on physical topology information, on traffic prediction or on optical impairments. In this respect, regenerators have been placed, for example, in the optical nodes having higher nodal degree or in the most centered, or the most requested. In this work, we only consider the regeneration assignment problem and suppose that regeneration modules are already pre-provisioned with a sufficient number in each optical node (i.e., in such a way no blocking can occur due to regenerator unavailability).

In [141] the authors have used the regenerator placement algorithm proposed in [159] and then applied the regeneration assignment algorithm proposed in Section 4.3, to assign regeneration sites for each optical channel during network operation. This algorithm has considered only the quality of transmission as a parameter in order to assign regeneration sites. Its goal was to minimize the number of regenerators used per channel by exploiting the maximum reach of the transceivers. Moreover, in [161] the authors propose a regeneration assignment algorithm that uses quality of transmission and wavelength availability information to select regeneration sites and perform wavelength conversion. Their goal was to study different regeneration assignment strategies in terms of costs and energy efficiency in translucent networks.

In fact, depending on the objectives to achieve, more or fewer regeneration sites can be assigned using a dedicated regeneration algorithm. In this respect, we consider in this work, the information on link optical power and link OSNR, to develop our power aware regeneration algorithm that allows avoiding power saturation problem in flex-grid networks.

5.2 Formalization of algorithm objective

In this thesis work, we have only considered the operational phase of the networks and thus online routing algorithm has been developed for the control plane. However, in order to facilitate the comprehension of our power aware regeneration algorithm, we use ILP formulation to model the objective of our algorithm.

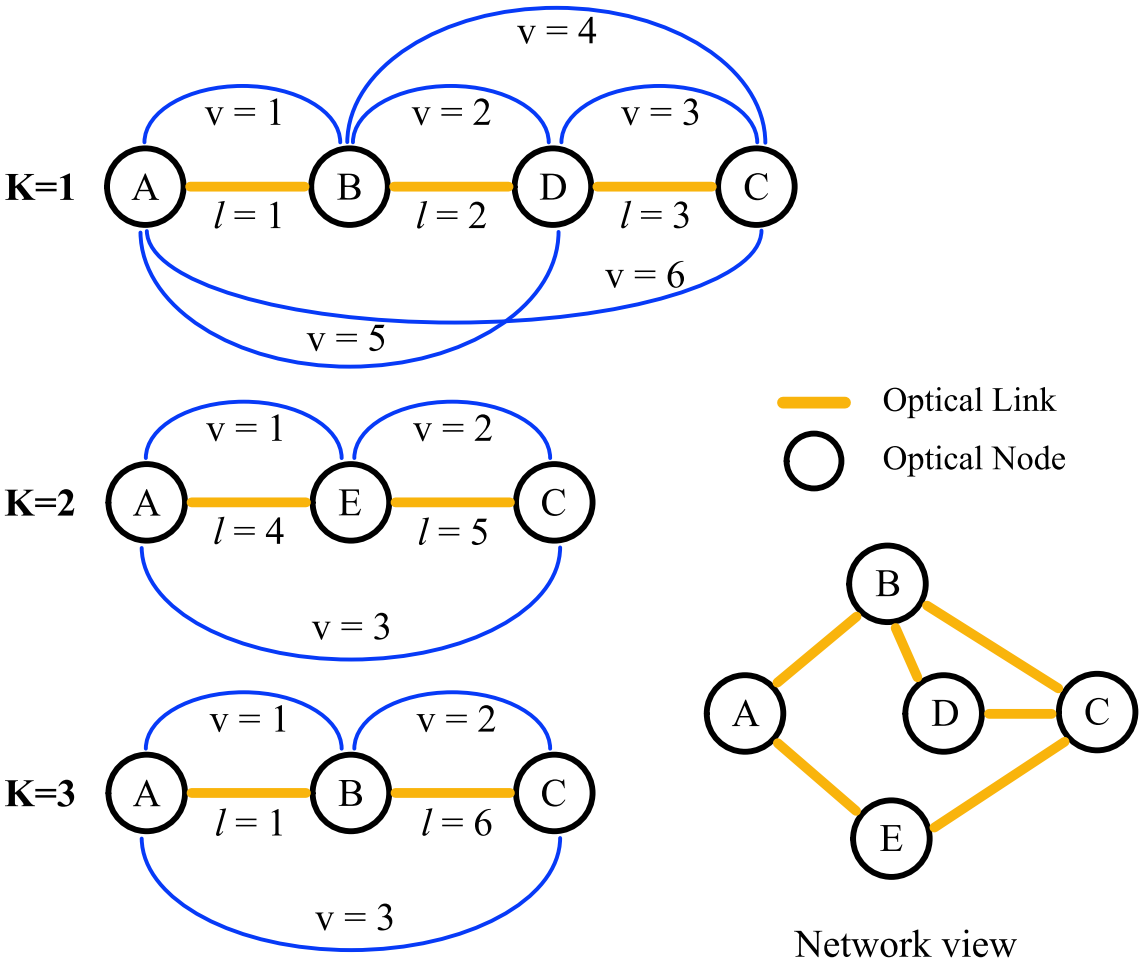

Figure 5.1: Set of optical sub-paths for the K shortest paths between A and C

To this end, we consider for this formulation a set of input data and variables defined in Table 5.1, and relies on the figure 5.1 to facilitate understanding them. Figure 5.1 shows the set of k possible paths (A-B-D-C, A-E-C, A-B-C) that an optical channel can undergo between two optical nodes (here node A and Node C). The index l used represents network links and v is to identify the possible combinations of transparent sub-paths v that can be created over a path k.

In Table 5.1, T represents the set of available transceivers in the network. O_t is the $OSNR_{min}$ required by the transceiver t. C_t is the cost of the transceiver t. D_t is the data rate achievable by the transponder t. K is the set of all possible optical paths between

Input data	
T	Set of transceiver types (1...t)
O_t	$OSNR_{min}$ of the transceiver of type t
C_t	Cost of transceiver of type t
D_t	Data rate of the transceiver of type t
K	set of optical paths between two optical nodes (1...k)
V_k	set of the sub-paths of the path k (1...v)
L	Set of network links (1...l)
ϵ	Constant ($\epsilon << 1$)
m_{tkv}	$OSNR_{margin}$ over the sub-path v ($m_{tkv} = OSNR_v - O_t$); $m_{tkv} > \epsilon$
W_l	current optical power level over the link l ($W_l = P_{real,l}/P_{max,l}$)
E_k	Set of links l of the path k
j	The optical link l having the highest power level
E_{kvl}	Equal to 1, if v passes through link l, with $v \in V_k$; 0 otherwise
Variables	
S_k	equal to 1 if the path k is a solution; 0 otherwise
S_{tkv}	equal to 1 if the path k is a solution using the transceiver t; 0 otherwise

Table 5.1: set of input data and variables

two nodes in the network, e.g., k=1 (ABDC), k=2 (AEC). V_k is the set of sub-paths that can be created over the path k, e.g., V_1 ={v=1 (AB), v=2 (BD), ..., v=6(AC)}. L is the set of network links, e.g., l=1 (AB), l=3 (DC), l=5 (EC). ϵ is a constant smaller than 1 (is a small coefficient used to weights the second part of the objective function). m_{tkv} represents the $OSNR_{margin}$ over the sub-path v ($m_{tkv} = OSNR_v - OSNR_{min,t}$). W_l is the current optical power level over the link l ($W_l = P_{real,l}/P_{max,l}$). E_k is the set of links l constituting the path k, e.g., E_2 ={AE, EC}. j is the optical link having the highest power level($W_j = \max_{l \in E_k}(W_l)$). E_{kvl} is an integer that equal to 1, if the sub-path v passes through link l, with $v \in V_k$; 0 otherwise. S_k is a variable that equal to 1 if the path k is a solution; 0 otherwise. Lastly, S_{tkv} is a variable equal to 1 if the path k is a solution using the transceiver t; 0 otherwise.

In fact, the goal of the algorithm is to assign regeneration sites in such a way it minimizes the added optical power over the optical link having the highest current optical power, while guaranteeing minimum number of regeneration sites. Therefore, using link power and link OSNR information, the algorithm selects the solution (i.e., combination of optical regeneration sites) that maximizes the $OSNR_{margin}$ over the transparent sub-path including the optical link having the highest optical power. In

this respect, the objective function of the algorithm can be written as follows:

$$\min \quad \sum_t \sum_k \sum_{v \text{ in } V_k} S_{tkv} C_t + \epsilon \sum_t \sum_k \sum_{v \text{ in } V_k} S_{tkv} E_{kvj} \times 1/m_{tkv} \tag{5.1}$$

$$\text{subject to} \quad S_k \geq S_{tkv}, \quad \forall t,k,v \tag{5.2}$$

$$\sum_k S_k = 1 \tag{5.3}$$

$$S_{tkv} \times OSNR_v \geq O_t \times S_{tkv}, \quad \forall t,k,v \tag{5.4}$$

$$S_{tkv} \times D_t \geq D \times S_{tkv}, \quad \forall t,k,v \tag{5.5}$$

$$\sum_{t,(v \text{ in } V_k)} S_{tkv} E_{kvl} = S_k, \quad \forall l \text{ from } E_k \tag{5.6}$$

Eq. (5.1) is the objective function that first minimizes the cost of the connection, then when several solutions have the same cost, it minimizes the inverse of the $OSNR_{margin}$ over the sub-path v including link j (i.e., the link with the highest power level). In other words, this function promotes the combination of t, k and v, that maximizes the $OSNR_{margin}$ over the sub-path including link j. Consequently, it maximizes the attenuation of channel power over the sub-path v (i.e., minimum added power over link j).

Eq. (5.2) ensures that the path k is a solution if any S_{tkv} is set to one. Eq. (5.3) is to select only one path from the k possible. Eq. (5.4) is to guarantee that the OSNR of any sub-path v should be bigger than the $OSNR_{min}$ (O_t) of the transponder t used (i.e., the equation allows selecting only feasible sub-paths). Eq. (5.5) is to ensure that the data rate of the transponder used satisfies the requested one (D). Finally, Eq. (5.6) is to avoid selecting several sub-paths v that pass through the same link l (i.e., if v is a solution then it must not have any common links l with any other selected sub-paths).

5.3 Power aware regeneration algorithm

To avoid power saturation problem, we developed an online power aware regeneration (PAR) algorithm that implements the objective function in the control plane. However, this implementation does not include the possibility to take into account several K shortest paths neither different type of transceivers. In this respect, the PAR algorithm, firstly, assigns regeneration sites like with the default regeneration algorithm (i.e., guaranteeing the minimum number of regeneration sites). Secondly, it tries to optimize their position in order to maximize the $OSNR_{margin}$ over the link with the highest power level. In contrast, the implementation of such an algorithm into the control plane requires several link and node parameters to be exchanged. Therefore, we assume that these parameters are made available to the control plane through the extensions described in Chapter 3 and 4 for OSPF-TE protocol.

In the following, we show through an example, the result obtained after the execution of the PAR algorithm over a regenerated optical path. Then, we present the functional description of the algorithm with its pseudo code.

5.3.1 PAR algorithm execution example

Let's assume that an optical channel must be established between a node A and a node F as shown in Figure 5.2. Moreover, we assume that the optical path between the two optical nodes is not physically feasible through one transparent segment (i.e., AF). Therefore, signal regenerations are required in intermediate nodes to receive correctly the optical signal in node F. Hence, depending on the goal of the applied regeneration algorithm, several regeneration sites can be designated accordingly.

As explained before, the goal of the PAR algorithm is to reduce the blocking due to power saturation while guaranteeing the minimum number of regeneration sites. Indeed, this goal can be achieved through maximizing the $OSNR_{margin}$ over the segment containing the optical link performing the highest power level. This link is identified through its power ratio (W_l), which is equal to the current aggregated link power ($P_{real,l}$) divided by the maximum power level ($P_{max,l}$) allowed over the link l. In this respect, the power ratio over an optical link l can be expressed as $W_l = P_{real,l}/P_{max,l}$.

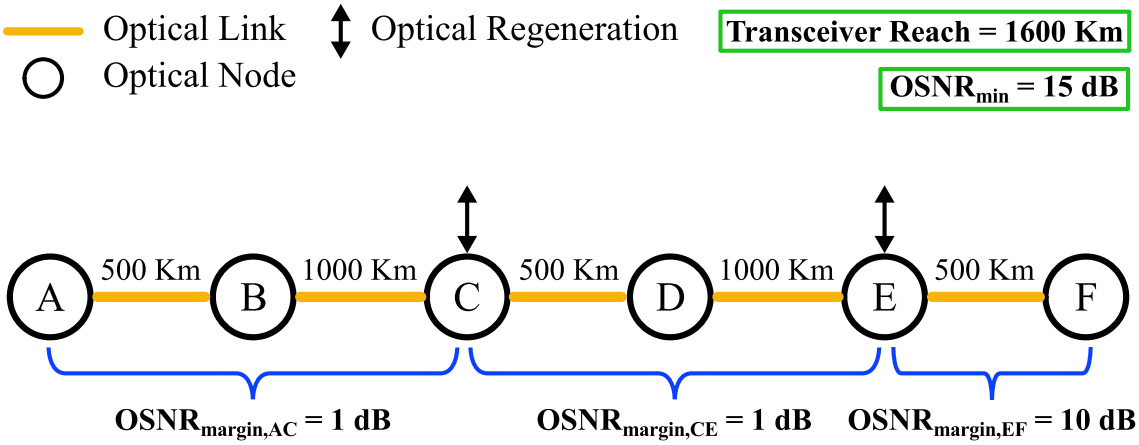

Figure 5.2: Regeneration sites assignment result using the default algorithm

Figure 5.2 shows the result obtained from the default regeneration algorithm defined in Section 4.3 when trying to establish the optical channel between node A and F. In order to get a working channel the algorithm identified two regeneration sites (C and E), by exploiting the maximum reach of the optical transceiver, guaranteeing minimum number of regeneration sites (i.e., minimum cost for the connection). Certainly, if the power adaptation process is applied over the optical channel of Figure 5.2, the highest power attenuation is performed over the EF segment since it performs the highest $OSNR_{margin}$ ($OSNR_{margin,EF}$ = 10 dB). However, if we consider an arbitrary optical power levels distribution over the optical links as shown in Figure 5.3, the selected regeneration sites do not offer the best solution. This is because our goal is to have the highest power attenuation over the link having the highest power ratio (called hereafter critical link), which is here AB and not EF.

In fact, to establish the optical channel between node A and node F, several regeneration assignment solutions having the same costs are possible (e.g., regeneration in

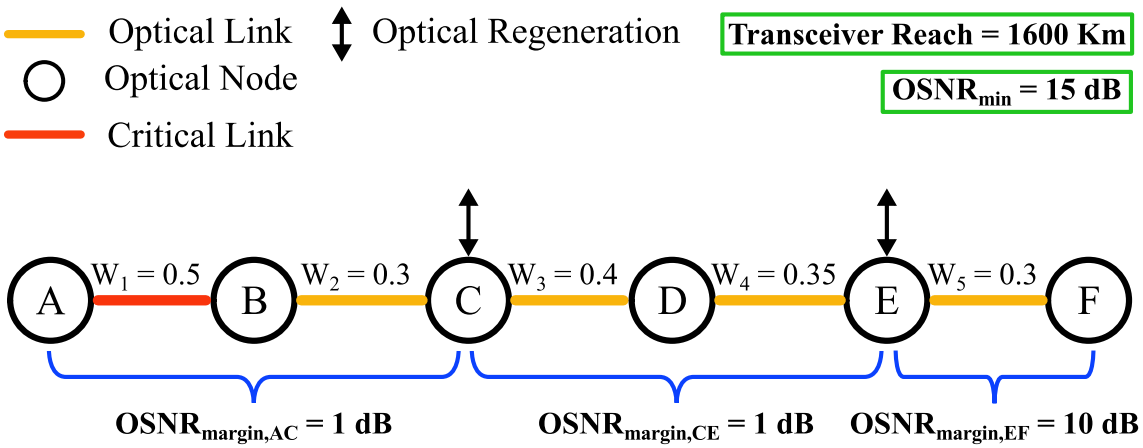

Figure 5.3: Regeneration sites assignment result using the default algorithm

node C and D, or in node B and D, or in node C and E). However, only one combination among the possible three allows having the maximum $OSNR_{margin}$ over the critical link AB. Therefore, if the PAR algorithm is applied, the obtained solution will be to regenerate in node B and D as shown in Figure 5.4. This regeneration combination allows having minimum number of regeneration sites and, at the same time, maximum $OSNR_{margin}$ over the transparent segment including the critical link AB.

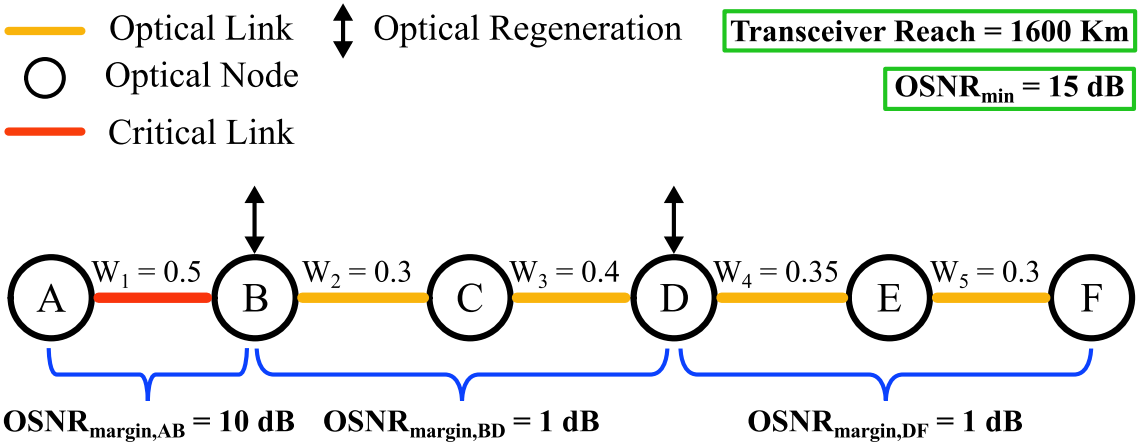

Figure 5.4: Regeneration sites assignment result using the PAR algorithm

Indeed, if we consider the selected regeneration sites of the Figure 5.4, the power attenuation that can be applied over the link AB is higher than the one that can be applied with the regeneration sites of Figure 5.3 ($OSNR_{margin,AC}$ = 1dB< $OSNR_{margin,AB}$ = 10dB). In this respect, this combination allows the minimization of the channel optical power over the critical link AB, which in turn reduces its aggregated power. In other words, the added optical power over the critical link AB is minimized after the establishment of the optical channel, which was not the case with the default regeneration algorithm. However, the algorithm does not guarantee that after setting up the

channel, that the critical link stays the same, and thus a new critical link might appear. Therefore, other regeneration assignment strategies can be considered to get a different power distributing among the links (e.g., maximizing the added power in the link with the lowest power).

5.3.2 Functional description

As explained before, the PAR algorithm requires a set of information on the computed optical path. This information concerns the optical nodes and links constituting the path. In this work, we suppose that regeneration sites are already calculated and thus the information on each regeneration site (i.e., link OSNR, link power level) is available to the control plane. Moreover, for simplicity reasons, we consider only the case where regeneration sites are already identified using the default regeneration algorithm.

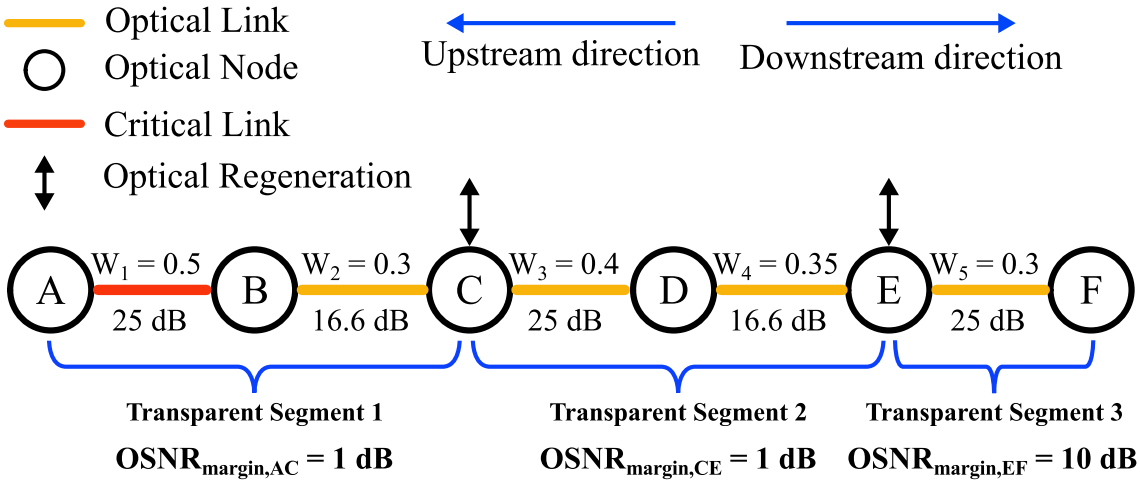

Figure 5.5: Regeneration sites assignment result using the default algorithm

In this respect, we present, in Figure 5.5, the result of the default regeneration algorithm when applied over an unfeasible optical path (AF) between ingress/egress nodes. In this example, the identified regeneration sites are Node C and Node E, and the critical link performing the highest power level is link AB.

In Table 5.2, we present the set of input data required by the PAR algorithm and we rely on the example of Figure 5.5 to clarify each parameter. In Table 5.2, V represents the number of transparent segments with the initial regeneration assignment result (e.g. $V = 3$ in Figure 5.5). C is the index of the transparent segment including the critical link (e.g., $C = 1$ in Figure 5.5). M is the number of downstream segments relative to the transparent segment containing the critical link ($M = V - C = 3 - 1 = 2$ in Figure 5.5). Tab_Regen is the set of regeneration sites calculated by the default default algorithm. The regeneration sites stored in the table are sorted in the downstream direction (e.g., Tab_regen[1] = C and Tab_regen[2] = E in Figure 5.5). Tab_OSNR_{margin} is the set of $OSNR_{margin}$ for the transparent segments with the

initial assignment result. The set of $OSNR_{margin}$ are sorted in the downstream direction (e.g., $Tab\_OSNR_{margin}[1] = 1$, $Tab\_OSNR_{margin}[2] = 1$ and $Tab\_OSNR_{margin}[3] = 10$ in Figure 5.5). Tab_OSNR_{link} is the set of OSNR degradation over every link of the optical path (e.g., $Tab\_OSNR_{link}[1]$ = 25 dB, $Tab\_OSNR_{link}[2]$ = 16.6 dB, $Tab\_OSNR_{link}[3]$ = 25 dB, $Tab\_OSNR_{link}[4]$ = 16.6 dB and $Tab\_OSNR_{link}[5]$ = 25 dB in Figure 5.5). N is the number of initial regeneration points (nodes) get from the default regenerator placement algorithm (e.g., $N = 2$ in Figure 5.5). Lastly, i is an integer variable used to browse the regeneration sites (e.g., when i=1, Tab_regen[i] = Tab_regen[1] = C in Figure 5.5).

Therefore, using these input data, the PAR algorithm presented in Algorithm 1 can executed and it will works as follows: The PAR algorithm first considers the same transparent segments generated by the default regeneration algorithm. Then it identifies the location of the critical link (i.e., in which transparent segment is located). Then it shifts the optical regeneration sites in the upstream direction in order to increase the $OSNR_{margin}$ over the transparent segment including the critical link.

Input data	
V	Number of transparent segments obtained with the initial assignment result.
C	The index of the segment containing the critical link (i.e., with the highest W).
$M = V - C$	Number of downstream segments relative to the segment containing the critical link.
Tab_Regen	The set of regeneration sites (here assigned by the default regeneration algorithm).
Tab_OSNR_{margin}	The set of $OSNR_{margin}$ for the transparent segments.
Tab_OSNR_{link}	The set of OSNR degradation over every link of the optical path.
N	Number of regeneration sites (nodes) in the path pre-computed with the default regenerator assignment algorithm.
i	Integer variable; it is used to browse the regeneration sites (the index of the regeneration node C in Tab_Regen is 1 and for the node E is 2 in Figure 5.5).

Table 5.2: Input data for the PAR_Upstream algorithm

In fact, moving the regeneration point in the upstream direction reduces the $OSNR_{margin}$ of the downstream segment and increases the $OSNR_{margin}$ of the upstream one. This is because the new downstream segment includes an additional link which certainly reduces its quality (the OSNR of any transparent segment decreases when any additional link is added to the segment).

The PAR algorithm before optimizing the regeneration sites, tests if the critical link is in the last segment. In this case the $OSNR_{margin}$ is already at the maximum

Algorithm 1 PAR_Upstream algorithm pseudo code

Input: Data presented in Table 5.2
Output: Tab_Regen and Tab_OSNR_{margin}

```
1: if (Critical link is in the last segment) (i.e. from a downstream point of view) then
2:     Exit PAR_Upstream algorithm
3: else
4:     i ← 0
5:     while M > 0 do
6:         M ← M − 1
7:         Shift_Upstream(N − i, M, Tab_Regen, Tab_OSNR_margin, Tab_OSNR_link)
8:         i ← i + 1
9:     end while
10: end if
```

value that we can have (because the default regeneration algorithm maximizes the $OSNR_{margin}$ of the last transparent segment). Therefore, no optimization is made for the regeneration sites. In contrast, if the critical link is not in the last segment, then there is a possibility to change the regeneration sites and thus to increase the $OSNR_{margin}$ for the segment including that link. This is the case of Figure 5.5 where PAR algorithm can be applied. The optimization result is presented in Figure 5.4.

5.4 Simulation and results

In Chapter 4, we noticed that the power saturation problem arises in flex-grid networks (i.e., in FX3S_PAPV_R) even if the power adaptation process was activated. Therefore, in this chapter, we use the PAR algorithm for the FX3S_PAPV_R scenario, in order to evaluate its performance. In this respect, we developed a new scenario, which we call "FX3S_PAPV_R_OPT", in which we implement the PAR algorithm. This scenario works exactly as the FX3S_PAPV_R, with the only difference in the regeneration placement method. In fact, for the new scenario FX3S_PAPV_R_OPT, the "Regeneration sites assignment" functional block of the path computation algorithm in Figure 4.3 is extended with the PAR algorithm.

The new "Regeneration site assignment" block works as follows: for any unfeasible path, the new "Regeneration sites assignment" function computes the required regeneration sites using the method of Section 4.3. Then, the PAR algorithm is applied over the obtained result. In the case where the optimization of regeneration sites is possible and allows increasing the $OSNR_{margin}$ over the highly powered link of a path p, the new assignment solution of regeneration sites is considered during the signaling phase. In contrast, if the application of PAR algorithm does not improve the $OSNR_{margin}$ of the highly powered link, then the initial regeneration sites assignment solution is considered during the signaling phase.

Algorithm 2 Pseudo code Shift_Upstream function

Input: $N-i, M, Tab\_Regen, Tab\_OSNR_{margin}, Tab\_OSNR_{link}$
Output: Tab_Regen and Tab_OSNR_{margin}
function SHIFT_UPSTREAM($N-i, M, Tab\_Regen, Tab\_OSNR_{margin}, Tab\_OSNR_{link}$)
Shift the $(N-i)$**th regeneration site in the upstream direction for one step**; (i.e., from the current node to neighbor previous node)
if ($OSNR_{new\_downstream\_segment} > OSNR_{min}$) (i.e. if the OSNR of the downstream segment relative to the $(N-i)$th regeneration site is bigger than the minimum acceptable OSNR) **then**
if (M=0) **then**
if (the critical link has changed segment) **then**
if ($OSNR_{margin,old} > OSNR_{margin,new}$) (i.e., compare the $OSNR_{margin}$ for the segment that was including the critical link with the $OSNR_{margin}$ of the segment that is including the link after regeneration site shifting) **then**
Shifting not accepted;
Exit Shift_Upstream() function;
else
Accept shifting;
Update Tab_Regen and Tab_OSNR_{margin} values;
Exit Shift_Upstream() function;
end if
end if
end if
Accept shifting;
Update Tab_Regen and Tab_OSNR_{margin} values;
Shift_Upstream($N-i$, M, Tab_Regen, Tab_OSNR_{margin}, Tab_OSNR_{link});
else
Exit Shift_Upstream() function
end if
end function

Simulations are performed using our distributed GMPLS-based network simulator over the European backbone network described Figure 5.6. It has 32 optical nodes and 42 optical links. All required information on optical links and nodes are disseminated in the network through the OSPF-TE extensions suggested in Chapter 3 and 4. Moreover, the same simulation parameters considered in Chapter 3 are also applied for the new developed scenario (e.g. link and amplifier parameters, traffic requests, number of runs, link design).

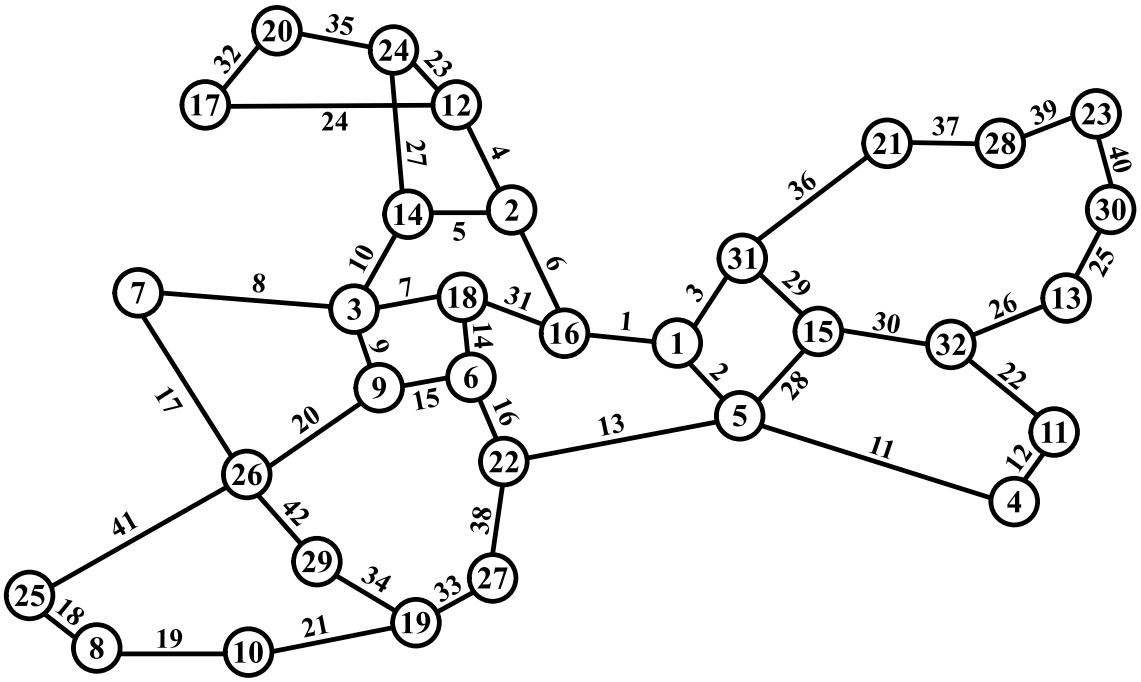

Figure 5.6: European backbone network with indexed links

5.4.1 Blocking probability and blocking reasons

Figure 5.7 shows the Blocking probability of the FX3S_PAPV_R_OPT scenarios as a function of network load in comparison with the main flexible scenarios simulated in Chapter 4 (i.e., FX3S_PAPV_R and FX3S_Full_R).

We can notice from Figure 5.7, that the scenario FX3S_PAPV_R_OPT that uses the PAR algorithm has less blocking in comparison with FX3S_PAPV_R. Apparently, the PAR algorithm allows to reduce the aggregated optical power level over the highly powered links that were causing the power saturation problem. Moreover, the FX3S_PAPV_R_OPT performs the same blocking probability as FX3S_Full_R which means that the power saturation problem is no longer occurring and thus the spectral limitation is the only source of blocking.

This analysis is confirmed in Figure 5.8, where we plotted the number of blocked requests per blocking reason for the three considered scenarios. Indeed, we can notice that in FX3S_PAPV_R_OPT, only No Spec blockings are arising and there is no longer blocking arising due to power saturation. This explains why the FX3S_PAPV_R_OPT scenario has the same performance as FX3S_Full_R.

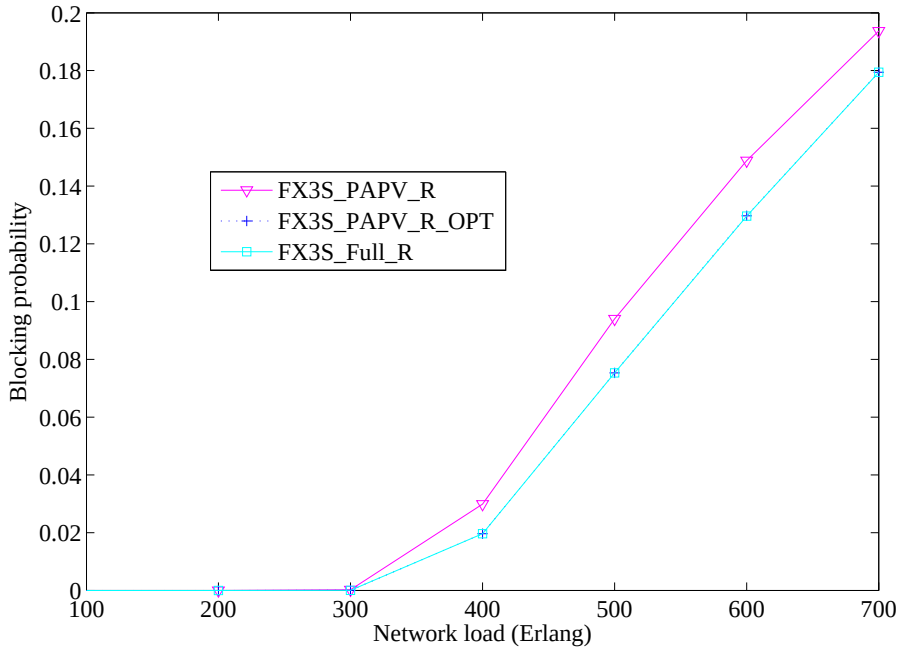

Figure 5.7: Blocking probability versus Network load

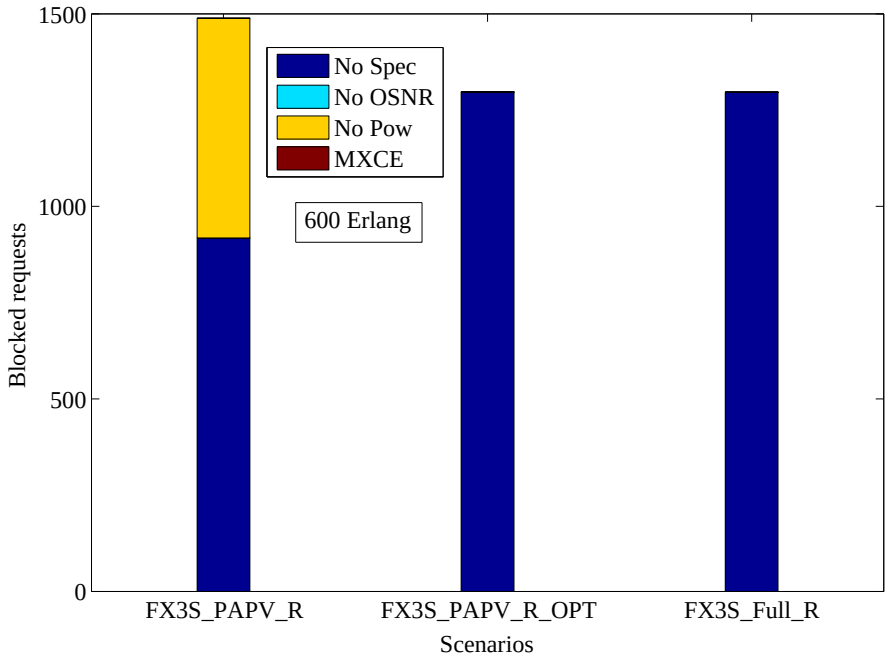

Figure 5.8: Blocking reasons per simulated scenarios

5.4.2 Evaluation in terms of power levels

We complete our analysis by comparing the optical power levels over each network link. Figure 5.9 shows the percentage of the remaining optical power over each link of the network, before and after the use of the PAR algorithm. We have in red the percentage of the remaining optical power over network links (sorted in ascending order) for the case of FX3S_PAPV_R scenario, and in yellow the remaining optical power over the same links for the case of FX3S_PAPV_R_OPT scenario.

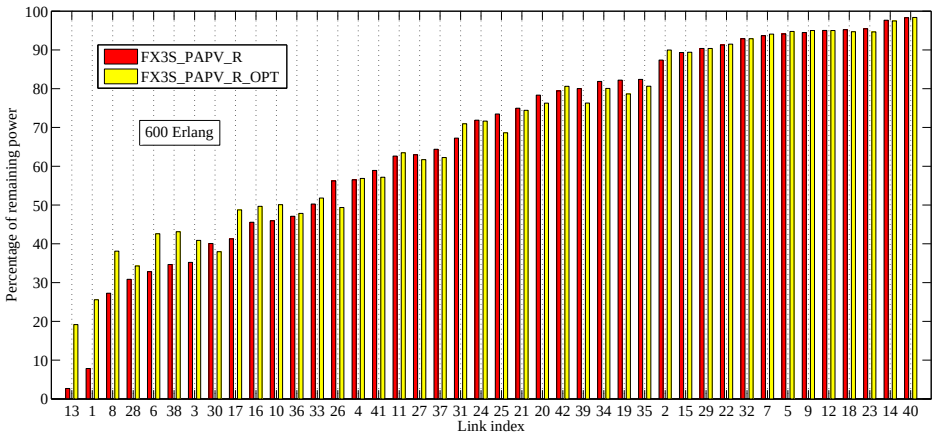

Figure 5.9: Percentage of the remaining optical power per link

We can notice from Figure 5.9 that, the PAR algorithm succeeded in reducing the optical power level for the highly loaded links, consequently, increasing their remaining power level. For instance the percentage of remaining optical power level over the link 13 goes from 3 % to 19 %. Figure 5.10 shows the normalized spectrum occupation (i.e., current spectrum occupation divided by the total allowed bandwidth) of each optical link. We can notice that even if the link 13 have high spectrum occupation the PAR algorithm succeeded in reducing its power level and increases its capacity (the normalized spectrum occupation increased from 0.825 to 0.9).

In fact, the PAR algorithm balances the power level distribution over network links: the power level of heavily used links is reduced while the power level of lightly-used link is increased. Figure 5.11, shows the percentage of gained power over each link after the use of the PAR algorithm. We can notice that, for links 13, 1 and 6 the remaining power levels have been increased. In contrast, this remaining power level has been decreased for links such as 39, 25, and 26 and thus they have a higher power level. This confirms the advantage of exchanging $OSNR_{margin}$ between the transparent segments constituting the optical paths. $OSNR_{margin}$ are transferred to high loaded links leading to an increase of the power levels of the other links of network.

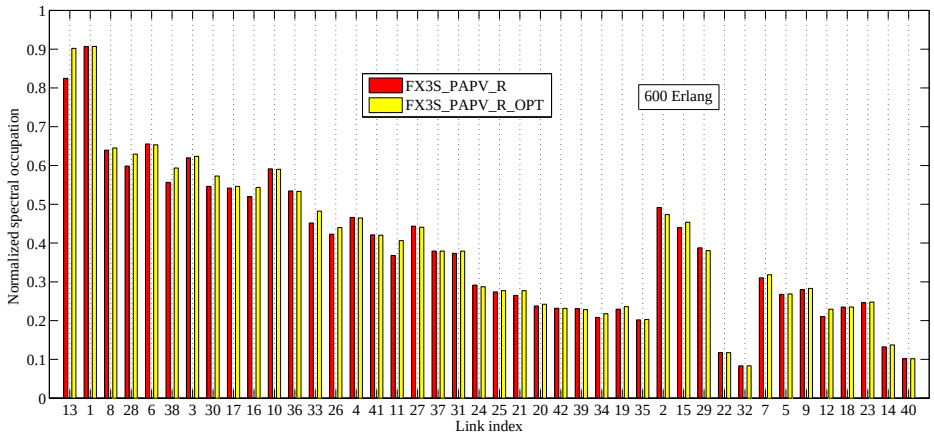

Figure 5.10: Normalized spectrum occupation over network links

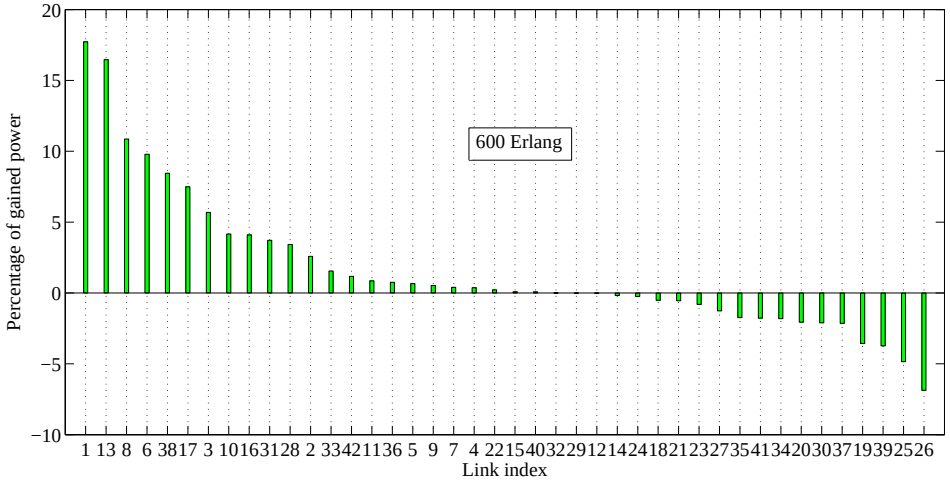

Figure 5.11: Percentage of gained power over each link after the use of the PAR algorithm

5.4.3 Evaluation in terms of optical regeneration

Figure 5.12 shows the number of regenerators used in the three simulated scenarios as a function of network load. As expected, the number of regenerators used in FX3S_PAPV_R_OPT is exactly the same as in the FX3S_Full_R scenario. Indeed, the capability of avoiding power saturation allows the FX3S_PAPV_R_OPT scenario to behave exactly as FX3S_Full_R where no power limitation exists over network links and thus the same set of optical connection are accepted in both scenarios.

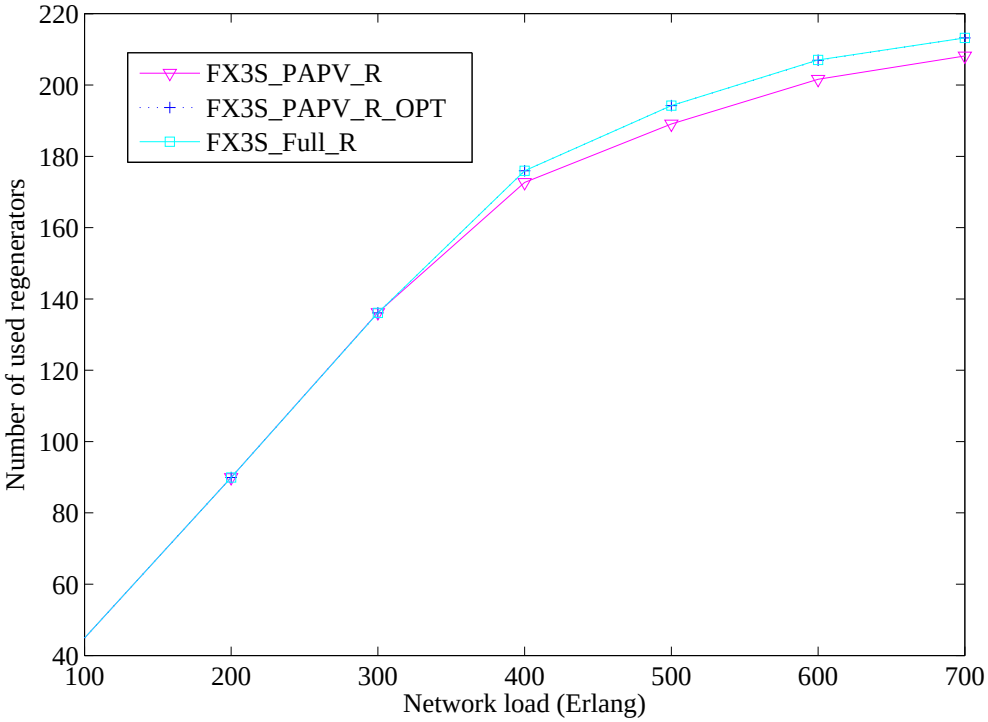

Figure 5.12: Number of regenerator used per scenario as a function of network load

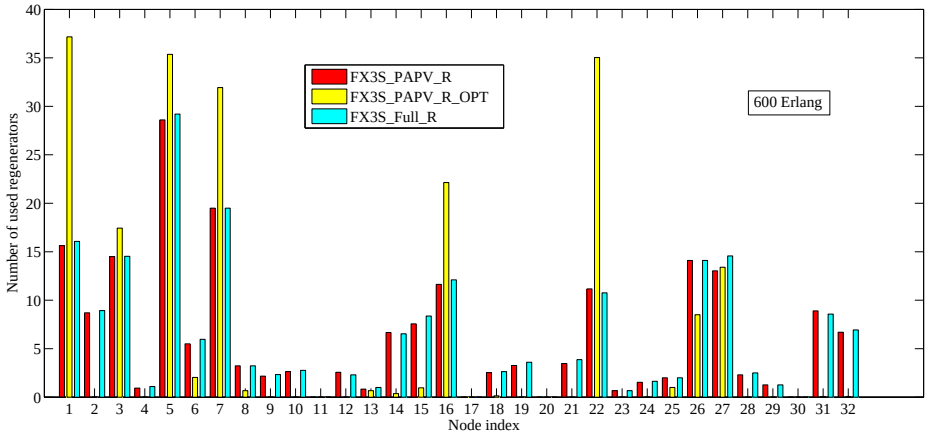

Figure 5.13: Number of regenerators used per node in each simulated scenario

However, even if the number of regenerators used in FX3S_PAPV_R_OPT is the same as in FX3S_PAPV_R, the regenerations are not performed in the same optical nodes. This can be noticed on Figure 5.13, where we show the number of regenerators used over network nodes per scenario. We plotted in yellow the regenerators used in

each node for the FX3S_PAPV_R_OPT scenario, in red for FX3S_PAPV_R and in blue for FX3S_Full_R. We can notice that the use of PAR algorithm has impacted the regeneration sites in FX3S_PAPV_R_OPT and thus they have different positions compared with the FX3S_Full_R scenario. For instance, in node 7 with FX3S_PAPV_R_OPT we have on average 32 regenerators used, whereas with FX3S_PAPV_R and FX3S_Full_R we have on average 19 regenerators used.

5.4.4 Simulations with other topologies

Simulations were repeated over the NSF topology (described by Figure 4.12) for the flexible scenario with power adaptation process (i.e., FX3S_PAPV_R). Figure 5.14 shows the blocking probability of the simulated scenarios as a function of network load. We can notice that the FX3S_PAPV_R_OPT scenario obtains exactly the same blocking probability as FX3S_PAPV_R.

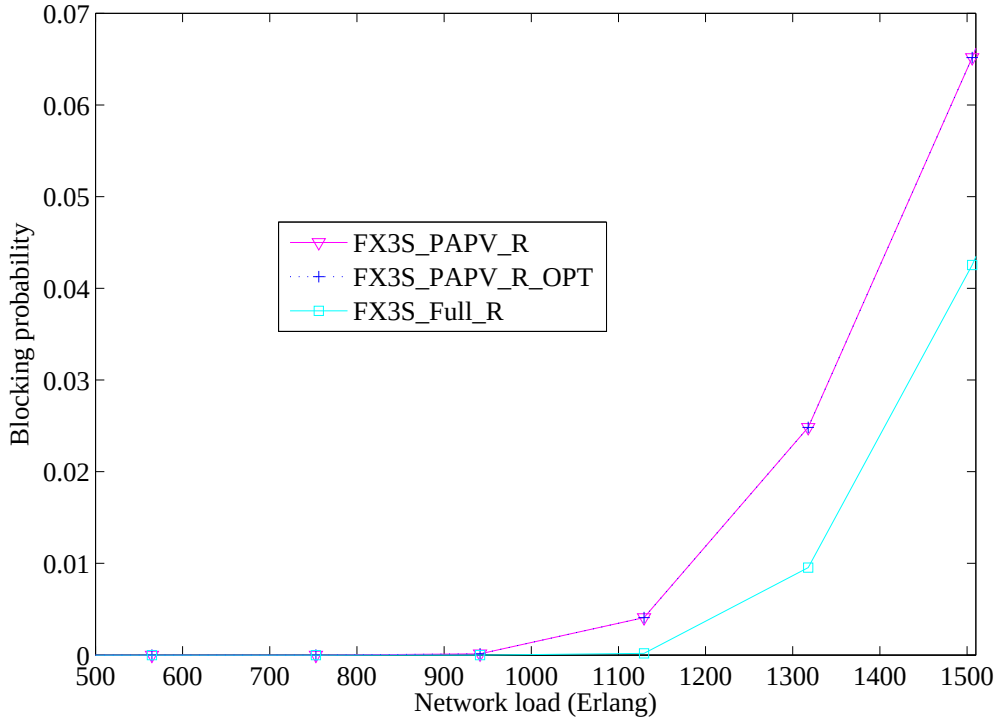

Figure 5.14: Blocking probability versus network load in NSF network

Indeed, the PAR algorithm used in FX3S_PAPV_R_OPT did not succeeded in avoiding the power saturation problem. This is confirmed by Figure 5.15 where No Pow blocking still arises with the same value on average compared to the FX3S_PAPV_R scenario. In fact, the NSF topology has very long optical links (as it can be noticed on Figure 4.12 in Chapter 4) and thus optical connections suffer from high signal degrada-

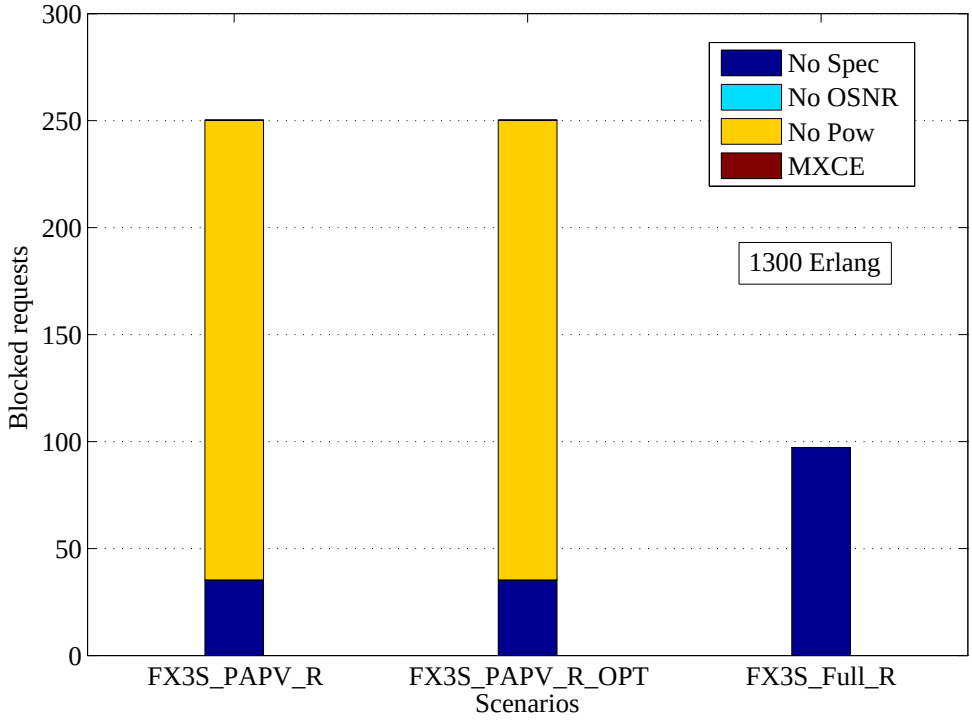

Figure 5.15: Blocking reasons per simulated scenarios

tion preventing the PAR algorithm from shifting the regeneration sites. Moreover, the maximum number of hops for any channel is three which reduces severely the flexibility to optimize regeneration sites (i.e., site optimization is possible only for 3-hops channel. Indeed, there is no choice for regenerator assignment when 2-hop channel is used, because it is mandatory to put assign regenerator in the central node. Moreover, no regenerator can be placed in a 1-hop channel. As a result, the PAR algorithm was not able to optimize regeneration sites and avoid the power saturation problem.

5.5 Conclusion

In this chapter, we focused on developing a solution to the persisting power saturation problem in flexible scenarios that uses the power adaptation process. To this end, we developed a power aware regeneration algorithm that places regeneration sites in such a way it allow reducing the power level over highly loaded links. The algorithm was implemented in the flexible scenarios that were not able to totally overcome the power saturation problem over the European and NSF topologies. The objective function of the algorithm was modeled through ILP formulation to facilitate understanding its goal. Finally, the functional description of the algorithm was described though an example.

Simulation results showed that the PAR algorithm succeeded in totally avoiding the power saturation problem over the European topology even when the network is highly loaded. In contrast, the algorithm was not capable of avoiding this saturation problem over the NSF topology. This result has demonstrated that the efficiency of the power aware regeneration algorithm depends on network topology in terms of channel length. This result shows the dependence between the efficiency of the power aware regeneration algorithm, the network topology and channels length. Moreover, it demonstrates that including power awareness in the regenerators assignment algorithm can improves the network utilization and allows benefiting from the flexible technology while keeping the legacy amplifiers.

CONCLUSIONS AND PROSPECTS

Exponential traffic growth in optical networks has triggered the evolution to flexible optical networks, promising a significant gain for network operators in terms of spectral efficiency and spectrum usage over their optical network infrastructures. However, deploying new optical links and replacing the existing optical equipment, makes the flex-grid technology very expensive for network operators in spite of its capacity increase promises. In this respect, network operators are trying to reduce the costs (i.e., purchasing and operational cost) of the migration to flexible networks by keeping in use the existing infrastructure.

In this thesis work, we have addressed the flexible technology and its impacts on the physical and the control plane of current optical transport networks. We focused on the power saturation problem that could possibly be encountered during the migration from fixed-grid to flex-grid networks when keeping in use the current network infrastructures. In particularly, we addressed the problem that has not been previously studied, regarding the power saturation in optical amplifiers due to the increase in the number of established optical channels.

The main objective of our work was, on the one hand, to evaluate this power saturation problem and propose a solution that can be easily implemented in an optical control plane. On the other hand, to demonstrate that improving the control plane intelligence allows optimizing network resources, and thus benefiting from the capacity increase offered by the flexible technology while keeping the existing network infrastructures.

It is in this context that the work was realized, the contributions and results are summarized as follows:

- We firstly introduced in Chapter 1, the evolution of optical networks as well as the data and control plane constituting the two main parts of an automated optical network. We presented the network design phase and the physical elements that can impact the design and the control of optical networks. Finally, we focused on the widely used GMPLS control plane protocol suite and provided a functional description of its routing and signaling protocols.

- Evolution towards flexible networks and impact of flexibility on the data plane and the control plane of current optical networks are presented in Chapter 2. We showed how the changes in the data plane by adding flexible optical equipment

can increase the complexity of the routing algorithm, requiring an improvement to the control plane protocols of any automated optical network. Then, we presented the existing works in literature that deal with flexibility, demonstrating that evolution towards automated flexible networks allows optimizing network resources and increases the capacity of current optical networks. Lastly, we highlighted the increase in channel number offered by the flexible technology, that can increases the optical power level in optical links, raising the importance of taking into account the optical power as a limitation when migrating to flexible network.

- In Chapter 3, we addressed the power saturation problem that could arise after the migration from fixed to flex-grid network when keeping in use existing network infrastructures. We focused in this chapter, on transparent optical networks under incremental traffic pattern, to simulate the case of static network. The power saturation problem was tackled as follows: Firstly, we developed a link design method that allowed us to determinate the power level over network links. Then, we identified the essential parameters required by an optical control plane to control and evaluate the power levels over network links. Secondly, we proposed a per channel power adaptation process that benefits from transmission power margins to reduce channel transmitted power. Subsequently, we proposed a path computation algorithm, with protocol extension to the routing and signaling protocols of the GMPLS protocol suite, in order to provide the practical implementation of such a power adaptation process.

  Simulation results demonstrated that the power levels of the fixed-grid infrastructure are not sufficient to handle the increase in the number of channels when migrating to flex-grid network. They showed also that the use of power adaptation process allows reducing the power saturation problem and thus increases the capacity of the network. Finally, they demonstrated that increasing the number of computed shortest paths does not allow to completely avoiding the power saturation problem even if the power adaptation process is used.

- In Chapter 4, we have extended our study to the case of translucent networks under dynamic traffic patterns to simulate the case of future automatic and flexible optical networks. The power adaptation process and the path computation algorithm were adapted to the case of regenerated optical channels. Then, we have proposed new extensions to the routing and signaling protocols to handle the optical regeneration and the power adaptation. Simulation results showed that the power saturation problem arises even at low network load and under dynamic traffic patterns. Moreover, as in Chapter 3, the increase in network capacity cannot be fully exploited, if the power adaptation process is not used in flexible scenarios. It has been shown also that the regeneration method used in the path computation algorithm can impact the performance and the cost of the network.

To go further, we have repeated the simulations over additional network topologies. Results have shown a strong dependence between the network topology and the arising of the power saturation problem. Topologies having optical links introducing low signal degradation will probably have enough power margins to avoid the power saturation problem, and can support the additional flex-grid channels when the power adaptation process is used.

- In Chapter 5, we have studied the persisting power saturating problem in flexible translucent optical networks. Therefore, we proposed a novel power aware regeneration algorithm that uses the power information of network links in order to select the regeneration sites. The algorithm was applied in flexible scenarios using the power adaptation process, where saturation problem is still arising. Simulation results have shown that the algorithm succeeded in avoiding the power saturation problem by changing the power distribution over network links. However, the performance of the algorithm showed a dependency on the network topology.

In summary, this work highlighted the importance of taking into account power information of optical links during the migration to flex-grid networks. It allowed understanding the impact of link optical power levels on the expected capacity gain of the flexible technology. Moreover, it allowed developing the protocol extensions and the path computation algorithms required to achieve the practical implementation of the per channel adaptation process in future flexible optical networks.

Perspectives

The results obtained in this thesis opens up many interesting research tracks that can be explored in the future:

- Implementation over platform: in this work, the theoretical study was realized to facilitate the implementation of the power adaptation process in optical control plane. However, the implementation of this process in a real platform is highly recommended to validate the theoretical study, to check whether the concept works, and that there is no missing parameter or criterion that should be taken into account.

- Improving the physical feasibility estimator: During simulations, only the flexibility in terms of channel spacing was considered, where only 3 and 4 slots channels are taken into account assuming fixed modulation format, baud and bit rate, and FEC. However, these considered parameters do not affect the required OSNR at the receiver side, since they were fixed and never changed during simulation. We think that with the introduction of programmable transceivers in future optical networks, it is important to have a physical feasibility estimator that is ca-

pable of computing the required $OSNR_{min}$ for any combination of flexibility parameters.

- Improving path computation algorithm: since the provisioning strategy considered in the control plane can impact the performance of the network, it is important to have an intelligent strategy that allows maximizing network capacity. Therefore, we recommend developing a path computation algorithm that allows exploiting efficiently network resources by using the offered flexibility parameters. More particularly, the algorithm should be capable, for example, of deciding when to adapt the channel power, or when to change the modulation format in order to exploit efficiently the OSNR margins.

- Improving the power adaptation signaling mechanism: As discussed in Chapter 1, the requested optical channel cannot sometime be successfully established, if the OSNR estimation is not sufficiently accurate. Therefore, we think that it is preferable to have a signaling mechanism that attenuates progressively the power of the channel to guarantee its operation.

- Interoperability between network operators: in this work, the real power values were used and stored in the databases of one network domain. However, for the context of multi-domain, we think that it is possible to secure power information by normalizing their values and thus guaranteeing privacy between the two domains.

- Improving regeneration algorithm: in Chapter 4 and Chapter 5, we showed that the regeneration placement algorithm has a direct impact on network performance. We believe that taking advantage of the set of flexibility parameters in addition to the wavelength conversion capability can allow improving network capacity. For example, developing a regeneration algorithm that uses wavelength converters, power information and other flexibility parameters (e.g., channel spacing, modulation format, baud rates, FEC), can help reducing spectral fragmentation, increasing network capacity and at the same time avoiding power saturation.

- Study of control plane scalability issues: in Chapter 3 and Chapter 4, we proposed several extensions to GMPLS control plane protocols. We think that adding some bytes to the already existing OSPF-TE and RSVP-TE messages will not really affect the performance of these protocols. However, it is always interesting to evaluate the performance of the control plane. Especially, when the control plane considers all flexibility parameters and integrates information on the internal switching capability of ROADMs.

- Implementation with other control plane protocols: with the emergence of SDN paradigm, it will be interesting to have interworking of GMPLS domain with an SDN controller. This interaction with an SDN controller (e.g., OpenDaylight or

ONOS [162, 163]) allows more sophisticated management of network resources. A direct example could be the optimization of channel power parameters (i.e., $C_{adaptation}$ coefficients) all over the network. Therefore, depending on the controller used and its associated protocols, several protocol extensions are required to handle this kind of improvement.

List of Publications

International Conferences

C1 M. Kanj, E. L. Rouzic, D. Amar, J. L. Auge, B. Cousin, and N. Brochier, "Optical power control to efficiently handle flex-grid spectrum gain over existing fixed-grid network infrastructures," in *2016 International Conference on Computing, Networking and Communications (ICNC)*, Feb 2016, pp. 1–7.

C2 D. Amar, M. Kanj, J. L. Auge, N. Brochier, E. L. Rouzic, C. Lepers, and B. Cousin, "On the legacy amplifier limitation in flexgrid optical networks," in *2015 International Conference on Photonics in Switching (PS)*, Sept 2015, pp. 172–174.

International Journals

J1 M. Kanj, E. L. Rouzic, J. Meuric, B. Cousin, and D. Amar, "Optical power control in GMPLS control plane," *IEEE/OSA Journal of Optical Communications and Networking*, vol. 8, no. 8, pp. 553–568, August 2016.

J2 D. Amar, N. Brochier, E. L. Rouzic, J. L. Auge, C. Lepers, B. Cousin, and M. Kanj, "Link design and legacy amplifier limitation in flex-grid optical networks," *IEEE Photonics Journal*, vol. 8, no. 2, pp. 1–10, April 2016.

Patent

P1 M. Kanj, and E. L. Rouzic, "Method for placing optical regenerators over flexible Grid wavelength switched optical networks," (under progress) .

BIBLIOGRAPHY

[1] S. Frisken, G. Baxter, D. Abakoumov, H. Zhou, I. Clarke, and S. Poole, "Flexible and grid-less wavelength selective switch using LCOS technology," in *2011 Optical Fiber Communication Conference and Exposition and the National Fiber Optic Engineers Conference*, March 2011, pp. 1–3.

[2] Y. Pointurier, "Design of low-margin optical networks," in *2016 Optical Fiber Communications Conference and Exhibition (OFC)*, March 2016, pp. 1–3.

[3] S. L. Woodward, "Roadm options in optical networks: Flexible grid or not?" in *2013 Optical Fiber Communication Conference and Exposition and the National Fiber Optic Engineers Conference (OFC/NFOEC)*, March 2013, pp. 1–3.

[4] Cisco, "Cisco visual networking index: Forecast and methodology, 2014-2019," White Paper, Cisco, May 2015. [Online]. Available: http://s2.q4cdn.com/230918913/files/doc_downloads/report_2014/white_paper_c11-481360.pdf

[5] B. Ramamurthy, H. Feng, D. Datta, J. P. Heritage, and B. Mukherjee, "Transparent vs. opaque vs. translucent wavelength-routed optical networks," in *OFC/IOOC . Technical Digest. Optical Fiber Communication Conference, 1999, and the International Conference on Integrated Optics and Optical Fiber Communication*, vol. 1, Feb 1999, pp. 59–61.

[6] S. Mechels, L. Muller, G. D. Morley, and D. Tillett, "1D MEMS-based wavelength switching subsystem," *IEEE Communications Magazine*, vol. 41, no. 3, pp. 88–94, Mar 2003.

[7] D. M. Marom, D. T. Neilson, D. S. Greywall, C.-S. Pai, N. R. Basavanhally, V. A. Aksyuk, D. O. Lopez, F. Pardo, M. E. Simon, Y. Low, P. Kolodner, and C. A. Bolle, "Wavelength-selective 1 x K switches using free-space optics and MEMS micromirrors: theory, design, and implementation," *Journal of Lightwave Technology*, vol. 23, no. 4, pp. 1620–1630, April 2005.

[8] C. V. Saradhi and S. Subramaniam, "Physical layer impairment aware routing (PLIAR) in WDM optical networks: issues and challenges," *IEEE Communications Surveys Tutorials*, vol. 11, no. 4, pp. 109–130, Fourth 2009.

[9] T. Xu, G. Jacobsen, S. Popov, J. Li, E. Vanin, K. Wang, A. T. Friberg, and Y. Zhang, "Chromatic dispersion compensation in coherent transmission system using digital filters," *Opt. Express, OE*, vol. 18, no. 15, pp. 16 243–16 257, Jul. 2010. [Online]. Available: http://www.osapublishing.org/abstract.cfm?uri=oe-18-15-16243

[10] R. Martinez, C. Pinart, F. Cugini, N. Andriolli, L. Valcarenghi, P. Castoldi, L. Wosinska, J. Comellas, and G. Junyent, "Challenges and requirements for introducing impairment-awareness into the management and control planes of ASON/GMPLS WDM networks," *IEEE Communications Magazine*, vol. 44, no. 12, pp. 76–85, Dec 2006.

[11] K. Christodoulopoulos, K. Manousakis, and E. Varvarigos, "Reach Adapting Algorithms for Mixed Line Rate WDM Transport Networks," *Journal of Lightwave Technology*, vol. 29, no. 21, pp. 3350–3363, Nov 2011.

[12] A. Nag and M. Tornatore, "Optical network design with mixed line rates," *Optical Switching and Networking*, vol. 6, no. 4, pp. 227–234, Dec. 2009. [Online]. Available: http://linkinghub.elsevier.com/retrieve/pii/S1573427709000538

[13] S. M. Sajjan, V. Seshasai, and D. G. Sadashivappa, "DWDM link design and power budget calculation," *International Journal of Advanced Research in Electrical, Electronics and Instrumentation Engineering*, vol. 4, April 2015.

[14] A. Gumaste and T. Antony, *DWDM network designs and engineering solutions*. Indianapolis, IN: Cisco Press, 2003.

[15] T. Zami, "Physical impairment aware planning of next generation WDM backbone networks," in *OFC/NFOEC*, March 2012, pp. 1–3.

[16] G. Bosco, A. Carena, R. Cigliutti, V. Curri, P. Poggiolini, and F. Forghieri, "Performance prediction for WDM PM-QPSK transmission over uncompensated links," in *2011 Optical Fiber Communication Conference and Exposition and the National Fiber Optic Engineers Conference*, March 2011, pp. 1–3.

[17] T. Zami, J. C. Antona, P. Peloso, E. L. Rouzic, A. Morea, M. Joindot, B. Fracasso, P. Gravey, and M. Gagnaire, "Dimensioning of WDM transparent networks based on the Quality of Transmission," in *Broadband Europe Conference, Brugges, Belgium*, vol. 8, 2004.

[18] P. Kulkarni, A. Tzanakaki, C. M. Machuka, and I. Tomkos, "Benefits of Q-factor based routing in WDM metro networks," in *2005 31st European Conference on Optical Communication, ECOC 2005*, vol. 4, Sept 2005, pp. 981–982.

[19] C. Politi, V. Anagnostopoulos, C. Matrakidis, and A. Stavdas, "Physical layer impairment aware routing algorithms based on analytically calculated Q-factor,"

in *2006 Optical Fiber Communication Conference and the National Fiber Optic Engineers Conference*, March 2006, pp. 1–3.

[20] R. Cardillo, V. Curri, and M. Mellia, "Considering transmission impairments in configuring wavelength routed optical networks," in *2006 Optical Fiber Communication Conference and the National Fiber Optic Engineers Conference*, March 2006, pp. 1–3.

[21] P. Poggiolini, G. Bosco, A. Carena, R. Cigliutti, V. Curri, F. Forghieri, R. Pastorelli, and S. Piciaccia, "The LOGON strategy for low-complexity control plane implementation in new-generation flexible networks," in *2013 Optical Fiber Communication Conference and Exposition and the National Fiber Optic Engineers Conference (OFC/NFOEC)*, March 2013, pp. 1–3.

[22] Y. Huang, J. P. Heritage, and B. Mukherjee, "Connection provisioning with transmission impairment consideration in optical WDM networks with high-speed channels," *Journal of Lightwave Technology*, vol. 23, no. 3, pp. 982–993, March 2005.

[23] W. Freude, R. Schmogrow, B. Nebendahl, M. Winter, A. Josten, D. Hillerkuss, S. Koenig, J. Meyer, M. Dreschmann, M. Huebner, C. Koos, J. Becker, and J. Leuthold, "Quality metrics for optical signals: Eye diagram, Q-factor, OSNR, EVM and BER," in *2012 14th International Conference on Transparent Optical Networks (ICTON)*, July 2012, pp. 1–4.

[24] E. L. Rouzic, "Physical impairment awareness in the context of an operator infrastructure," in *2009 International Conference on Photonics in Switching*, Sept 2009, pp. 1–4.

[25] A. Jajszczyk, "The ASON approach to the control plane for optical networks," in *Proceedings of 2004 6th International Conference on Transparent Optical Networks (IEEE Cat. No.04EX804)*, vol. 1, July 2004, pp. 87–90.

[26] ITU Telecommunication Standardization, "Protocol for automatic discovery in SDH and OTN networks," ITU-T Recommendation G.7714.1/Y.1705.1, International Telecommunication Union, Geneva, Apr. 2003.

[27] ——, "ASON routing architecture and requirements for link state protocols," ITU-T Recommendation G.7715.1/Y.1706.1, International Telecommunication Union, Geneva, Feb. 2004.

[28] Y. Lee, G. Bernstein, J. Martensson, T. Takeda, T. Tsuritani, and O. G. de Dios, "Path computation element communication protocol (PCEP) requirements for wavelength switched optical network (WSON) routing and wavelength assignment," Internet Requests for Comments, RFC Editor, RFC 7449, February 2015.

[29] ITU Telecommunication Standardization, "Distributed Call and Connection Management: Signalling mechanism using GMPLS RSVP-TE," ITU-T Recommendation G.7713.2/Y.1704.2, International Telecommunication Union, Geneva, Mar. 2003.

[30] T. W. Um, J. K. Choi, Y. A. Kim, H. H. Lee, H. W. Jung, and S. G. Jong, "Signaling and control procedures using generalized MPLS protocol for IP over an optical network," *ETRI journal*, vol. 24, no. 2, pp. 69–80, 2002. [Online]. Available: http://etrij.etri.re.kr/etrij/journal/article/article.do?volume=24&issue=2&page=69

[31] M. Veeraraghavan and H. Wang, "A comparison of in-band and out-of-band transport options for signaling," in *IEEE Global Telecommunications Conference Workshops, 2004. GlobeCom Workshops 2004*, Nov 2004, pp. 345–351.

[32] H. Zang, J. P. Jue, B. Mukherjee, and others, "A review of routing and wavelength assignment approaches for wavelength-routed optical WDM networks," *Optical Networks Magazine*, vol. 1, no. 1, pp. 47–60, 2000.

[33] D. Amar, E. L. Rouzic, N. Brochier, and C. Lepers, "Class-of-service-based multilayer architecture for traffic restoration in elastic optical networks," *IEEE/OSA Journal of Optical Communications and Networking*, vol. 8, no. 7, pp. A34–A44, July 2016.

[34] J. P. Jue, "Lightpath establishment in wavelength-routed WDM optical networks," in *Optical networks*. Springer, 2001, pp. 99–122. [Online]. Available: http://link.springer.com/chapter/10.1007/978-1-4613-0291-9_5

[35] G. N. Rouskas, "Routing and Wavelength Assignment in Optical WDM Networks," *Wiley Encyclopedia of Telecommunications*, (John Proakis, Editor), John Wiley & Sons, 2001.

[36] B. V. Caenegem, W. V. Parys, F. D. Turck, and P. M. Demeester, "Dimensioning of survivable WDM networks," *IEEE Journal on Selected Areas in Communications*, vol. 16, no. 7, pp. 1146–1157, Sep 1998.

[37] I. Chlamtac, A. Ganz, and G. Karmi, "Lightpath communications: an approach to high bandwidth optical wan's," *IEEE Transactions on Communications*, vol. 40, no. 7, pp. 1171–1182, Jul 1992.

[38] A. Norouzi, A. Zaim, and B. B. Ustundag, "An integrated survey in optical networks: Concepts, components and problems," *IJCSNS International Journal of Computer Science and Network Security*, vol. 11, no. 1, January 2011.

[39] D. Levi, P. Meyer, and B. Stewart, "Simple Network Management Protocol (SNMP) Applications," Internet Requests for Comments, RFC Editor, RFC 3413, December 2002. [Online]. Available: http://www.rfc-editor.org/rfc/rfc3413.txt

[40] B. A. A. Nunes, M. Mendonca, X. N. Nguyen, K. Obraczka, and T. Turletti, "A Survey of Software-Defined Networking: Past, Present, and Future of Programmable Networks," *IEEE Communications Surveys Tutorials*, vol. 16, no. 3, pp. 1617–1634, Third 2014.

[41] E. Mannie, "Generalized multi-protocol label switching (gmpls) architecture," Internet Requests for Comments, RFC Editor, RFC 3945, October 2004.

[42] D. Katz, K. Kompella, and D. Yeung, "Traffic Engineering (TE) Extensions to OSPF Version 2," Internet Requests for Comments, RFC Editor, RFC 3630, September 2003.

[43] D. Awduche, L. Berger, D. Gan, T. Li, V. Srinivasan, and G. Swallow, "RSVP-TE: Extensions to RSVP for LSP Tunnels," Internet Requests for Comments, RFC Editor, RFC 3209, December 2001.

[44] J. Lang, "Link Management Protocol (LMP)," Internet Requests for Comments, RFC Editor, RFC 4204, October 2005.

[45] F. Paolucci, F. Cugini, A. Giorgetti, N. Sambo, and P. Castoldi, "A Survey on the Path Computation Element (PCE) Architecture," *IEEE Communications Surveys Tutorials*, vol. 15, no. 4, pp. 1819–1841, Fourth 2013.

[46] S. Azodolmolky, M. Klinkowski, E. Marin, D. Careglio, J. S. Pareta, and I. Tomkos, "A survey on physical layer impairments aware routing and wavelength assignment algorithms in optical networks," *Computer Networks: The International Journal of Computer and Telecommunications Networking archive*, vol. 53, no. 1, pp. 926–944, May 2009.

[47] X. Chen and Y. Zhang, "Intelligence on Optical Transport SDN," *International Journal of Computer and Communication Engineering*, vol. 4, no. 1, pp. 5–8, 2015. [Online]. Available: http://www.ijcce.org/index.php?m=content&c=index&a=show&catid=45&id=445

[48] D. Kreutz, F. M. V. Ramos, P. E. Veríssimo, C. E. Rothenberg, S. Azodolmolky, and S. Uhlig, "Software-Defined Networking: A Comprehensive Survey," *Proceedings of the IEEE*, vol. 103, no. 1, pp. 14–76, Jan 2015.

[49] D. King, A. Farrel, and N. Georgalas, "The role of SDN and NFV for flexible optical networks: Current status, challenges and opportunities," in *2015 17th International Conference on Transparent Optical Networks (ICTON)*, July 2015, pp. 1–6.

[50] R., R. Munoz, R. Martínez, R. Vilalta, L. Liu, T. Tsuritani, I. Morita, V. López, O. G. de Dios, and J. P. Fernández-Palacios, "SDN based Provisioning orchestration of OpenFlow/GMPLS flexi-grid networks with a stateful hierarchical PCE," in *OFC 2014*, March 2014, pp. 1–3.

[51] R. Casellas, R. Martinez, R. Munoz, R. Vilalta, and L. Liu, "Control and orchestration of multidomain optical networks with GMPLS as inter-SDM controller communication [Invited]," *IEEE/OSA Journal of Optical Communications and Networking*, vol. 7, no. 11, pp. B46–B54, November 2015.

[52] A. Morea, G. Rizzelli, and M. Tornatore, "On the energy and cost trade-off of different energy-aware network design strategies," in *2013 Optical Fiber Communication Conference and Exposition and the National Fiber Optic Engineers Conference (OFC/NFOEC)*, March 2013, pp. 1–3.

[53] S. Shimazaki, Y. Tamura, D. Hanawa, K. Oguchi, T. Watanabe, and T. Takahashi, "Cost comparison of different roadm architectures," in *2013 19th Asia-Pacific Conference on Communications (APCC)*, Aug 2013, pp. 501–504.

[54] ITU Telecommunication Standardization, "Spectral grids for WDM applications: DWDM frequency grid," ITU-T Recommendation G.694.1, International Telecommunication Union, Geneva, Feb. 2012.

[55] S. L. Woodward, "ROADM options in optical networks: Flexible grid or not?" in *2013 Optical Fiber Communication Conference and Exposition and the National Fiber Optic Engineers Conference (OFC/NFOEC)*, March 2013, pp. 1–3.

[56] P. Wright, A. Lord, and L. Velasco, "The network capacity benefits of Flexgrid," in *2013 17th International Conference on Optical Networking Design and Modeling (ONDM)*, April 2013, pp. 7–12.

[57] P. Wright, A. Lord, and S. Nicholas, "Comparison of optical spectrum utilization between flexgrid and fixed grid on a real network topology," in *OFC/NFOEC*, March 2012, pp. 1–3.

[58] E. Pawlowski, K. Takiguchi, M. Okuno, K. Sasayama, A. Himeno, K. Okamoto, and Y. Ohmori, "Variable bandwidth and tunable centre frequency filter using transversal-form programmable optical filter," *Electronics Letters*, vol. 32, no. 2, pp. 113–114, Jan 1996.

[59] G. Baxter, S. Frisken, D. Abakoumov, H. Zhou, I. Clarke, A. Bartos, and S. Poole, "Highly programmable wavelength selective switch based on liquid crystal on silicon switching elements," in *2006 Optical Fiber Communication Conference and the National Fiber Optic Engineers Conference*, March 2006, pp. 1–3.

[60] M. C. Mora, A. M. Minguez, and P. R. Horche, "Design of equalized ROADMs devices with flexible bandwidth based on LCoS technology," in *2014 19th European Conference on Networks and Optical Communications - (NOC)*, June 2014, pp. 41–46.

[61] Y. Li, L. Gao, G. Shen, and L. Peng, "Impact of ROADM colorless, directionless, and contentionless (CDC) features on optical network performance [invited]," *IEEE/OSA Journal of Optical Communications and Networking*, vol. 4, no. 11, pp. B58–B67, Nov 2012.

[62] A. Chiu, G. Choudhury, G. Clapp, R. Doverspike, M. Feuer, J. Gannett, J. Jackel, G. Kim, J. Klincewicz, T. Kwon, G. Li, P. Magill, . . Simmons, R. Skoog, J. Strand, A. Lehmen, B. Wilson, S. Woodward, and D. Xu, "Architectures and Protocols for Capacity Efficient, Highly Dynamic and Highly Resilient Core Networks [Invited]," *IEEE/OSA Journal of Optical Communications and Networking*, vol. 4, no. 1, pp. 1–14, January 2012.

[63] K. Roberts, D. Beckett, D. Boertjes, J. Berthold, and C. Laperle, "100G and beyond with digital coherent signal processing," *IEEE Communications Magazine*, vol. 48, no. 7, pp. 62–69, July 2010.

[64] G. Bosco, V. Curri, A. Carena, P. Poggiolini, and F. Forghieri, "On the performance of nyquist-wdm terabit superchannels based on pm-bpsk, pm-qpsk, pm-8qam or pm-16qam subcarriers," *Journal of Lightwave Technology*, vol. 29, no. 1, pp. 53–61, Jan 2011.

[65] X. Liu, S. Chandrasekhar, and P. J. Winzer, "Digital signal processing techniques enabling multi-tb/s superchannel transmission: An overview of recent advances in dsp-enabled superchannels," *IEEE Signal Processing Magazine*, vol. 31, no. 2, pp. 16–24, March 2014.

[66] O. Gerstel, M. Jinno, A. Lord, and S. J. B. Yoo, "Elastic optical networking: a new dawn for the optical layer?" *IEEE Communications Magazine*, vol. 50, no. 2, pp. s12–s20, February 2012.

[67] K. Roberts and C. Laperle, "Flexible transceivers," in *2012 38th European Conference and Exhibition on Optical Communications*, Sept 2012, pp. 1–3.

[68] O. Rival, A. Morea, H. Drid, N. Brochier, and E. L. Rouzic, "Upgrading optical networks with elastic transponders," in *2012 38th European Conference and Exhibition on Optical Communications*, Sept 2012, pp. 1–3.

[69] G. Shen and Q. Yang, "From coarse grid to mini-grid to gridless: How much can gridless help contentionless?" in *2011 Optical Fiber Communication Conference and Exposition and the National Fiber Optic Engineers Conference*, March 2011, pp. 1–3.

[70] P. S. Khodashenas, J. M. Rivas-Moscoso, D. Klonidis, D. M. Marom, and I. Tomkos, "Evaluating the performance of ultra-fine spectrum granularity flexible optical networks," in *2015 17th International Conference on Transparent Optical Networks (ICTON)*, July 2015, pp. 1–4.

[71] O. Pedrola, A. Castro, L. Velasco, M. Ruiz, J. P. Fernández-Palacios, and D. Careglio, "CAPEX study for a multilayer IP/MPLS-over-flexgrid optical network," *IEEE/OSA Journal of Optical Communications and Networking*, vol. 4, no. 8, pp. 639–650, Aug 2012.

[72] J. Shen, J. Chen, and Y. Sun, "Fragmentation aware routing and spectrum assignment algorithm for elastic optical networks," in *TENCON 2015 - 2015 IEEE Region 10 Conference*, Nov 2015, pp. 1–4.

[73] R. Wang and B. Mukherjee, "Spectrum management in heterogeneous bandwidth networks," in *2012 IEEE Global Communications Conference (GLOBECOM)*, Dec 2012, pp. 2907–2911.

[74] ——, "Provisioning in Elastic Optical Networks with Non-Disruptive Defragmentation," *Journal of Lightwave Technology*, vol. 31, no. 15, pp. 2491–2500, Aug 2013.

[75] A. N. Patel, P. N. Ji, J. P. Jue, and T. Wang, "Defragmentation of transparent Flexible optical WDM (FWDM) networks," in *2011 Optical Fiber Communication Conference and Exposition and the National Fiber Optic Engineers Conference*, March 2011, pp. 1–3.

[76] Y. Sone, A. Hirano, A. Kadohata, M. Jinno, and O. Ishida, "Routing and spectrum assignment algorithm maximizes spectrum utilization in optical networks," in *2011 37th European Conference and Exhibition on Optical Communication*, Sept 2011, pp. 1–3.

[77] F. Cugini, F. Paolucci, G. Meloni, G. Berrettini, M. Secondini, F. Fresi, N. Sambo, L. Poti, and P. Castoldi, "Push-Pull Defragmentation Without Traffic Disruption in Flexible Grid Optical Networks," *Journal of Lightwave Technology*, vol. 31, no. 1, pp. 125–133, Jan 2013.

[78] T. Takagi, H. Hasegawa, K. i. Sato, Y. Sone, A. Hirano, and M. Jinno, "Disruption Minimized Spectrum Defragmentation in Elastic Optical Path Networks that Adopt Distance Adaptive Modulation," in *2011 37th European Conference and Exhibition on Optical Communication*, Sept 2011, pp. 1–3.

[79] R. Proietti, R. Yu, K. Wen, Y. Yin, and S. J. B. Yoo, "Quasi-hitless defragmentation technique in elastic optical networks by a coherent RX LO with fast TX wavelength tracking," in *2012 International Conference on Photonics in Switching (PS)*, Sept 2012, pp. 1–3.

[80] Y. Yin, M. Zhang, Z. Zhu, and S. J. B. Yoo, "Fragmentation-aware routing, modulation and spectrum assignment algorithms in elastic optical networks," in *2013 Optical Fiber Communication Conference and Exposition and the National Fiber Optic Engineers Conference (OFC/NFOEC)*, March 2013, pp. 1–3.

[81] A. Rosa, C. Cavdar, S. Carvalho, J. Costa, and L. Wosinska, "Spectrum allocation policy modeling for elastic optical networks," in *High Capacity Optical Networks and Emerging/Enabling Technologies*, Dec 2012, pp. 242–246.

[82] D. A. A. Melo and others, "Adaptive optical transceivers: concepts and challenges," *Journal of Communication and Information Systems*, vol. 29, no. 1, 2014. [Online]. Available: http://www.academia.edu/download/43244255/Adaptive_Optical_Transceivers_Concepts_a20160301-29901-11sydlh.pdf

[83] X. Zhang, H. Zheng, R. Casellas, O. de Dios, and D. Ceccarelli, "GMPLS OSPF-TE Extensions in support of Flexi-grid DWDM networks," Working Draft, IETF Secretariat, Internet-Draft, draft-ietf-ccamp-flexible-grid-ospf-ext-05, August 2016. [Online]. Available: http://www.ietf.org/internet-drafts/draft-ietf-ccamp-flexible-grid-ospf-ext-05.txt

[84] F. Zhang, X. Zhang, A. Farrel, O. G. de Dios, and D. Ceccarelli, "RSVP-TE Signaling Extensions in Support of Flexi-Grid Dense Wavelength Division Multiplexing (DWDM) Networks," Internet Requests for Comments, RFC Editor, RFC 7792, March 2016.

[85] G. Martinelli and A. Zanardi, "GMPLS Signaling Extensions for Optical Impairment Aware Lightpath Setup," Working Draft, IETF Secretariat, Internet-Draft, draft-martinelli-ccamp-optical-imp-signaling-03, October 2010. [Online]. Available: http://www.ietf.org/internet-drafts/draft-martinelli-ccamp-optical-imp-signaling-03.txt

[86] F. Agraz, Y. Ye, J. Han, C. Saradhi, and A. Francescon, "RSVP-TE Extensions in Support of Impairment Aware Routing and Wavelength Assignment in Wavelength Switched Optical Networks (WSONs)," Working Draft, IETF Secretariat, Internet-Draft, draft-agraz-ccamp-wson-impairment-rsvp-00, October 2010. [Online]. Available: http://www.ietf.org/internet-drafts/draft-agraz-ccamp-wson-impairment-rsvp-00.txt

[87] Y. Lee, G. Bernstein, D. Li, and G. Martinelli, "A Framework for the Control of Wavelength Switched Optical Networks (WSON) with Impairments," Internet Requests for Comments, RFC Editor, RFC 6566, March 2012.

[88] N. Sambo, F. Cugini, G. Bottari, P. Iovanna, and P. Castoldi, "Distributed setup in optical networks with flexible grid," in *2011 37th European Conference and Exhibition on Optical Communication*, Sept 2011, pp. 1–3.

[89] V. López, B. Huiszoon, J. Fernández-Palacios, O. G. de Dios, and J. Aracil, "Path computation element in telecom networks: Recent developments and standardization activities," in *2010 14th Conference on Optical Network Design and Modeling (ONDM)*, Feb 2010, pp. 1–6.

[90] A. Farrel, J.-P. Vasseur, and J. Ash, "A Path Computation Element (PCE)-Based Architecture," Internet Requests for Comments, RFC Editor, RFC 4655, August 2006. [Online]. Available: http://www.rfc-editor.org/rfc/rfc4655.txt

[91] A. Giorgetti, F. Cugini, N. Sambo, F. Paolucci, N. Andriolli, and P. Castoldi, "Path state-based update of PCE traffic engineering database in wavelength switched optical networks," *IEEE Communications Letters*, vol. 14, no. 6, pp. 575–577, June 2010.

[92] Y. Lee, G. Bernstein, and W. Imajuku, "Framework for GMPLS and PCE Control of Wavelength Switched Optical Networks (WSON)," Internet Requests for Comments, RFC Editor, RFC 6163, April 2011.

[93] J. Vasseur and J. L. Roux, "Path Computation Element (PCE) Communication Protocol (PCEP)," Internet Requests for Comments, RFC Editor, RFC 5440, March 2009. [Online]. Available: http://www.rfc-editor.org/rfc/rfc5440.txt

[94] G. Meloni, F. Paolucci, N. Sambo, F. Cugini, M. Secondini, L. Gerardi, L. Potì, and P. Castoldi, "PCE architecture for flexible WSON enabling dynamic rerouting with modulation format adaptation," in *2011 37th European Conference and Exhibition on Optical Communication*, Sept 2011, pp. 1–3.

[95] R. Casellas, R. Muñoz, J. M. Fàbrega, M. S. Moreolo, R. Martínez, L. Liu, T. Tsuritani, and I. Morita, "Gmpls/pce control of flexi-grid dwdm optical networks using co-ofdm transmission [invited]," *IEEE/OSA Journal of Optical Communications and Networking*, vol. 4, no. 11, pp. B1–B10, Nov 2012.

[96] J. L. Augé, "Can we use flexible transponders to reduce margins?" in *2013 Optical Fiber Communication Conference and Exposition and the National Fiber Optic Engineers Conference (OFC/NFOEC)*, March 2013, pp. 1–3.

[97] A. Mitra, A. Lord, S. Kar, and P. Wright, "Effect of link margin and frequency granularity on the performance of a Flexgrid optical network," in *39th European Conference and Exhibition on Optical Communication (ECOC 2013)*, Sept 2013, pp. 1–3.

[98] ——, "Effect of link margins and frequency granularity on the performance and modulation format sweet spot of multiple flexgrid optical networks," in *Optical Fiber Communications Conference and Exhibition (OFC), 2014*, March 2014, pp. 1–3.

[99] D. J. Ives, P. Bayvel, and S. J. Savory, "Adapting Transmitter Power and Modulation Format to Improve Optical Network Performance Utilizing the Gaussian Noise Model of Nonlinear Impairments," *Journal of Lightwave Technology*, vol. 32, no. 21, pp. 4087–4096, Nov 2014.

[100] ——, "Assessment of options for utilizing SNR margin to increase network data throughput," in *2015 Optical Fiber Communications Conference and Exhibition (OFC)*, March 2015, pp. 1–3.

[101] D. McGhan, W. Leckie, and C. Chen, "Reconfigurable coherent transceivers for optical transmission capacity and reach optimization," in *OFC/NFOEC*, March 2012, pp. 1–3.

[102] A. Eira, J. Pedro, and J. Pires, "On the impact of optimized guard-band assignment for superchannels in flexible-grid optical networks," in *2013 Optical Fiber Communication Conference and Exposition and the National Fiber Optic Engineers Conference (OFC/NFOEC)*, March 2013, pp. 1–3.

[103] M. Jinno, B. Kozicki, H. Takara, A. Watanabe, Y. Sone, T. Tanaka, and A. Hirano, "Distance-adaptive spectrum resource allocation in spectrum-sliced elastic optical path network [Topics in Optical Communications]," *IEEE Communications Magazine*, vol. 48, no. 8, pp. 138–145, August 2010.

[104] T. Takagi, H. Hasegawa, K. Sato, T. Tanaka, B. Kozicki, Y. Sone, and M. Jinno, "Algorithms for maximizing spectrum efficiency in elastic optical path networks that adopt distance adaptive modulation," in *36th European Conference and Exhibition on Optical Communication*, Sept 2010, pp. 1–3.

[105] M. Salsi, O. Bertran-Pardo, J. Renaudier, W. Idler, H. Mardoyan, P. Tran, G. Charlet, and S. Bigo, "WDM 200Gb/s single-carrier PDM-QPSK transmission over 12,000km," in *2011 37th European Conference and Exhibition on Optical Communication*, Sept 2011, pp. 1–3.

[106] B. T. Teipen, M. H. Eiselt, K. Grobe, and J.-P. Elbers, "Adaptive Data Rates for Flexible Transceivers in Optical Networks," *Journal of Networks*, vol. 7, no. 5, May 2012. [Online]. Available: http://ojs.academypublisher.com/index.php/jnw/article/view/6612

[107] X. Zhou, L. E. Nelson, and P. Magill, "Rate-adaptable optics for next generation long-haul transport networks," *IEEE Communications Magazine*, vol. 51, no. 3, pp. 41–49, March 2013.

[108] G. H. Gho, L. Klak, and J. M. Kahn, "Rate-Adaptive Coding for Optical Fiber Transmission Systems," *Journal of Lightwave Technology*, vol. 29, no. 2, pp. 222–233, Jan 2011.

[109] L. E. Nelson, G. Zhang, M. Birk, C. Skolnick, R. Isaac, Y. Pan, C. Rasmussen, G. Pendock, and B. Mikkelsen, "A robust real-time 100G transceiver With soft-decision forward error correction [Invited]," *IEEE/OSA Journal of Optical Communications and Networking*, vol. 4, no. 11, pp. B131–B141, Nov 2012.

[110] F. Chang, K. Onohara, and T. Mizuochi, "Forward error correction for 100 G transport networks," *IEEE Communications Magazine*, vol. 48, no. 3, pp. S48–S55, March 2010.

[111] G. Gao, J. Zhang, W. Gu, Z. Feng, and Y. Ye, "Dynamic power control for mixed line rate transparent wavelength switched optical networks," in *36th European Conference and Exhibition on Optical Communication*, Sept 2010, pp. 1–3.

[112] A. Carena, V. Curri, G. Bosco, P. Poggiolini, and F. Forghieri, "Modeling of the Impact of Nonlinear Propagation Effects in Uncompensated Optical Coherent Transmission Links," *Journal of Lightwave Technology*, vol. 30, no. 10, pp. 1524–1539, May 2012.

[113] A. Alvarado, D. J. Ives, S. J. Savory, and P. Bayvel, "On the Impact of Optimal Modulation and FEC Overhead on Future Optical Networks," *Journal of Lightwave Technology*, vol. 34, no. 9, pp. 2339–2352, May 2016.

[114] D. J. Ives and S. J. Savory, "Transmitter optimized optical networks," in *2013 Optical Fiber Communication Conference and Exposition and the National Fiber Optic Engineers Conference (OFC/NFOEC)*, March 2013, pp. 1–3.

[115] E. Palkopoulou, G. Bosco, A. Carena, D. Klonidis, P. Poggiolini, and I. Tomkos, "Nyquist-WDM-Based Flexible Optical Networks: Exploring Physical Layer Design Parameters," *Journal of Lightwave Technology*, vol. 31, no. 14, pp. 2332–2339, July 2013.

[116] D. J. Ives, P. Bayvel, and S. J. Savory, "Physical layer transmitter and routing optimization to maximize the traffic throughput of a nonlinear optical mesh network," in *2014 International Conference on Optical Network Design and Modeling*, May 2014, pp. 168–173.

[117] D. Amar, N. Brochier, E. L. Rouzic, J. L. Auge, C. Lepers, B. Cousin, and M. Kanj, "Link design and legacy amplifier limitation in flex-grid optical networks," *IEEE Photonics Journal*, vol. 8, no. 2, pp. 1–10, April 2016.

[118] P. Poggiolini, "The GN Model of Non-Linear Propagation in Uncompensated Coherent Optical Systems," *Journal of Lightwave Technology*, vol. 30, no. 24, pp. 3857–3879, Dec. 2012.

[119] F. Vacondio, C. Simonneau, L. Lorcy, J.-C. Antona, A. Bononi, and S. Bigo, "Experimental characterization of Gaussian-distributed nonlinear distortions," in *European Conference on Optical Communications*. Optical Society of America, 2011, pp. We–7.

[120] A. Carena, V. Curri, G. Bosco, P. Poggiolini, and F. Forghieri, "Modeling of the Impact of Nonlinear Propagation Effects in Uncompensated Optical Coherent

Transmission Links," *Journal of Lightwave Technology*, vol. 30, no. 10, pp. 1524–1539, May 2012.

[121] G. Bosco, A. Carena, R. Cigliutti, V. Curri, P. Poggiolini, and F. Forghieri, "Performance prediction for WDM PM-QPSK transmission over uncompensated links," in *Optical Fiber Communication Conference*. Optical Society of America, 2011.

[122] A. Nag, M. Tornatore, and B. Mukherjee, "Power management in mixed line rate optical networks," in *Integrated Photonics Research, Silicon and Nanophotonics and Photonics in Switching*. Optical Society of America, 2010.

[123] A. Bononi, P. Serena, and A. Morea, "Regeneration savings in coherent optical networks with a new load-dependent reach maximization," in *2014 The European Conference on Optical Communication (ECOC)*, Sept 2014, pp. 1–3.

[124] R. Martinez, R. Casellas, R. Munoz, and T. Tsuritani, "Experimental translucent-oriented routing for dynamic lightpath provisioning in gmpls-enabled wavelength switched optical networks," *Journal of Lightwave Technology*, vol. 28, no. 8, pp. 1241–1255, April 2010.

[125] M. Kanj, E. L. Rouzic, D. Amar, J. L. Auge, B. Cousin, and N. Brochier, "Optical power control to efficiently handle flex-grid spectrum gain over existing fixed-grid network infrastructures," in *2016 International Conference on Computing, Networking and Communications (ICNC)*, Feb 2016, pp. 1–7.

[126] D. Amar, M. Kanj, J. L. Auge, N. Brochier, E. L. Rouzic, C. Lepers, and B. Cousin, "On the legacy amplifier limitation in flexgrid optical networks," in *2015 International Conference on Photonics in Switching (PS)*, Sept 2015, pp. 172–174.

[127] A. Mitra, S. Kar, and A. Lord, "Effect of frequency granularity and Link Margin at 100g and beyondFlexgrid Optical Networks," in *Communications (NCC), 2014 Twentieth National Conference on*. IEEE, 2014, pp. 1–5.

[128] A. Mitra, A. Lord, S. Kar, and P. Wright, "Effect of link margin and frequency granularity on the performance of a flexgrid optical network," *Optics express*, vol. 22, no. 1, pp. 41–46, 2014.

[129] F. Vacondio, O. Rival, C. Simonneau, E. Grellier, A. Bononi, L. Lorcy, J.-C. Antona, and S. Bigo, "On nonlinear distortions of highly dispersive optical coherent systems," *Optics Express*, vol. 20, no. 2, pp. 1022–1032, 2012.

[130] E. Mannie, "Generalized Multi-Protocol Label Switching (GMPLS) Architecture," Internet Requests for Comments, RFC Editor, RFC 3945, October 2004.

[131] X. Zhang, R. Casellas, O. G. de Dios, and D. Ceccarelli, "Gmpls ospf-te extensions in support of flexi-grid dwdm networks," Working

Draft, IETF Secretariat, Internet-Draft draft-ietf-ccamp-flexible-grid-ospf-ext-04, April 2016. [Online]. Available: http://www.ietf.org/internet-drafts/draft-ietf-ccamp-flexible-grid-ospf-ext-04.txt

[132] F. Zhang, X. Zhang, A. Farrel, O. G. de Dios, and D. Ceccarelli, "RSVP-TE Signaling Extensions in Support of Flexi-Grid Dense Wavelength Division Multiplexing (DWDM) Networks," Internet Requests for Comments, RFC Editor, RFC 7792, March 2016.

[133] G. Martinelli, X. Zhang, G. Galimberti, A. Zanardi, D. Siracusa, F. Pederzolli, Y. Lee, and F. Zhang, "Information model for wavelength switched optical networks (wsons) with impairments validation," Working Draft, IETF Secretariat, Internet-Draft, draft-ietf-ccamp-wson-iv-info-02, October 2015. [Online]. Available: http://www.ietf.org/internet-drafts/draft-ietf-ccamp-wson-iv-info-02.txt

[134] Y. Lee, G. Bernstein, D. Li, and G. Martinelli, "A framework for the control of wavelength switched optical networks (wsons) with impairments," Internet Requests for Comments, RFC Editor, RFC 6566, March 2012.

[135] I. Hussain, R. Rao, M. Sosa, and A. Dhillon, "TE extensions to OSPF for GMPLS control of Flex-Grid Networks," Working Draft, IETF Secretariat, Internet-Draft, draft-dhillon-ccamp-flexgrid-ospfte-ext-00, March 2014. [Online]. Available: http://www.ietf.org/internet-drafts/draft-dhillon-ccamp-flexgrid-ospfte-ext-00.txt

[136] F. Zhang, Y. Lee, J. Han, G. Bernstein, and Y. Xu, "OSPF-TE Extensions for General Network Element Constraints," Internet Requests for Comments, RFC Editor, RFC 7580, June 2015.

[137] G. Martinelli and A. Zanardi, "GMPLS Signaling Extensions for Optical Impairment Aware Lightpath Setup," Working Draft, IETF Secretariat, Internet-Draft draft-martinelli-ccamp-optical-imp-signaling-03, October 2010. [Online]. Available: http://www.ietf.org/internet-drafts/draft-martinelli-ccamp-optical-imp-signaling-03.txt

[138] B. Braden, L. Zhang, S. Berson, S. Herzog, and S. Jamin, "Resource reservation protocol (rsvp) – version 1 functional specification," Internet Requests for Comments, RFC Editor, RFC 2205, September 1997. [Online]. Available: http://www.rfc-editor.org/rfc/rfc2205.txt

[139] D. Amar, E. Le Rouzic, N. Brochier, J.-L. Auge, C. Lepers, N. Perrot, and S. Fazel, "How problematic is Spectrum Fragmentation in operator's Gridless network?" in *International Conference on Optical Network Design and Modeling, 2014*. IEEE, 2014, pp. 67–72.

[140] R. Martinez, R. Casellas, R. Munoz, T. Tsuritani, and T. Otani, "Experimental GMPLS routing for dynamic provisioning in translucent wavelength switched optical networks," in *2009 Conference on Optical Fiber Communication - incudes post deadline papers*, March 2009, pp. 1–3.

[141] N. Sambo, A. Giorgetti, F. Cugini, N. Andriolli, L. Valcarenghi, and P. Castoldi, "Accounting for Shared Regenerators in GMPLS-Controlled Translucent Optical Networks," *Journal of Lightwave Technology*, vol. 27, no. 19, pp. 4338–4347, Oct 2009.

[142] H. Guo, T. Tsuritani, S. Okamoto, and T. Otani, "Demonstration of GMPLS-controlled inter-domain transparent optical networks," in *2008 34th European Conference on Optical Communication*, Sept 2008, pp. 1–2.

[143] F. Cugini, N. Sambo, A. Giorgetti, L. . Valcarenghi, P. Castoldi, E. L. Rouzic, and J. Poirrier, "GMPLS extensions to Encompass Shared Regenerators in Transparent Optical Networks," in *33rd European Conference and Exhibition of Optical Communication*, Sept 2007, pp. 1–2.

[144] N. Sambo, F. Cugini, N. Andriolli, A. Giorgetti, L. Valcarenghi, and P. Castoldi, "Lightweight RSVP-TE extensions to account for Shared Regenerators in Translucent Optical Networks," in *2007 Photonics in Switching*, Aug 2007, pp. 35–36.

[145] N. Sambo, N. Andriolli, A. Giorgetti, F. Cugini, L. Valcarenghi, and P. Castoldi, "Distributing Shared Regenerator Information in GMPLS-Controlled Translucent Networks," *IEEE Communications Letters*, vol. 12, no. 6, pp. 462–464, June 2008.

[146] G. Bernstein, Y. Lee, D. Li, W. Imajuku, and J. Han, "Routing and Wavelength Assignment Information Encoding for Wavelength Switched Optical Networks," Internet Requests for Comments, RFC Editor, RFC 7581, June 2015.

[147] G. Bernstein, S. Xu, Y. Lee, G. Martinelli, and H. Harai, "Signaling extensions for wavelength switched optical networks," Internet Requests for Comments, RFC Editor, RFC 7689, November 2015.

[148] Y. Lee, G. Bernstein, D. Li, and W. Imajuku, "Routing and wavelength assignment information model for wavelength switched optical networks," Internet Requests for Comments, RFC Editor, RFC 7446, February 2015.

[149] D. C. Rider, J. C. Slezak, A. V. W. Smith, and A. Lucent, *Regenerators placement mechanism for wavelength switched optical networks*. Erteilung, Mar. 2002. [Online]. Available: http://www.google.ch/patents/US8571415

[150] F. Zhang, Y. Lee, J. Han, G. Bernstein, and Y. Xu, "OSPF-TE Extensions for General Network Element Constraints," Internet Requests for Comments, RFC Editor, RFC 7580, June 2015.

[151] G. Bernstein, Y. Lee, D. Li, W. Imajuku, and J. Han, "General Network Element Constraint Encoding for GMPLS-Controlled Networks," Internet Requests for Comments, RFC Editor, RFC 7579, June 2015.

[152] Y. Lee and G. Bernstein, "GMPLS OSPF Enhancement for Signal and Network Element Compatibility for Wavelength Switched Optical Networks," Internet Requests for Comments, RFC Editor, RFC 7688, November 2015.

[153] L. Berger, "Generalized Multi-Protocol Label Switching (GMPLS) Signaling Resource ReserVation Protocol-Traffic Engineering (RSVP-TE) Extensions," Internet Requests for Comments, RFC Editor, RFC 3473, January 2003.

[154] A. Farrel, D. King, Y. Li, and F. Zhang, "Generalized Labels for the Flexi-Grid in Lambda Switch Capable (LSC) Label Switching Routers," Internet Requests for Comments, RFC Editor, RFC 7699, November 2015.

[155] C. Margaria, G. Martinelli, S. Balls, and B. Wright, "Label Switched Path (LSP) Attribute in the Explicit Route Object (ERO)," Internet Requests for Comments, RFC Editor, RFC 7570, July 2015.

[156] R. Casellas, R. Muñoz, R. Martínez, R. Vilalta, L. Liu, T. Tsuritani, I. Morita, V. López, O. G. de Dios, and J. P. Fernández-Palacios, "SDN orchestration of OpenFlow and GMPLS flexi-grid networks with a stateful hierarchical PCE [invited]," *IEEE/OSA Journal of Optical Communications and Networking*, vol. 7, no. 1, pp. A106–A117, Jan 2015.

[157] X. Yang and B. Ramamurthy, "Sparse regeneration in translucent wavelength-routed optical networks: Architecture, network design and wavelength routing," *Photonic network communications*, vol. 10, no. 1, pp. 39–53, 2005. [Online]. Available: http://link.springer.com/article/10.1007/s11107-005-1694-y

[158] E. Yetginer and E. Karasan, "Regenerator placement and traffic engineering with restoration in GMPLS networks," *Photonic Network Communications*, vol. 6, no. 2, pp. 139–149, 2003. [Online]. Available: http://link.springer.com/article/10.1023/A:1024731113866

[159] N. Sambo, N. Andriolli, A. Giorgetti, P. Castoldi, and G. Bottari, "Multiple path based regenerator placement algorithm in translucent optical networks," in *2009 11th International Conference on Transparent Optical Networks*, June 2009, pp. 1–4.

[160] R. Martínez, R. Casellas, R. Muñoz, B. García-Manrubia, P. Pavón-Marino, M. Klinkowski, and D. Careglio, "Experimental study on the impact of regenerator placement strategies when dynamically provisioning in translucent GMPLS WSON networks," in *2011 Optical Fiber Communication Conference and Exposition and the National Fiber Optic Engineers Conference*, March 2011, pp. 1–3.

[161] A. V. Manolova, A. Giorgetti, I. Cerutti, N. Sambo, N. Andriolli, R. Munoz, R. Martinez, R. Casellas, S. Ruepp, and P. Castoldi, "Wavelengths and Regenerators Sharing in GMPLS-Controlled WSONs," in *2010 IEEE Global Telecommunications Conference GLOBECOM 2010*, Dec 2010, pp. 1–5.

[162] The LINUX Foundation, "Opendaylight: Open source sdn platform," accessed october, 2016. [Online]. Available: www.opendaylight.org

[163] ——, "ONOS project," accessed october, 2016. [Online]. Available: http://onosproject.org